UNIVERSITÀ DEGLI STUDI DI NAPOLI FEDERICO II

SCUOLA DI MEDICINA E CHIRURGIA
AREA DIDATTICA DI FARMACIA E BIOTECNOLOGIE PER LA SALUTE

DOTTORATO IN SCIENZA DEL FARMACO
XXXIV CICLO

SKINCARE AND HAIRCARE ACTIVE INGREDIENTS DEVELOPMENT

Doctoral Dissertation of:

Dott. Ritamaria Di Lorenzo

Tutor:
Prof. Sonia Laneri

The Chair of the Doctoral Program:
Prof. Maria Valeria D'Auria

2019/2021

COLLABORATIONS

This doctoral research project was carried out under Prof. Sonia Laneri.

The in vitro analysis on cell coltures was performed by collaborating with Arterra Bioscience Spa, Naples (Italy), an Italian biotechnology company with consolidated know-how in molecular, cellular, and plant biology and extensive experience in the identification of active molecules.

Part of the research project took place at the Institute for Advanced Chemistry of Catalonia (Barcelona, Spain), here studies on hair diffusion and thermal properties were conducted in collaboration with Prof. Luisa Coderch (DermoCosmetic Assessment service,) expert on hair morphological and functional organization and in the evaluation of cosmetic products' efficacy on human hair.

INDEX

ABSTRACT……

CHAPTER 1……1

1.1 INTRODUCTION…… 1

1.2 STUDY DESIGN……...3

1.3 MATERIALS AND METHODS……6

1.3.1 SNAIL MUCUS PICKING AND STERILIZATION……....6

1.3.1.1 MICROBIOLOGICAL CHARACTERIZATION……...6

1.3.2 GLYCOLIC ACID AND ALLANTOIN CHEMICAL CHARACTERIZATION……..…..6

1.3.2.1 SNAIL MUCUS TREATMENT……..……6

1.3.2.2 REAGENT AND CHEMICALS FOR CHEMICALS CHARACTERIZATION…..……6

1.3.2.3 STANDARDS PREPARATION……7

1.3.2.4 CHROMATOGRAPHIC APPARATUS…….....7

1.3.2.5 CHROMATOGRAPHIC ANALYSIS……7

1.3.3 CREAMS PREPARATION……..8

1.3.3.1 FORMULATION DEVELOPMENT……..8

1.3.3.2. CREAMS APPLICATION AND SKIN ANALYSIS……9

1.4 STATISTICAL ANALYSIS……10

1.5 RESULTS……10

1.5.1 ALLANTOIN AND GLYCOLIC ACID DETECTION……10

1.5.2 IN VIVO DATA……12

1.5.2.1 TRANS EPIDERMAL WATER LOSS……...12

1.5.2.2 SKIN HYDRATION……..14

1.6 DISCUSSION……..16

1.7 CONCLUSIONS……17

CHAPTER 2……...18

2.1 INTRODUCTION……18

2.1.1 CIRSIUM ERIOPHORIUM……21

2.1.1.1 CIRSIUM ERIOPHORIUM CHEMICAL PROPERTIES……22

2.1.1.2 CIRSIUM ERIOPHORIUM FUNCTIONAL PROPERTIES……23

2.2 STUDY DESIGN……24

2.3 MATERIALS AND METHODS ……26

2.3.1 PLANT TISSUE COLTURES AND EXTRACT PREPARATION……26

2.3.2 CHEMICAL ANALYSIS……..27

2.3.3 CELL COLTURES……..28

2.3.4. 5-ALPHA REDUCTASE ACTIVITY……28

2.3.5 GENE EXPRESSION ANALYSIS OF CYTOKINE GENES……29

2.3.6 GENE EXPRESSION AND ACTIVITY OF KALLIKREIN 5……30

2.3.7 ELISA ASSAY FOR COLLAGEN MEASURE……30

2.3.8 IN VIVO STUDIES……31

2.3.8.1 APPARATUS……31

2.3.8.2 CREAM COMPOSITION……31

2.3.8.3 TEST CONDITIONS……32

2.3.8.4 VOLUNTEERS SELECTION……32

2.3.8.5 INCLUSION AND EXCLUSION CRITERIA……32

2.4 STATISTICAL ANALYSIS……33

2.5 RESULTS……33

2.5.1 CHEMICAL CHARACTERIZATION OF C. ERIOPHORIUM CELL COLTURE EXTRACT AND PHENOLIC QUANTIFICATION……33

2.5.2 IN VITRO STUDIES……36

2.5.2.1 5-α REDUCTASE ACTIVITY……..36

2.5.2.2 KALLIKREIN 5 ACTIVITY……..37

2.5.2.3 ANTI-INFLAMMATORY ACTIVITY……...38

2.5.2.4 COLLAGEN I PRODUCTION……39

2.5.3 IN VIVO STUDIES……..40

2.5.3.1 ACTIVITY IN SEBUM PRODUCTION……..40

2.5.3.2 ACTIVITY ON PORE SIZE……41

2.5.3.3 SKIN HYDRATION……..43

2.6 DISCUSSION……..44

2.7 CONCLUSIONS……45

CHAPTER 3……...46

3.1 INTRODUCTION……46

3.2 STUDY DESIGN……48

3.3 MATERIALS AND METHODS……49

3.3.1 IN VITRO STUDIES……49

3.3.1.1 REAGENT AND CHEMICALS……....49

3.3.1.2 DETERMINATION OF OCTANOL/WATER PARTITION COEFFICIENT……...49

3.3.1.3 VALIDATION OF OCTANOL/WATER PARTITION COEFFICIENT……...50

3.3.1.4 TISSUE PREPARATION……50

3.3.1.5 CHROMATOGRAPHIC ANALYSIS FOR SKI PERMEATION STUDY……51

3.3.1.6 VALIDATION OF FBA-EXTRACTION METHOD AND HPLC ANALYSIS……..51

3.3.1.6.1 SELECTIVITY……52

3.3.1.6.2 SENSITIVITY……52

3.3.1.6.3 PRECISION AND ACCURACY……..53

3.3.1.6.4 MATRIX EFFECT……53

3.3.1.7 SKIN PERMEATION AND RETENTION……53

3.3.1.7.1 PERMEABILITY CALCULATION……...54

3.3.2 IN VIVO STUDY……..54

3.3.2.1 CLINICAL TRIAL……..55

3.3.2.2 STUDY POPULATION……56

3.3.2.3 CREAM COMPOSITION……56

3.4 STATISTICAL ANALYSIS……57

3.5 RESULTS……57

3.5.1 IN VITRO STUDIES……57

3.5.1.1 PARTITION COEFFICIENT AND SILICO PARAMETERS...58

3.5.1.2 DOSAGE METHOD USED TO DETERMINE FBA LEVELS……..58

3.5.1.3 VALIDATION OF THE ANALYTICAL METHOD……60

3.5.1.4 SKIN PERMEATION……61

3.5.2 IN VIVO STUDY……..61

3.5.2.1 ERYTHEMA INDEX……61

3.6 DISCUSSION……..63

3.7 CONCLUSIONS……65

CHAPTER 4……...66

4.1 INTRODUCTION……66

4.1.1 FICUS CARICA……67

4.1.1.1 F. CARICA CHEMICAL PROPERTIES……68

4.1.1.2 F. CARICA FUNCTIONAL PROPERTIES……...69

4.2 STUDY DESIGN……70

4.3 MATERIALS AND METHODS……72

4.3.1 IN VITRO STUDIES…… 72

4.3.1.1 PLANT CELL COLTURING AND EXTRACT PREPARATION……72

4.3.1.2 SKIN CELLS EXPLANTS……...73

4.3.1.3 GENE EXPRESSION ANALYSIS……73

4.3.1.4 DETERMINATION OF LIPID PEROXIDES……75

4.3.1.5 LIPOFUSCIN MEASUREMENTS……75

4.3.1.6 EPIDERMAL LIPID MEASUREMENT……75

4.3.1.7 MEASURING OF CARBONYLATED PROTEINS IN CELLS AND SKIN EXPLANTS……..75

4.3.1.8 cAMP MEASUREMENT……76

4.3.1.9 DETERMINATION OF FICIN AMOUNT AND ACTIVITY……...77

4.3.2 IN VIVO STUDIES……..77

4.3.2.1 STUDY POPULATION……78

4.3.2.2 CREAM COMPOSITION……79

4.4 STATISTICAL ANALYSIS……80

4.5 RESULTS……81

4.5.1 IN VITRO STUDIES……81

4.5.1.1 EXTRACT PREPARATION……81

4.5.1.2 ACTIVITY OF FcHEx EPINEPHRINE SIGNALING…82

4.5.1.3 ACTIVITY OF FcHEx ON THE INFLAMMATORY CYTOKINE IL-6……..……...83

4.5.1.4 LIPID PEROXIDE MEASUREMENT……..…83

4.5.1.5 CARBONYLATED PROTEIN DETERMINATION…...84

4.5.1.6 LIPOFUSCIN MEASUREMENTS…….……86

4.5.1.7 ACTIVITY OF FcHEx ON THE CERAMIDE PRODUCTION……...87

4.5.2 IN VIVO STUDIES……..…89

4.5.2.1 TRANS EPIDERMAL WATER LOSE EVALUATION.89

4.5.2.2 SKIN SEBUM AND DESQUAMATION LEVEL DETECTION……..……..91

4.5.2.3 SKIN LIGHTNESS……...92

4.5.2.4 SKIN pH…….94

4.6 DISCUSSION……..94

4.7 CONCLUSIONS…….97

CHAPTER 5……...98

5.1 INTRODUCTION……98

5.2 STUDY DESIGN……..……100

5.3 MATERIALS AND METHODS…..……101

5.3.1 PERCENTAGE NO TRANSFER REMOVAL RATIO……..103

5.4 STATISTICAL ANALYSIS……..104

5.5 RESULTS……..104

5.6 DISCUSSION……106

5.7 CONCLUSIONS……...107

CHAPTER 6……108

6.1 INTRODUCTION……..108
6.2 STUDY DESIGN……..111
6.3 MATERIALS AND METHODS……...111
6.3.1 AIR SAMPLES……..111
6.3.2 LIPID EXTRACTIONS……111
6.3.3 LIPIDS ANALYSIS……112
6.3.4 THERMOGRAVIMETRIC ANALYSIS……112
6.3.5 MOISTURE CONTENT……112
6.3.6 ATR-FTIR……...113
6.3.7 DYNAMIC WATER VAPOUR SORPTION……113
6.4 STATISTICAL ANALYSIS……..115
6.5 RESULTS……..115
6.5.1 HAIR LIPID ANALYSIS TLC-FID……115
6.5.2 THERMOGRAVIMETRIC ANALYSIS……119
6.5.3 AIR MOISTURE……120
6.5.4 DYNAMIC VAPOR SORPTION……..122
6.5.5 ATR-FTIR……...124
6.6 DISCUSSION……126
6.7 CONCLUSIONS……...127

CHAPTER 7……128
7.1 INTRODUCTION…… 128
7.2 STUDY DESIGN……..132
7.3 MATERIALS AND METHODS……...132
7.3.1 HAIR SAMPLES…… 132
7.3.1.1 WASHING PROCESS…….....133

7.3.2 DYNAMIC VAPOR SORPTION……....133

7.3.3 IR SPECTROSCOPY FTIR-ATR……...134

7.3.4 MOISTURE CONTENT…….....135

7.3.5 LIPID EXTRACTIONS…….....135

7.3.5.1 LIPDS ANALYSIS…….....135

7.4 RESULTS.. …….....136

REFERENCES…….... 137

ACKNOWLEDGMENTS……153

CURRICULUM VITAE……154

PUBLICATIONS……..155

‘

ABSTRACT

The present Doctoral Thesis deals with studies for evaluating the effectiveness of active products transmitted in cosmetics according to EU Regulation 1223/2009. This regulation governs the production and sale of cosmetic products and therefore has the purpose of harmonizing cosmetic legislation to create a single legal instrument of reference for all Member States of the European Union. In particular, according to Article 11, the information documentation relating to cosmetic products held by the person responsible for placing them on the market must provide evidence of the effects attributed to them.
The cosmetic claim must be supported by demonstrable, relevant, and clear evidence founded on peer-reviewed data obtained through in vivo, ex vivo, or in vitro studies or with a combination thereof.

The European Commission, up to now according to the Colipa orientation to avoid slowing down or hindering technical-scientific innovation, has preferred to avoid the publication of a list of accepted claims and scientific studies that could be used as this could limit innovation in the sector. Herein, the possibility to develop a range of tests supporting a cosmetic claim.

The first study was carried out to provide by using chromatographic method contents of two of the essential active ingredients contained in the *Helix aspersa* mucus:

- Allantoin, which regenerates the epidermal layers and acts as a nourishing and protective ingredient
- Glycolic acid stimulates collagen and elastin production in the dermis and promotes epidermis renewal. It removes dead cells from the skin surface, thus giving the skin a brighter and more uniform, smooth, and hydrated appearance.

Different percentages of snail mucus cosmetic creams were prepared, whose ability to hydrate the skin was evaluated by comparing the skin hydration and trans-epidermal water loss (TEWL) to a placebo, with a short-term human in-use test.

Afterward, the use of functional substances of vegetable origin was investigated in treating different skin concerns.

In Europe, functional plants are defined as Botanicals or Herbals used as they are or in processed form as ingredients for food, food supplements, cosmetics, medical devices, and drugs.

As scientific evidence shows, all plant species/derivatives are potentially suitable for use medicines, cosmetics, or other products for human or animal use, respecting any restrictions that arise from the compatibility of the plant for the specific use and the conformity of the finished product, which derives from the specific reference legislation.

For functional substances in the cosmetic field, reference is made to raw materials capable of giving specificity to the finished cosmetic product.

The use of the plant or meristematic cells to develop new cosmetic active ingredients has numerous advantages over standard plant extracts, which is why ingredients obtained from undifferentiated plant cells in liquid culture have been considered in recent years by both cosmetic brands and final consumers. One of the most crucial advantages is safety, as all the purified extracts or compounds derived from plant cell cultures are clean or relatively free of pathogens or environmental contaminants. Cells cultures grow in the laboratory with sterile and controlled conditions without coming into contact with potentially harmful substances. Furthermore, the cells do not contain allergens.

The second significant benefit is bio-sustainability; indeed, no agricultural land is exploited during the production process, no pesticides or fertilizers are used, there is reduced water consumption and little waste. The third advantage is that meristematic cells can be cultured in the laboratory-based on specific growth parameters monitored to obtain an optimal stimulation of the production of certain substances, the accumulation of which is of interest for cosmetic applications. In this way, it is possible to obtain plant extracts based on substances obtained from plant stem cells with a high concentration of reproducible molecules. Plant extracts are also always standardized, and producers can count on a reproducible supply of active material, not dependent on seasons or environmental conditions. This state assures high levels of consistency from one production batch to another, making these ingredients more suitable for meeting specific biological functions. [21-23]

Today, the market trend is to use plant-based ingredients in unlimited amounts and reduce possible side effects. Hence the need to study two new botanical extracts of *Cirsium eriophorum* and *Ficus carica*, the first active as pore-refiner, the other as an anti-stress.

Facial pore enlargement is considered a significant esthetic concern in skincare cosmetics. The pores live up to the critical function of keeping the skin surface hydrated and protected against external agents. The stress factors and the hormonal triggers can cause pore enlargement, causing a higher skin propensity to microbe aggressions and inflammatory reactions. Thus, two of the most requested activities in skincare cosmetics are reducing excessive sebum production and keeping functional pores, and *Cirsium eriophorum* cell culture extract was investigated for its role in sebum-control, skin desquamation, and anti-inflammation. The extract could govern essential markers related to sebum secretion and pore spread, like the 5α-reductase enzyme, which plays an essential role in sebum production, and the Kallikrein 5, a trypsin-like serine protease, which promotes skin flaking and antimicrobial response.
Finally, the *C. eriophorum* extract shows a sebum-normalizing and pore refining activity in people with oily or acne-prone skins, suggesting its role in rebalancing altered skin conditions involved in pore-enlargement.

Scientific evidence associated with the detoxifying effect of fruits and vegetables, the growing awareness of the long-term issues related to the use of chemical-filled cosmetics, the aging of the population, and the increase in living standards are the factors responsible for the growth of food-derived ingredients in the cosmetics market. Psychological stress activates catecholamine production, determines oxidation processes, and alters the lipid barrier functions in the skin. A *Ficus carica* cell suspension culture extract (FcHEx) was tested in vitro and in vivo to evaluate its action on managing the stress-hormone-damaged skin.
The in vivo experiments were corroborated by the in vitro test results. The FcHEx reduced the epinephrine, lipid peroxide, interleukin 6, and protein carbonylation productions; it generated ceramide synthesis ameliorating the lipid barrier performance. The extract of the *Ficus carica* cell suspension cultures reduced the trans epidermal water loss, desquamation, and sebum production, diminishing the facial greying, suggesting its role in alleviating the signs of psychological stress in the skin.

The in vivo activity of a butyrate derivative and its skin diffusion properties were analyzed within the framework of a new cosmetic active ingredient investigation.
Nasty sensorial properties and disadvantageous physicochemical butyrate properties strongly limit its cosmetic use. Nevertheless, some butyrate derivatives,

like phenylalanine butyramide, are odorless and maintain the pharmacokinetics safety profile of the butyric acid. This study assessed the FBA's skin permeation and its soothing and anti-reddening action to purpose its transmission in cosmetic products. The FBA permeation tests were evaluated *in vitro* using Franz cell, while the soothing action was determined *in vivo* through a colorimetric test.
The results show that FBA is an innovative butyric acid derivative that exploits its benefits in the cosmetic field.

Afterward, following a market need emerging with the COVID-19 disease, spread worldwide since December 2019, that has made it necessary to use personal protective equipment, especially face masks, due to the high transmission rate of COVID -19 [139] and propensity to airborne infection [140]. This condition has made it extremely difficult to wear makeup products, registering a sale decline. The producers have tried to compensate for inconvenience, like uneven foundation, smudged and messy masks, by developing new no transfer products.
Whereby no transfer means the ability of a cosmetic product to completely resist the "transfer" from one surface to another, and therefore to remain adhered to the area of original application without "transferring" to the surface with which it comes into contact, in particular face masks defining a new claim word, better known as mask-proof.
Companies are looking for tests that provide reliable scientific results, with objective scientific evidence, compliant with European guidelines, which can only be conducted by trained and qualified technical personnel and advanced scientific instruments.
Herein, the development of a mask-proof protocol to test the no transferability of cosmetic products on surgical masks. The in vivo measurements are conducted with calibrated devices inside a closed room, maintained at controlled temperature and humidity, on a panel of volunteers selected respecting the Declaration of Helsinki on Ethical Principles for Medical Research.

During the period as visiting Ph.D. Student, from June to October 2021, at the Institute for Advanced Chemistry of Catalonia, IQAC (Barcelona, Spain), and more precisely, with the Cosmetic and Textile innovation group managed by Prof. Luisa Coderch, my work focused on identifying the key drivers of diffusion on hair and key factors between Caucasian and Chinese diffusion differences, like lipid’s impact, pH and solvent impact. The project was sponsored by the Hair Fiber Discovery Domain

of L’ORÉAL Research & Innovation, Aulnay-sous-Bois – France. A non-disclosure agreement covers the results of this project, so they cannot be reported in this thesis.

The second project carried out during the period spent at IQAC was about studying the effect of lipids on hair aging. The lipid quantification and analysis were done using thin-film chromatography coupled to a flame detector (TLC-FID). Next, a study was made of the calorimetric behavior of the different lipids extracts obtained from the hair samples using thermogravimetric (TGA) and dynamic vapor sorption (DVS) analysis. Their moisture content was assessed, and liposomes were formed to determine the organization of these lipids by Fourier-transform infrared spectroscopy (FTIR). These tests allowed us to characterize the differences between white and brown Caucasian hairs and determine the role of the external and internal lipids in the hair aging process.

CHAPTER 1

Helix aspersa mucus bioactive molecules analysis and in vivo moisturizing efficacy assessment

1.1 Introduction

Snail mucopoly-saccharide, commonly called burr, also known as slime or bava, is a secretion produced by glands at the snail's foot.
Snails are rich in secondary metabolites used in cosmetics and medicine; their slime is abundant in collagen, elastin, glycoproteins and mucopolysaccharides [1], hyaluronic acid, allantoin, and glycolic acid, all of which have skin benefits broadly studied and recognized.[2]

Extraction, or deburring, of this material from the animal is carried out under adequate temperature and humidity conditions, without adding salt or other chemical substances.
Deburring occurs manually using food-grade containers and a stainless-steel device operated by hand that simulates stimulation. This manipulation does not affect the animal's quality of life, thus achieving an optimal result for the production yield of burrs per unit in kg of treated snails and, due to the absence of damage and stress, ensuring most survival.

The collected snail slime passes through various stages of filtration, initially to remove residues and clean it. After due diligence checks, the mucus is stabilized using a preservative. It is then passed through pharmaceutical-grade filters to

remove bacteria before being subjected to microbiology control before and after adding preservatives.

The ingredient exhibits healing and emollient properties for the skin thanks in part to its natural content of allantoin, or 5-ureidohydantoin, one of the several oxidated-uric-acid-derived products [3,4], which promotes epidermal turnover and favors moisturizing, soothing, and revitalizing actions. Allantoin helps cell proliferation and wound healing, increases the extracellular matrix's water content, and forms complexes with irritant and sensitizing substances.[5]

The presence of glycolic acid, or alpha-hydroxyacetic acid, has an excellent capability to penetrate the skin, where reduces cohesion forces between corneocytes by direct action on the desmosomes, promoting gentle exfoliation of the superficial layers of skin. This action, in turn, speeds cellular turnover and produces an increase in fibroblast activity and the production of collagen and elastin and modulates matrix degradation [5-7];

The other snail mucus components have hydrating properties that aid the skin barrier and help lock in moisture so that the skin can be softer, glowing, and moisturized with the consistent use of snail mucin.[9]

The Snail Slime ingredient (INCI: Snail Secretion Filtrate) appears as an amber liquid, transparent or slightly opalescent. It is completely miscible in water, is insoluble in vegetable or mineral oils, and is dispersible in o/w emulsions. The pH can vary from 5.7 to 6.5.

Although there is a wide range of research about the snail slime single components, there is a lack of peer-reviewed papers regarding its direct use on human beings.

The study aimed to establish its benefits on human skin, first determining the allantoin and glycolic acid concentrations in snail mucus of *Helix aspersa Muller* to assess its potential as a source of valuable molecules to formulate effective serums or creams with moisturizing properties.

The RD Cosmetics of Federico II University – Pharmacy Department (Naples, Italy) performed the single-blind trial.

The research laboratory is, equipped with material and technical means suitable for non-invasive clinical research, compatible with human subjects' safety requirements, according to the Helsinki Declaration [10].

1.2 Study Design

Snail mucus (**SM**) was kindly provided by an Italian natural breeding farm of *Helix Aspersa*. The mucus microbiological characterization was necessary to assure the raw material's safety. After that, the allantoin and glycolic acid (Figure 1.1) dosages were performed in several snail mucin batches.

Figure 1.1. Chemical structure, a) glycolic acid, b) allantoin.

The SM was adequately treated before the chemical characterization by HPLC, according to the El Mubarak [9] method, and results were compared with high-quality allantoin (**A**) and glycolic acid (**GA**) standards.

Meanwhile, creams with different SM % (Figure 1.2) were prepared to evaluate their in vivo efficacy compared to a placebo. Creams were tested on 20 healthy volunteers following the Helsinki Declaration of ethical principles for medical research. They signed informed consent and were subjected to case history and a clinical examination.

Figure 1.2. Exemplification snail mucin cosmetic cream

The upper forearm was selected as a test site (Figure 1.3), and panelists had to apply each cream to different delimited areas. Then the skin hydration and trans epidermal water loss detection were performed at different times (1 and 24 hours

after creams application) and compared with the baseline (T_0) using Student *t*-test setting $p < 0.05$ significant.

SPSS software performed statistical tests. The testing skin parameters were recorded in a controlled temperature and humidity lab after 30-minutes acclimatizations utilizing worldwide recognized tools for the cosmetic efficacy assessments, such as the Corneometer® CM 825 and the Tewameter® TM 300 (C+K electronic GmbH).

Figure 1.3. Exemplification test site image

TEWL is an indicator of the skin barrier integrity; there is a water gradient through the stratum corneum (SC), water vapor is continuously spread from the body to the skin surface and the environment. TEWL refers to the total amount of water the dermal and epidermal tissues exchanged to the external environment through the horny state.

The evaporimeter (Tewameter® TM 300, Figure 1.4) measures the water vapor released from a surface, basing on the Fick diffusion law. The diffusion current provides the water vapor quantity (g / m^2) transported in the time (h), so the measurement values will be expressed in g / hm^2.

The smaller the TEWL, the more the skin barrier remains unaltered in its integrity, so more water is retained in the SC.

Figure 1.4. Tewameter® TM 300 (C+K electronic GmbH)

Corneometer® CM 825 (Figure 1.5) is the most employed device to determine the hydration level of the upper skin layer (SC).

Nowadays, the terms "corneometry" and level of skin hydration are synonymous.

Measurement is based on the capacitance of the SC, which is a dielectric medium because it contains water.

Water has a high dielectric constant, and with increasing hydration, the SC dielectric properties change.

Gold tracks on the head of the probe create an electric field between the tracks with alternating attraction. One track builds up an excess of electrons (negatively charged), the other lacks their (plus charge). When put on the skin surface, the scattered field crosses the first layer of the skin—the Corneometer® CM 825 measures the change in the dielectric constant due to skin surface hydration changing.

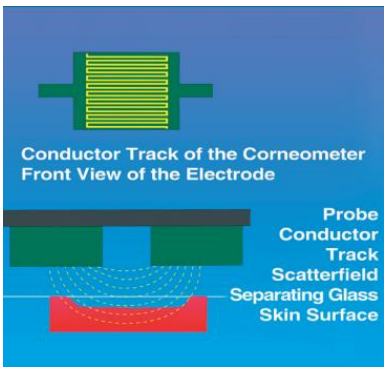

Figure 1.5. Corneometer® CM 825 (C+K electronic GmbH) measurement principle

The values of TEWL and those of the Corneometer are therefore directly related to the skin hydration and moisture degree; then, they can measure the physio-balancing power of a cosmetic product.

1.3 Materials and Methods

1.3.1 Snail mucus picking and sterilization

Terra Fertilis Italy (Campi Flegrei, Zona Agricola di Pregio – Italy), a snail natural breeding farm, kindly provided *Helix aspersa Muller* mucus sample lots: C 121701; D 151701; E 191701.

1.3.1.1. Microbiological Characterization

100 µL of SM was plated on culture media tryptic soy agar dishes (Biomerieux Italia S.p.a., Italy).
The colony-forming units (CFU) were detected after 24 to 48 hours at 37 ° C. The contaminating bacteria identification was performed by Gram staining (Liofilchem S.r.l., Italy), then stratifying SM on Sabouraud medium plates (Biomerieux Italia S.p.a, Italy) contaminating fungi were detected.
The sample presented a total bacterial amount of less than 100 CFU/g, molds and yeasts, and the total absence of pathogens.

1.3.2 Glycolic Acid and Allantoin Chemical Characterization

HPLC chemically analyzed the A and GA content in different SM batches extract following the El Mubarak et al.[9] method with some modifications.

1.3.2.1 Snail mucus treatment

1 mL of Snail Mucus (SM) was dissolved in 4 mL potassium phosphate buffer (pH 2.7; 10 mM), then it was stirred with a Vortex device for 15 minutes. After that, 1 mL is dissolved in further 4 mL sodium phosphate buffer (pH 2.7; 10 mM). In the end, the sample is filtered with a Corning filter (0.8 µm).

1.3.2.2 Reagent and chemicals for chemicals characterization

High-quality standard Allantoin was supplied from FLUKA (St Louis, MO, USA) with purity > 98.0 % and Glycolic acid from Sigma-Aldrich (St Louis, MO, USA) with a purity of 99.0 %.
Ultra-pure water from a MilliQ® instrument (Millipore, Billerica, MA, USA) was used.
HPLC grade acetonitrile (CH_3CN) and methanol (CH_3OH) were purchased from Honeywell Burdick & Jackson (Seelze, Germany); sodium hydroxide (NaOH) from Merck KgaA (Darmstadt, Germany) n-hexane ($CH_3(CH_2)_4CH_3$) from Fisher Scientific (Hampton, UK), and monosodium phosphate (NaH_2PO_4), phosphoric acid (H_3PO_4).
All solvents were filtered through 0.22 µm filters (Titan Membrane, Millipore).

1.3.2.3 Standards preparation

A and GA standards were prepared at 3 concentration levels: 1, 0.5, 0.25 mg/mL in potassium phosphate buffer (pH 2.7; 10 mM).

The procedure takes the calculated volumes or milligrams of GA and A, placing them in the respective flasks, previously labeled with the type of dilution and making up to volume with the buffer solution.

1.3.2.4 Chromatographic apparatus

The chromatographic system consisted of an HPLC Jasco LC-Net II/ADC (JASCO International Co., Ltd. Tokyo, Japan) with a 20 µL Rheodyne 8125 injector (Rheodyne, Rohnert Park, CA, USA), the UV Detector Jasco MD-2010 plus (JASCO International Co., Ltd. Tokyo, Japan) (λ 200 nm), and reversed-phase Vision HT C18 High Load 5 µm (250 mm × 4.60 mm, 4 µm) column (Grace, Munich, Germany).

1.3.2.5 Chromatographic analysis

SM samples were eluted on a Vision HT C18 High Load column 250 mm × 4.6 mm ID, 5 µm particle size, using the eluting conditions reported in Table 1.1.

Table 1.1. HPLC eluting conditions.

Time (min)	Eluent	%	Flow
Pre-run	CH_3CN	100	1 $mL.min^{-1}$
1 - 8	NaH_2PO_4	100	1 $mL.min^{-1}$
9 - 26	NaH_2PO_4 : CH_3CN	30 : 70	1 $mL.min^{-1}$
27 - 30	CH_3CN	100	1 $mL.min^{-1}$

The flow rate of the mobile phase was 1 mL/min. Elution was monitored at 200 nm wavelength.

20 µL of the three standards and the SM solutions were injected with a Hamilton syringe three times. A washing run of 100 % acetonitrile followed each sample injection to eliminate any contamination.

1.3.3 Creams preparation

Compared to a placebo, three creams with different SM %w/w were prepared to test in vivo the influence of the investigated active ingredient on the skin barrier recovery and hydration.

1.3.3.1 Formulation development

The four creams used for the in vivo efficacy assessment is an o/w emulsion containing ingredients listed in Table 1.2, and with different SM % (w/w): 0 % (placebo), 2 %, 5 %, and 10 %.

The oil phase (O) ingredients were heated until their fusion (≈ 65°C); meanwhile, the deionized water was heated to the same temperature. Then the two phases were joined, shaking vigorously.

In the end, the emulsion was put in an ice bath, and when cool, the remaining components were added.

The emulsion pH was 5.0 ± 0.5 (calculated with a pHmeter Crison GPL20) and viscosities 26 570 to 29 460 mPa s (L4, 20 rpm) were calculated with a rheometer Visco Basic Plus, Fungilab.

Table 1.2. Creams ingredient lists.

	Ingredient Class	INCI Name	% (w/w)	Origin
Phase O	Emollient	Cetyl alcohol	2.5	ACEF Spa (Fiorenzuola d'Arda, Italy)
	Emollient	Prunus Amygdalus Dulcis Oil	2.5	
	Emulsifier	Polyglyceryl-3-methyl glucose distearate	5.0	
	Emulsifier	Triticum Vulgare Germ Oil	7.5	
Phase W	Antioxidant	Tocopheryl Acetate	1.0	
	Parfum	Parfum	0.1	Farotti essenze (Rimini, Italy)
	Base	Aqua	q.b. to 100	
	Active Ingredient	Snail Mucus	0, 2, 5, 10	Terra Fertilis Italy (S.r.l.)
	Preservatives	Sodium benzoate, potassium sorbate phenoxyethanol	0.5	ACEF Spa (Fiorenzuola d'Arda, Italy)

1.3.3.2 Creams application and skin analysis

About 0.5 ± 0.10 g of SM creams (placebo, 2 %, 5 %, and 10 %) were applied on four volunteers' upper forearm areas (each one ~ 4 cm^2).

The instrumental measurements occurred in an air-conditioned room at T = 20 ± 5 ° C and controlled humidity (50 ± 5 % RH) after 30-minutes acclimatization.

At the baseline (T_0), after 1 and 24 hours (T_{1h} and T_{24h}), the following instrumental evaluations were carried out :

- TEWL with Tewameter® TM 300
- Skin hydration level detected with Corneometer® CM 825
- Software CK-MPA-Multi-Probe-Adapter FB for the data analysis

All tools are from C+K electronic GmbH, and they are periodically calibrated according to the investigating laboratory's corresponding procedure.

1.4 Statistical analysis

Unpaired Student t-test was set for continuous and independent data, paired Student t-test for paired data.

Statistical tests were performed using SPSS software (version 15). The Pearson's correlation coefficient was used to assess the correlation between the continuous variable. For all tests, significance was achieved at $p < 0.05$.

1.5 Results

The chromatographic snail slime characterization results correlate the in vivo data with the SM rate transmitted in the cosmetic creams and the allantoin and glycolic acid detected in them. In this way, it is possible to estimate the active dosage necessary to obtain a specific skin effect.

1.5.1 Allantoin and Glycolic acid detection

According to European medicines agency guidelines, validation, linearity, LLOD, LLOQ, precision, and accuracy are considered.

Direct dilution of SM in water or buffer was not possible and led to poor recoveries. Sound separation and recovery levels were achieved by dissolving SM in buffer solution (1 mL SM + 4 mL phosphate buffer pH 2.7; 10 mM) using an ultrasonic bath for 15 minutes.[9]

Three different flow rate values for the mobile phase (0.5, 0.7, and 1.0 mL/min) were tested. The value of 1 mL/min determined the best separation.

The detection wavelength was set at 200 nm (maximum absorbance) after spectra monitoring with a UV detector.

In these conditions, GA (2.82 ± 0.07 minutes) elutes earlier than A (3.9 ± 0.06 minutes). The linearity, LLOD, and LLOQ of the analytical procedure are summarized in Table 3.

Table 1.3. Linearity Data (Line Equation with a Standard Calibration Curve) in Spiked Samples of SM (n = 5 for Each Concentration Level).

Component	**Line Eq.**	**R^2**	**LLOD** (mg/mL)	**LLOQ** (mg/mL)
Allantoin	y = 28.114 x + 0.65	0.9972	0.004	0.0125
Glycolic acid	y = 70.482 x + 9.2	0,9926	0.130	0.2500

Intra- and inter-day repeatability are reported in Table 1.4.

Table 1.4. RSD (%) and Recoveries for 3 Consecutive Days in Spiked Samples of SM (n = 5 at Each Concentration Level).

Component	**Theoretical concentration (mg/mL)**		**Recovery %**	**RSD %**
Allantoin	1.0	Day 1	105.26	2.54
		Day 2	100.00	3.00
		Day 3	105.26	2.63
		Total	103.50	2.58
	0.5	Day 1	99.20	2.16
		Day 2	98.30	1.90
		Day 3	99.10	0.44
		Total	98.90	1.36
	0.25	Day 1	100.00	0.87
		Day 2	113.10	3.80
		Day 3	113.20	2.08
		Total	108.70	1.58
Glycolic acid	1.0	Day 1	98.40	1.70
		Day 2	95.24	2.49
		Day 3	99.00	2.40
		Total	97.50	1.01
	0.5	Day 1	86.90	2.13
		Day 2	90.59	1.54
		Day 3	91.24	2.12
		Total	89.60	3.50
	0.25	Day 1	100.00	2.12
		Day 2	109.00	4.21
		Day 3	113.00	3.56
		Total	107.30	1.10

Results shown in Table 1.5 on method stability agree with data reported by El Mubarak et al.[9]

A and GA were detected in three different SM batches at a rate of 1:10 (mL) with the buffer solution.

Table 1.5. Values of A and GA in SM batches (Concentration expressed in g/L).

Products	Allantoin	Glycolic acid
SM (g/L) lot 1	0.37 ± 0.60	3.29 ± 0.125
SM (g/L) lot 2	0.40 ± 0.30	3.42 ± 0.423
SM (g/L) lot 3	0.45 ± 0.52	3.35 ± 0.443
Average	0.41	3.35

1.5.2 In vivo data

Twenty females between 20 and 65 enrolled in the study applied on four different areas of the upper forearm 0.5 ± 0.1 g of the investigated product massaging until absorption.

TEWL and corneometry values were measured after 1 and 24 hours by cream's application, and data were statistically compared with the baseline.

All participants completed the study, and no adverse events were observed.

1.5.2.1 Transepidermal water loss

The loss of transepidermal water (TEWL) is an indicator of the integrity of the skin barrier. Water vapor in the stratum corneum is continuously spread from the body to the skin surface and the environment. TEWL refers to the total amount of water the dermal and epidermal tissues exchanged to the external environment through the horny state.

TEWL was evaluated by an evaporimeter which measures the water vapor released from a surface. The measurement basis on the Fick diffusion law (Eq.1). The diffusion current provides the quantity of water vapor (g / m^2) transported in the time unit (h), so the measurement values will be expressed in g / hm2. The smaller is the TEWL, the more the skin barrier is intact.

$$\frac{dm}{dt} = -D \cdot A \cdot \frac{dp}{dx}$$

Equation 1.1 Fick diffusion law

The average values obtained at the different times (T_0, T_{1h}, and T_{24h}) for each tested cream are reported in Table 1.6 and represented in Figure 1.4.

Table 1.6. TEWL values after a single topical SM cream application. *$p < 0.05$

Time (h)	**Cream type**	**Nr. of Volunteers**	**TEWL average values** (g/hm^2)	**Variation compared to T_0** (%)	***P***
0	Placebo	20	14.0 ± 3.2		
	SM 2 %	20	11.1 ± 1.4		
	SM 5 %	20	12.6 ± 2.4		
	SM 10 %	20	12.4 ± 2.5		
1	Placebo	20	13.8 ± 1.9	+ 2.5	0.018*
	SM 2 %	20	10.8 ± 1.3	- 1.2	0.050
	SM 5 %	20	12.8 ± 1.5	+ 4.1	0.038*
	SM 10 %	20	13.0 ± 2.0	+ 6.1	0.044*
24	Placebo	20	13.9 ± 2.0	+ 0.86	0.049*
	SM 2 %	20	10.1 ± 2.0	- 7.8	0.082
	SM 5 %	20	11.2 ± 1.9	- 10.1	0.047*
	SM 10 %	20	10.6 ± 2.2	- 14.9	0.016*

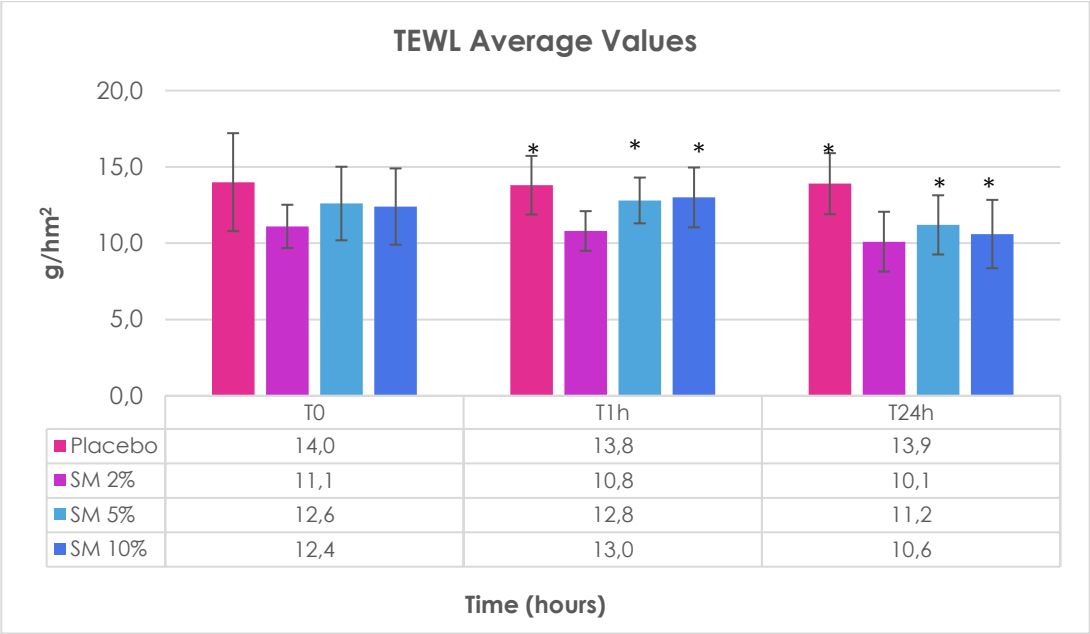

	T0	T1h	T24h
Placebo	14,0	13,8	13,9
SM 2%	11,1	10,8	10,1
SM 5%	12,6	12,8	11,2
SM 10%	12,4	13,0	10,6

Figure 1.4. TEWL Average Values after a single SM cream topical application. *$p < 0.05$

Results show that after 1 hour, only the 2 % SM cream lowers TEWL values by - 1.2 %, and this trend is confirmed after 24 h when a - 7.8 % decrease is registered. In comparison, the 5 and 10 % SM creams show action on the transepidermal water loss only after 24 hours by their application, when a statistically significant percentage decrease is highlighted. Placebo cream has no efficacy in the recovery of the skin barrier.

1.5.2.2 Skin hydration

Corneometer® CM 825 is the most used device to evaluate the hydration level of the stratum corneum, the upper layer of the skin.

The average values registered at the different measuring times (T_0, T_{1h}, and T_{24h}) for each tested product are reported in Table 1.7 and represented in Figure 1.5.

Table 1.7. Corneometry Measurements after a single SM cream topical application. *$p < 0.05$

Time (h)	Cream type	Nr. of Volunteers	TEWL average values (g/hm^2)	Variation compared to baseline (%)	*p*
0	Placebo	20	35.7 ± 6.8		
	SM 2 %	20	32.9 ± 4.6		
	SM 5 %	20	31.7 ± 5.8		
	SM 10 %	20	32.2 ± 6.8		
1	Placebo	20	37.2 ± 7.6	+ 5.8	0.050
	SM 2 %	20	36.2 ± 4.3	+ 11.1	0.025 *
	SM 5 %	20	35.5 ± 5.2	+ 15.3	0.035 *
	SM 10 %	20	36.4 ± 7.9	+ 15.2	0.049 *
24	Placebo	20	35.7 ± 6.9	+ 1.8	0.031 *
	SM 2 %	20	37.9 ± 5.2	+ 15.8	0.0026 **
	SM 5 %	20	35.2 ± 5.4	+ 12.8	0.050
	SM 10 %	20	38.2 ± 8.3	+ 20.3	0.017 *

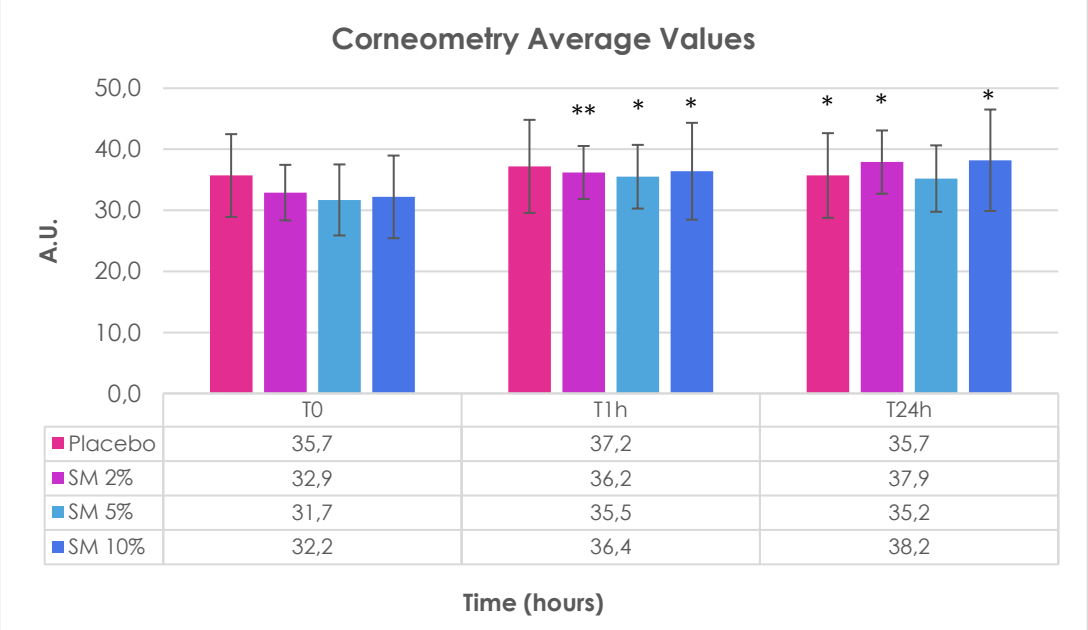

Figure 1.5. Corneometry Average Values after a single SM cream topical application. *$p < 0.05$, **$p < 0.01$

Corneometry data tell us that all SM creams increase skin hydration after 1 and 24 hours. The highest percentage increase is obtained with the 10 % SM cream, suggesting that the high concentrations of the snail mucin bioactive molecules influence the skin water content. After one hour, there are similar results for both 5 and 10 % SM cream, but also suitable for the 2 % cream, showing that this lower SM concentration results enough to satisfy consumer expectations. Placebo cream also shows hydrating efficacy but is lower than active creams.

1.6 Discussion

Allantoin and glycolic acid were analyzed in 3 different snail mucus batches (at concentration of 1 mL mucus/10 mL buffer solution). Both compounds are highly polar molecules that interact with end-capping (as it happens with Vision HT C18 High Load column silica column) mainly via H-bonding.

The effect of mobile phase pH was studied associated with the retention time, peak height, and shape. Buffer solutions of different pH values were prepared by adding phosphoric acid 0.1 M to 10 mM NaH_2PO_4.
According to El Mubarak et al.[9] the optimal mobile phase pH was 2.7, comparing the curves in the resulting pH/time plots. Increasing the mobile phase concentration to 20 mM NaH_2PO_4 did not determine a change in peak shape and analytes' retention time. Three different flow rate values for the mobile phase (0.5, 0.7, and 1.0 mL/min) were tested. The value of 1 mL/min determined an excellent separation.

To validate the analytic procedure, method linearity was detected: the constant addition method was used to construct calibration curves. The correlation coefficient of the linear regression line is considered linear in the range studied because it is approximately 1 (R^2 glycolic acid = 0.9926; R^2 allantoin = 0.9972). Successively, was found the lowest amount of analyte in the sample (relative standard deviation < 15 %), the accuracy (relative error < 20 %), and the method precision under the same operating conditions over a short interval of time. Method validation showed high recovery, precision, and sensitivity.

After one hour by the SM creams application, the trans epidermal water loss does not change significantly, maintaining levels close to the baseline.
After applications of SM cream 5 % and 10 %, TEWL values increased much.
In low concentration, glycolic acid is believed to facilitate progressive weakening of cohesion of the stratum corneum intercellular material, resulting in uniform exfoliation of its outermost layers[11] and evaporation of the matrix water. Instead, we note a decrease in TEWL values immediately after 2 % snail mucus cream application.
After 24 hours, the water is regenerated and accumulated in the inter-corneocyte spaces creating a more compact hydrolipidic film as shown by the significant decrease of the TEWL for all three active formulations (at 2 %, 5 %, 10 %).

Regarding the results of corneometry, all formulations, with increasing concentration of SM, immediately after applying the tested cream, determine a highly statistically significant (p = 0.0026 - 0.050) improvement in hydration. This result may be due to allantoin in the snail mucus, an extremely moisturizing substance. In addition, snail mucus by itself has a moisturizing action capable of supporting the effect of allantoin.

1.7 Conclusions

A snail mucus cosmetic cream with moisturizing properties was formulated. The amount of mucus added was evaluated according to allantoin and glycolic acid content in *H. aspersa Muller* mucus of common Campania land (Italy), and TEWL and corneometry measured skin hydration. An HPLC method developed and validated according to the European Commission Decision 2002/657/EC allowed quantifying glycolic acid (3.35 g/L) and allantoin (0.41 g/L) in the mucus. A cream containing mucus (2 %) gives a desirable moisturizing action.

CHAPTER 2

Sebum production and skin inflammatory response modulated by *Cirsium eriophorum* cell culture extract

2.1 Introduction

Excess sebum secretion, a slackening of the pore wall, and an abnormal keratinization process cause pores to widen.[12]

In dermo-cosmetology, pore refers to the openings of the adnexa at the skin surface. It can be applied to the sudoriparous glands hole, which secretes sweat and eliminates toxins from the body and the orifices of the hair follicles (Figure 2.1).

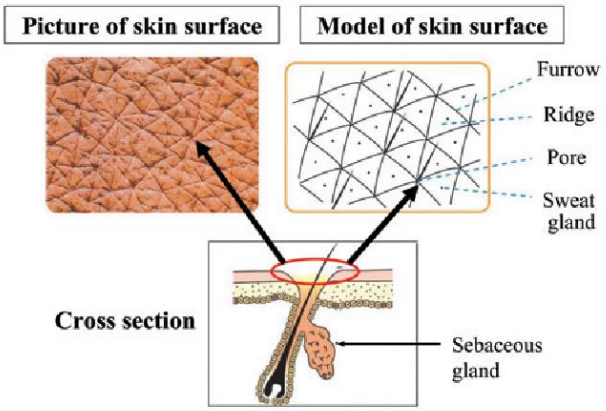

Figure 2.1. Model of a pore (Cosmetic&Toiletries, Feb 17th, 2009. Improving the Appearance of Facial Pores)

Enlarged facial pores are crucial cosmetic worries, as they are often associated with comedones, pustules, papules, and cysts [13].

They represent an easy way-in for harmful or potentially pathogenic aggressors, leading to local inflammatory reactions [14].

Pore widening is influenced by many exogenous and endogenous factors. Indeed, pore dilation is often associated with skin shininess problems. A high level of sebum production by the sebaceous gland leads to widening the pore associated with the gland [15], particularly in the nasal area.

Shiny skin, irritation, and a feeling of discomfort are the primary physiological effects of hyper-seborrhoea. Since excess sebum is a factor favoring pore dilation, a treatment targeting the reduction of seborrheic secretion would benefit from attenuating their dilatation (Figure 2.2). [16]

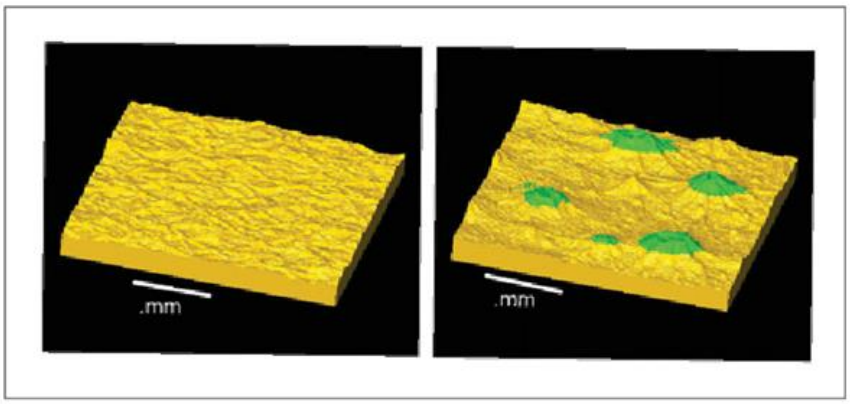

Figure 2.2. Skin replicas of inconspicuous facial pores (left) and conspicuous facial pores (right) with large pores shown in green

The visible pore numbers increase up to the 40s, whereas the activity of the sebaceous glands diminishes with age. Factors other than sebum thus seem to be involved in pore dilation.

The loss of collagen and elastin (matrix components) results in pore wall slackening and modifications of characteristic structures located only in the area of dilated pores (stalagmite structures) are observed with age (Figure 2.3).[17,16]

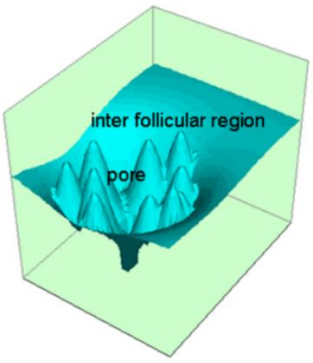

Figure 2.3. Epidermal-dermal 3D junction around a pore (the stalagmite-like structure)

In young skin, pores are visible mainly in the nasal and forehead areas, the primary cause of their dilation being excessive sebum production. In women's 40s, the pores appear recessed and distorted because of skin slackening, above all on the cheeks.[17]

Finally, the third factor in pore dilation seems to be related to an abnormal accelerated keratinization process leading to the accumulation of nucleated cells around the pores (Figure 2.4).[14]

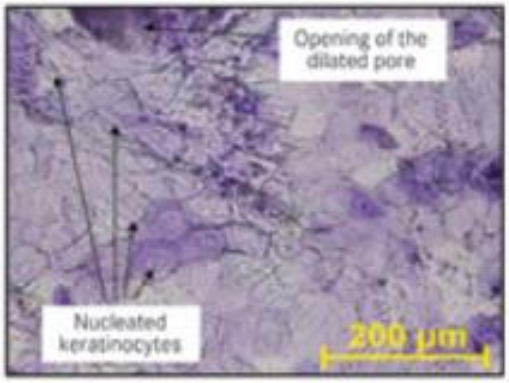

Figure 2.4. Nucleated keratinocytes around the opening of the dilated pore

The physiology of the corneocytes located around dilated pores has shown that they are frequently surrounded by nucleated cells compared to non-dilated pores.[14]
The presence of cells that have abnormally retained their nucleus when they arrive on the skin surface indicates parakeratosis, which is accelerated and incomplete keratinization of keratinocytes to corneocytes. Parakeratosis can be caused by conditions like inflammation, certain stimuli, or the abundance in the sebum of unsaturated fatty acids such as oleic acid.[18]

Keratinocyte differentiation must be stimulated, promoting the nucleated cells renewal around dilated pores by new mature corneocytes.

Therefore, minimizing the facial pore size and decreasing sebum secretion are the most desired targets to treat oily and acne-prone skin.
This study proposes a natural active ingredient, *C. eriophorum* cell culture extract, targeting the leading causes of the dilated pore appearance:

- Target 1 : Excess sebum secretion
- Target 2 : Pore wall slackening
- Target 3 : Abnormal keratinization process

The first target was achieved acting on the enzyme 5α-reductase, associated with sebum formation and secretion [19].
Target 2 acting on trypsin-like serine proteases Kallikrein 5 (KLK5), linked to physiological peeling and removal of pore-clogging dead skin cells [20]; and the third one stimulating human fibroblasts responsible for building the skin scaffold and for keeping it firm and strong.
The in vitro tests were corroborated by a single-blind clinical trial on healthy human volunteers on the in vivo performance of the investigated active ingredient.

2.1.1 *Cirsium eriophorum*

Cirsium eriophorum (Figure 2.5), also known as Wooly thistle, is a biennial plant belonging to the Asteraceae family.
It originates in Central Europe and is found up to 2100 meters above sea level in the Alps, in dry and calcareous soils, paths, pastures, and uncultivated fields.
It is 50-150 cm high and has a stem whose hypogeal or underground part is a large rhizome while the epigeal or aerial part is slightly branchy with a cylindrical section with the surface striated and covered by a white-tomentose down.
The leaves are large, green, sessile, pinnate-matched, thorny with bristly and bristly hairs.

Figure 2.5. *Cirsium eriophorum*

The inflorescence is formed by a large and globular terminal flower head with bracteal patent leaves that do not exceed the flower head, which is provided with an ovoid or pyriform envelope with short apical spines of the restiform scales and with dense fluffy-felted hairs, which give rise to an external checkerboard or rhombic appearance. From this envelope, the tubular and hermaphrodite flowers, of a purple-red color, come out in the form of a large brush and, once ripe, release silky pappi, destined to release the seeds (achenes).

The fruit of *Cirsium eriophorum* is an achene surmounted by a thick pappus of feathery hairs. Pollinating agents are moths and bees.

Between June and September, the plant blooms in summer at an altitude of 2000 m and also tolerates the winter temperatures of the Alps well, surviving at - 20 ° C.

2.1.1.1 *Cirsium eriophorum* : chemical properties

Plants belonging to the genus Cirsium have been widely used in food and biomedical applications due to their content of active phytochemicals, such as flavonoid glycosides, phenolic acids, sterols, triterpenes, and lignans [24], with antimicrobial, anti-inflammatory activities and antiphlogistic [25,26].

Cirsium eriophorum extract is a potential dermo-cosmetic active ingredient from cell suspension cultures containing phenolic and polyphenolic compounds.

Polyphenols are organic molecules produced by the secondary metabolism of plants, fungi, and animals and are of considerable importance in the food, pharmacological and cosmetic fields.

The main functions of these chemical compounds are:

• Antioxidant: protect cells from free radicals damaging process and cellular aging caused by smoke, pollutants and UV rays, viral attacks, and physical stress;

• Anti-inflammatory: they protect cells from oxidative stress and have properties that control cholesterol levels;

• Anti-carcinogenic: they show a positive impact in the early stages of cancer development, protecting cells against the attack of carcinogens, especially concerning some forms of cancer such as that of the skin;

• Antibacterial, antipruritic, antiparasitic and cytotoxic;

• Anti-teratogenic: they limit the oxidation of lipids and LDL particles, which are mainly responsible for arteriosclerosis, stroke, and cardiovascular disease.

Among the phenolic compounds present in the extract of Cirsium eriophorum, there is chlorogenic acid, chemically known as 3-caffeoylquinic acid; it is a natural organic substance, an ester that is obtained from the reaction of caffeic acid with (L) -quinic or quinic acid; it has an antioxidant power comparable to that of caffeic acid, but lower than that of di-hydrocaffeic acid. Thanks to its antioxidant and anti-inflammatory properties, caffeic acid is often found in skincare regimens, and studies show promising results, such as the reduced formation of wrinkles induced by UVB irradiation or the inhibition of oxidative stress.

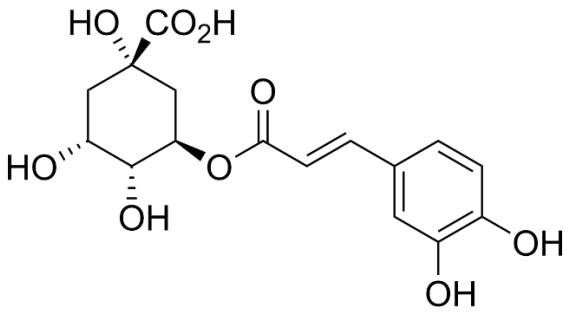

Figure 2.6. Cholorogenic acid (3-caffeoylquinic acid)

2.1.1.2 *Cirsium eriophorum* : functional properties

Cirsium eriophorum is a poorly held plant for its insidious thorns, but its root has diuretic, detoxifying, hepato-stimulating, and sweating properties. It is

used in the therapeutic field to treat urinary stones, water retention, joint and muscle pain of rheumatic origin, colds, and flu.

It is an edible plant: the receptacle is used in human nutrition.

This study, aimed at evaluating both in vitro and in vivo the sebum-balancing / skin-purifying action of the extract, demonstrates its ability to reduce the expression and activity of essential markers associated with sebum production and pores enlargement. Skin cells, in particular the 5α-reductase enzyme, and inhibit the expression of pro-inflammatory mediators in skin cells.

The extract effectively improves the functionality of the epidermal barrier, restoring an average level of sebum, and reducing pore size, thus proposing itself as a potential dermo-cosmetic ingredient helpful in relieving complications related to acne-prone seborrheic skin.

2.2 Study design

Plants of the genus *Cirsium* (family of Asteraceae) have been extensively used in biomedical applications [25], due to their content of active phytochemicals, with known antimicrobial, anti-inflammatory, and antiphlogistic activities [26-28].

C. eriophorum cell cultures are obtained by inducing the proliferation of meristematic leaf were transmitted in cosmetic formulations and, after a chemical characterization, tested in vitro on skin cell cultures and in vivo on oily acne-prone skins to demonstrate a pore-refining and sebum-regulating activity.

CeCCE samples were chemically analyzed by the UHPLC-Orbitrap platform in MS and MS/MS levels to investigate and dose their phenolic profile.

Then, the water-soluble extract derived from *C. eriophorum* cell cultures was tested in vitro through the following essay :

- 5α-Reductase (5α-R) activity inhibition
- Kallikrein 5 (KLK5) expression increase
- Pro-inflammatory cytokines negatively modulation
- Collagen synthesis increase

5α-reductase plays a central role in sebum production; the trypsin-like serine protease Kallikrein 5 promotes skin exfoliation and antimicrobial response. Both are essential markers associated with hyperseborrhea and pore slackening.
Hence, it is crucial to investigate the natural extract's ability to fight them, guaranteeing a pore minimizing refining effect and a diminished sebum secretion. Meanwhile, the fibroblast stimulation can fight pore wall slackening, and the negative modulation of pro-inflammatory cytokines helps to turn off possible exacerbations.
The trial was performed by the skin analysis laboratory of the University of Naples Federico II, Pharmacy Department, under Professor Sonia Laneri, in the same conditions as for the study on *Helix aspersa* mucus. The effect of CeCCE was assessed by clinical evaluation of many skin parameters involved in dilated pores before and after four weeks of twice-daily treatment.
Tested in comparison with a placebo, CeCCE formulated at 0.5 % in emulsions which formulation was indicated by VitaLab Srl and kept in secrecy according to the agreement stipulated between University and the company.
The protocol used in the single-blind study has provided TEWL, Corneometry, Sebumetry, and Porosity measurements on twenty female volunteers between 20 and 40s with combination, oily acne-prone skin.
Readings occurred at different times: baseline (D_0), after two weeks of treatment (D_{14}), and after four weeks of treatment (D_{28}).
Measurements got using peer-reviewed skin analysis devices :

- Tewameter® TM 300
- Corneometer® CM 825
- Visioscope® PC 35 equipped with Sebufix® F16
- VisioFace® 1000 D

All tools are from C+K electronic GmbH, Köln, Germany.

The TEWL and corneometry are directly related to the skin's healthy state in terms of hydration and moisture, as thoroughly previously illustrated (Cap. 1, par. 1.2).
Sebumetry is used to quantify skin fat, i.e., the quantity of sebum that comes out of the follicular pore.
The total amount of superficial skin lipids is measured with the Sebometer (Visioscope® PC 35). It is a videocamera with polarized parallel or circular light

equipped with stickers (Sebufix® F16) placed on the volunteers' faces to analyze the skin's sebum in a semi-quantitative way.

The principle of measurement is based on the fact that lipids present in the investigation area form spots on the particular opaque film of the adhesive: the sebum present is visible as black spots in its micro-pores.

Under normal conditions, this lipidic material protects the skin from dehydration. It performs a slight antibacterial action, while in conditions of increased activity of sebaceous glands, this hyperfunction is concretized in its excessive production due to various imperfections and skin alterations, often representing the prelude of the acne.

The quality-quantitative analysis of the pores is carried out using the VisioFace® 1000 D equipped with Canon EOS series camera, over 10 Megapixels with 210 White light LEDs lighting.

In every square centimeter of skin, there are about 150 pores: they connect the glands to the surface, which, more deeply, produce sebum to form the hydrolipidic layer. In perfectly balanced situations, the pores have a diameter of about 50 microns, and this ideal dimension can be compromised (dilation) by some factors.

The driest and normal skins are less at risk, while the fatter and combination skin are more exposed because they tend to have larger pores and produce more sebum.

Pore obstruction with keratin mixed with excess sebum is responsible for the appearance of blackheads.

In assessing the sebum-normalizing, mattifying, and pore-refining action, it is good to quantify the pore number and diameter, the amount of sebum present, and check the healthy skin state.

All results were presented as means ± standard deviations (SD) of three independent experiments, and a paired-samples t-test was conducted considering a *p*-value lower than .05 statistically significant.

2.3 Materials and Methods

2.3.1 Plant tissue cultures and extract preparation

Cell cultures were obtained by C*. eriophorum* plants (Plant World Seeds, Devon, UK) by inducing the proliferation of meristematic leaf cells on solid agar plates until obtaining calluses.

The cells were transferred to the liquid growth medium (Gamborg B5 medium, supplemented with 500 mg/L myo-inositol, 30 g/L sucrose, and phytohormones) and grown as suspension cultures at 27°C in the dark under orbital shaking. Once the cultures of about 300 g/L were obtained, the cells were collected and lysed in a phosphate buffer at pH 7.4 to prepare a water-soluble extract, which was lyophilized (**CeCCE**). The powder was dissolved in water or cell culture media at the appropriate concentrations for testing.

2.3.2 Chemical analysis

In a 1% TFA water solution samples of CeCCE were dissolved and the resulting solution analyzed by Liquid Chromatography-Mass Spectrometry (LC-MS/MS).

High-resolution mass spectrometer based on Orbitrap technology (Q-Exactive, ThermoFisher, Bartlesville) and connected to an EASY-Spray source a UHPLC (Ultra-High-Performance Liquid Chromatography; UltiMate 3000 UHPLC, ThermoFisher Dionex, Bartlesville) was interfaced.

The samples loaded onto an EASY-Spray analytical column (15 cm x 75 µm ID PepMap RSLC C18, 3 µm, 100 Angstrom; Thermo Scientific, Bartlesville) with 0.1% formic acid in water (solvent A) at a flow of 300 ml/min, were previously desalted using a 0.1% formic acid solution on a C18 PepMap 100 precolumn (Thermo Scientific, Bartlesville).

Increasing concentration of solvent B (acetonitrile/0.1% formic acid) were used for the elution of column. Operating in positive ion mode with a vaporization temperature of 350 °C, a capillary temperature of 280 °C, and a capillary voltage of 1.9 kV mass data (MS) and MS/MS were acquired. By selecting, with a dynamic exclusion range of 15 s, the most intense five ions (isolation window 1.0 m/z, stepped collision energy 20, 40) the mass spectrometer was set in data-dependent acquisition mode. The ions selected for this set were the one with a single and double charge.

Compounds fragmentation MS/MS datas were analyzed in triplicate and processed to identify the metabolites using the Compound Discoverer 2.1 Software (ThermoFisher, Bartlesville)

2.3.3 Cell cultures

Derived from immortalized keratinocytes HaCaT (AddexBio Technologies, San Diego, CA) and from neonatal foreskin, Human Dermal Fibroblasts (HDF, Cell Applications, Inc., San Diego, CA) were maintained supplemented at humidified atmosphere at 37 ° C, 95 % air and 5 % CO_2 with 10 % of fetal bovine serum in DMEM. Medium supplemented with Human Keratinocyte Growth Supplement in a 95 % air, 5 % CO_2, and humidified atmosphere at 37° C was used for maintaining Human Epidermal Keratinocytes (HEK, Gibco/Life Technologies, Carlsbad, CA) in EpiLife.

2.3.4 5-alpha reductase activity

8 x 10^3 HDF were treated for 24 hr with 100 nM CeCCE plus testosterone, after seeding in 96-well plates.
As a positive control, a 10 nM concentration of synthetic aza-steroid Finasteride was used. The supernatants were collected and stored at 4 ° C for analysis after the treatment.
Using 20 ng/ml BSA-conjugated dihydrotestosterone (BSA-DHT) in Na_2CO_3 50 mM, pH 9.0, at 4 ° C multiwell plates were coated. Then incubation of the multiwell plates with 50 µl of biotin conijugated anti-DHT primary antibody (Cloud-Clone Corp. CCC) dissolved in 1 % Bovine Serum Albumin (BSA) containing PBS, and 50 µl of cell supernatant, after a previous washing with phosphate buffer (PBS) was performed. 2 hr after, incubation of the plates with peroxidase in PBS containing 1 % BSA with 5 µg/ml of streptavidin-conjugated Horse Radish was conducted as following a three times wash. By the absorbance at 490 nm the color developed by a 0.5 mg/ml solution of O-Phenylene Diamine (OPD) in 0.012 % H_2O_2 was measured[29].
Expressed as percentages the reported values were the means of the three independent experiments. In these as calculated by the paired-samples t-test the observed differences were statistically significant.

2.3.5 Gene expression analysis of cytokine genes

In a 6-well plates, were seeded and treated for 16 hr with RA 1 μM or CeCCE 1.5 x 10^5 HaCaT.

Parallelly, were grown until OD = 0.45 cultures of Staphylococcus epidermidis cells (NCTC 11047 - Sigma Aldrich, Germany) overnight.

Then to the keratinocyte cultures (1:20 dilution in the cell culture medium), were added and incubated, for about additional 3 hr, 1 x 10^8 Staphylococcus epidermidis cells.

Next the total extracted with GenElute Mammalian Total RNA Purification Kit (Sigma-Aldrich, Milano, Italy) RNA, was treated with deoxyribonuclease (DNAse) I (Thermo Fisher Scientific, Dallas, TX) for 30 min at 37 ° C.

Using the RevertAid First Strand cDNA Synthesis Kit (Thermo Fisher Scientific, Dallas, TX) reverse transcription was performed.

Reduced amplified 18_S rRNA product within the range to be used as endogenous standard were obtained by mean of a Semi-quantitative PCR performed using Quantum RNA kit (Thermo Fisher Scientific) containing competimers and primers to amplify 18_S ribosomal RNA (18S rRNA).

Specific oligonucleotides were used for conducting the amplification reactions:

- IL-1αRev: TGTAATGCAGCAGCCGTGAG;
- (IL-1αFor: ATGGCCAAAGTTCCAGACAT;
- IL-1βRev: AAGGACATGGAGAACACCAC;
- IL-1βFor: ATGGCAGAAGTACCTGAGCT;
- IL-8Rev: CTCTTCAAAAACTTCTCCACAACC;
- IL-8For: GCCACCGGAGCACTCCATAA;
- TNFαRev: TCATACCAGGGCTTGGCCTCA)
- TNFαFor: ATGAGCACTGAAAGCATGATCC;

2′ at 94 ° C followed by 35 cycles of 94 ° C for the 30 s, 50 ° C for 30 s, and 72 ° C for 30 s, with a 10 min final extension at 72 ° C was the general scheme in the Mastercycler ProS (Eppendorf, Milano, Italy).

Subsequently, with the Geliance 200 Imaging system (Perkin Elmer, Woodbridge, Ontario, Canada), after the PCR products were loaded on 1.5 % agarose gel, amplification bands were quantified and visualized.

The analyzed gene corresponding amplification band was reported as a percentage of bacteria treated cells (set as 100%; Wang, Bell, Keeney, & Strobel, 2010) after being normalized to the 18S corresponding amplification band. the reported values are the means of three independent experiments and the observed differences showed as calculated by the t-test paired-samples to be statistically significant.

2.3.6 Gene expression and activity of Kallikrein 5

1.5×10^5 HEK were treated for 6 hr with RA 1 μM or CeCCE for KLK5 gene expression analysis using a 6-well plates for the seeding.
The GenElute Mammalian Total RNA Purification Kit (Sigma-Aldrich) was used to extract the total RNA from the cells collected after the treatment.
As described above the RNA was subsequently processed for the cytokine gene expression analysis. KLK5For: ATCACAGCCTTGCTTCTG and KLK5Rev: GACCTTAGGGAAGTGCACT were the oligos used in this amplification reactions.
To induce cell differentiation in the presence or not of the extractor 1 μM RA for KLK5 activity evaluation, at confluency 1.2 mM $CaCl_2$ was added to a 6-well plates with the cell already seeded in them.
48 hr later, at pH 8.0, in 50 mM Tris–HCl + 50 mM $CaCl_2$ with 1 mM Na-Benzoyl-d,l-arginine 4-nitroanilide hydrochloride (DL-BAPA, Sigma-Aldrich), the cell culture media were incubated aftere being collected.
The absorbance at 410 nm was measured 72 hr after incubation at 37 ° C. The values reported in the graph, means of three independent experiments, were expressed as percentages compared to $CaCl_2$ treated cells.

2.3.7 ELISA assay for collagen measure

8×10^4 HDF were seeded and 24 hr-treated in a 6-well plates with the cell extract or (transforming growth factor-beta) TGFβ 2.5 ng/ml as the positive control, to determine Pro-Collagen I production.
The cells were washed three times with the "ELISA buffer" (PBS 1x, 0.5 mM $CaCl_2$, 1 mM $MgCl_2$, 0.1 % Triton X100) after being fixed in 4 % paraformaldehyde for 10 min were treated with 3 % of BSA for 30 min in ELISA buffer after an even earlier previous washing in Phosphate-buffered saline (PBS; Thermo Fisher Scientific).

The amount of Procollagen I was measured by a colorimetric reaction, using 0.35 mg/ml solution of OPD (Sigma-Aldrich, Milano, Italy) and 0.012 % H_2O_2 in 50 mM citrate buffer (di Martino et al., 2017) added to the cells incubated with the anti-mouse secondary antibody (Biorad, CA) for 1 hr, as following a wash after a 2 hr incubation with the primary antibody (sc-166,572, Santa Cruz Biotechnology, Dallas, TX) at room temperature.

The values, which represented the means of three independent experiments, were reported as percentages to the untreated control (set as 100%). As calculated by the paired-samples t-test the observed differences were statistically significant.

2.3.8 In vivo studies

The test was made according to the principles of the Helsinki Declaration (1964) and subsequent revisions endorsed by the European Community (fourth revision, called Somerset West, South Africa, 1996; Saunders & Wainwright, 2003) and according to the Colipa Guidelines for the evaluation of the efficiency of cosmetic products (May 2008).

2.3.8.1 Apparatus

TEWL and skin hydration were measured with a Tewameter TM 300 Probe and Corneometer CM 825.

Sebum secretion was obtained by Visioscope PC35 equipped with Sebufix F16, while for pore counting and type, we used a VisioFace 1000D connected to the Software CSI (Complete Skin Investigation).

Instruments and software are from C+K electronic GmbH, Köln, Germany.

2.3.8.2 Cream composition

The CeCCE cream contained: Phase O (*Triticum Vulgare germ oil* 5.0 %); Emulsifiers (Cetyl alcohol 2%, Polyglyceryl-3methylglucose distearate 5.0 %, Cetearyl alcohol 3.0 %); Phase W Aqua (q.b to 100); Cirsium extract (0.5 %); Preservants (Potassium sorbate, sodium benzoate 0.5 %) and Parfum (0.1%). The placebo cream contained all these components without CeCCE. All the ingredients were bought from ACEF Spa (Fiorenzuola D'Arda, Italy) and Parfum by Farotti Srl (Rimini, Italy).

The creams (active and Placebo) were prepared, shaking vigorously the oil phase (O) at 70 °C with the aqueous phase, heated up to the same temperature, by a Silverson L5M-A Laboratory Mixer.
Subsequently, the cream was cooled in an ice bath, and the remaining components were added at room temperature.
The pHmeter Crison GPL20 measured the cream's pH, and they were 5.5 – 5.4; the viscosity of both the creams (CeCCE and Placebo) was 29.254 – 30.156 mPa (L4, 20 rpm) and was calculated by a rheometer Visco Basic Plus, Fungilab Sa.

2.3.8.3 Test conditions

Skin biophysical parameters were detected in a chamber (T = 25 ± 2 ° C; relative humidity 40 ± 5 %), after an acclimation period of approximately 30 min, at the beginning (D_0), after two weeks (D_{14}), and after four weeks (D_{28}) of twice-daily treatment with the test product (2 mg/cm^2).

2.3.8.4 Volunteers selection

A panel of 40 volunteers, aged 20 to 40, with combination or oily skin, applied a dermo-cosmetic cream containing 0.5 % p/p plant extract or the corresponding Placebo twice daily for four weeks on faces.
Biophysical parameters were monitored over 2 and 4 weeks of product use.
Volunteers were selected based on inclusion and non-inclusion specific criteria and on their ability to respect the constraints required by the protocol.
According to the Helsinki Declaration of ethical principles for medical research, all volunteers signed an informed consent sheet and claimed not to be allergic to the dermo-cosmetic cream components.
Each volunteer had a card with the instruction for dermo-cosmetic cream use and, at the end of the study, answered a questionnaire to determine product compliance.

2.3.8.5 Inclusion and exclusion criteria

The subjects included in the study were females and males aged between 20 and 40 with phototype I-IV (Fitzpatrick Scale), with combination or oily skin, impure and acne-prone skin, in functional health status, without systemic pathologies. The volunteers do not apply products other than those studied

on the test sites seven days before and during the study period. In this study, pregnant or lactating women, subjects with a history of skin hyper-reactivity or reactions of intolerance to cosmetic products/ingredients, affected by skin diseases (eczema, psoriasis, lesions), subjects with photosensitivity, overexposed to intensive sunlight (natural or artificial) the month preceding the study or expected to be exposed to UV rays during the study period, were excluded.

2.4 Statistical analysis

All the in vitro experiments were conducted in triplicates and repeated three times. The results were presented as means ± standard deviations (SD) of three independent experiments.

A paired-samples t-test was conducted using the GraphPad QuickCalcs Website: https://www.graphpad.com/quickcalcs/ttest1.cfm; a *p*-value lower than .05 was considered statistically significant.

For the in vivo tests, statistical tests were performed using SPSS software 15.0 for Windows (SPSS Science, Chicago, IL). Student t-test was assessed. A *p*-value <.05 was considered significant.

2.5 Results

2.5.1 Chemical characterization of *C. eriophorum* cell culture extract and phenolic quantification

The most abundant phenols present in the CeCCE extract were identified (Table 2.1) and quantified by LC-HRMS (Orbitrap) analysis. Thirteen phenolics, including nine phenolic acids, three caffeoylquinic acids derivatives, and two di-caffeoylquinic acids, were identified.

Table 2.1. Validation parameter for phenolics analysis by UHPLC–MS/MS

Phenolic compounds	RT (min)	Formula	Theoretical m/z	Experimental m/z	Calculated errors Δppm	LC/MSn data (%base peak)
Phenolic acid						
Caffeic acid	4.65	$C_9H_7O_4$	179.0338	179.0332	-3.2	MS^2[179] 135.0451 (100)
Caffeic acid glucosidic derivatives	1.55	$C_{15}H_{18}O_9$	341.0866	341.0877	0.40	179.0345 (100), 135.0400 (10)
p-Coumaric acid	9.71	$C_9H_{10}O_5$	163.04007	163.04028	1.29	119.05023
Sinapinic acid hexoside	6.29	$C_{17}H_{22}O_{10}$	385.1128	385.1139	0.11	223.0610 (100), 208.0400 (20),179.0698 (10)
Ferulic acid hexoside	6.42	$C_{16}H_{20}O_9$	355.123	355.1034	0.10	93.0507 (100), 178.0280 (10)
Protocatechuic acid	2.45	$C_7H_6O_4$	153.183	153.0193	0.06	109.0292 (100)
Hydroxybenzoic acid	2.88	$C_7H_6O_3$	137.02442	137.02458	1.17	93.03431
Gallic acid	7.55	$C_7H_7O_5$	169.01425	169.01639	3.81	
Caffeoylquinic acids						
5-O-caffeoylquinic acid	4.94	$C_{16}H_{17}O_9$	353.0867	353.0875	0.7	MS^2[353] 191.0557(100),179.0343 (7), 173. 0450 (5)
1-O-caffeoylquinic acid	4.27	$C_{16}H_{18}O_9$	353.0867	353.0877	0.2	191.0555 (100), 179.0343 (10)
3-O-caffeoylquinic acid (chlorogenic acid)	2.68	$C_{16}H_{17}O_9$	353.0867	353.0877	0.2	MS^2[353] 191.0548(100),179.0338 (46), 135.0443(7))
Dicaffeoylquinic acids						
1.5-O-dicaffeoylquinic acid	15.53	C25H23O12	515.1184	5151.1176	-1.54	MS^2 [515]: 353.0853(100), 191.0552(5), 179.0342(5
4.5-O-dicaffeoylquinic acid		C25H23O12	515.1184	515.1182	-0.3	MS^2[515] 353.0865(100)

Validation parameters for the quantification of the phenolics by UPLC are explained in Table 2.2. The caffeoylquinic acid derivatives were the most representative class of phenols, and the chlorogenic acid, the most concentrated phytochemicals in the extract (Table 2.3).

Table 2.2. Validation parameter for phenolic analysis by UHPLC–MS/MS

Phenolic compounds	**Linearity** (mg/g)	**R^2**	**LOD** (mg/g)	**LOQ** (mg/g)	**RSD %** (*n* = 3), (50 mg/g)
Phenolic acid					
Caffeic acid	0.5 - 2	0.998	0.542	2.50	1.19
Caffeic acid exoses	3 – 4	0.995	3.147	3.781	1.24
Coumaric acid	0.1 - 1	0.998	0.207	0.822	0.9
Sinapinic acid hexoside	0.1 - 3	0.991	0.105	0.458	1.17
Ferulic acid hexoside	0.01 – 0.1	1.000	0.012	0.092	1.27
Protocatechuic acid	1 - 5	0.912	3.5	5.236	1.24
Hydroxybenzoic acid	1 - 5	0.991	0.100	2	1.8
Gallic acid	1 - 5	0.991	0.994	1.526	1.52
Caffeoylquinic acids					
1-O-caffeoylquinic acid	5 - 13	0.992	11.983	12.578	1.22
3-O-caffeoylquinic acid	1 - 120	0.991	102.321	104.567	1.19
Dicaffeoylquinic acids					
1.5-O-dicaffeoylquinic acid	1 - 3	0.991	0.45	3.567	1.23
4.5-O-dicaffeoylquinic acid	3 - 5	0.991	4.231	5.012	1.21

Table 2.3. Polyphenols composition of CeCCE

Compound	**Concentration CeCCE** (mg/g of powder)
Phenolic acid	
Caffeic acid	1.81
Caffeic acid exoses	3.41
Coumaric acid	0.61
Sinapinic acid hexoside	0.26
Ferulic acid hexoside	0.08
Protocatechuic acid	4.70
Hydroxybenzoic acid	1.55
Gallic acid	1.23
Caffeoylquinic acids	
1-O-caffeoylquinic acid	12.39
3-O-caffeoylquinic acid (chlorogenic acid)	103.34
Dicaffeoylquinic acids	
1.5-O-dicaffeoylquinic acid	2.16
4.5-O-dicaffeoylquinic acid	4.77

2.5.2 In vitro studies

2.5.2.1 5α-reductase activity

Pore dilation in oily and acne-prone skins is often associated with sebum overproduction, which is, in turn, regulated by the activity of the enzyme 5α-Reductase (**5α-R**).

The 5α-R activity was first induced in human dermal fibroblasts by testosterone 100 nM. Then the cells were treated with CeCCE at two concentrations and with the compound (5α,17β)-(1,1-Dimethylethyl)-3-oxo-4-aza-androst-1-ene-17-carboxamide, a 5α-R inhibitor, known as Finasteride

(Rattanachitthawat, Pinkhien, Opanasopit, Ngawhirunpat, & Chanvorachote, 2019), as a positive control.

Significant inhibition of the testosterone-induced enzymatic activity was produced by CeCCE 0.002 % (52.2 %) and 0.01 % (44.5 %), even more potent than those obtained with Finasteride (Figure 2.6).

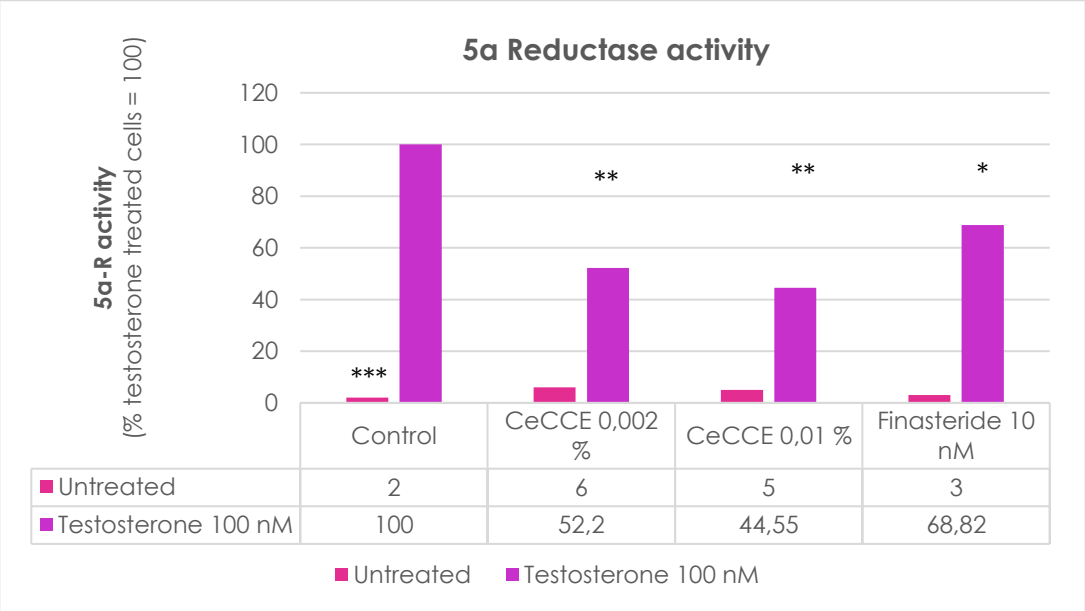

Figure 2.6. 5α Reductase activity. The error bars represent standard deviations; all the measures are statistically significant (*$p < .05$; **$p < .01$; ***$p < .001$)

2.5.2.2 Kallikrein 5 activity

We analyzed the involvement of CeCCE in the regulation of kallikrein activity, as kallikreins are necessary enzymes modulating hyper-keratinization, which is often associated with pore dilation [30].

Skin keratinocytes were treated with the cell extract or RA as the positive control, and the expression level and the enzymatic activity of Kallikrein 5 (**KLK5**), the main protease involved in desmosome degradation, were measured.

The CeCCE extract at 0.002 and 0.01 % increased both expression and enzymatic activity significantly similar to those obtained with RA, indicating a potential effect of the extract in promoting skin desquamation (Figure 2.7a, 2.7b).

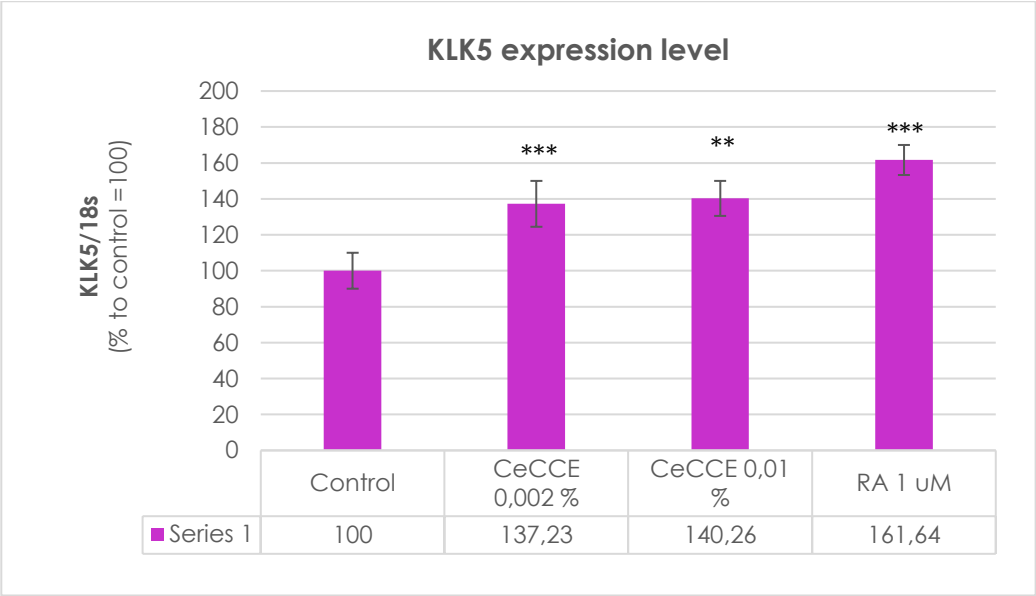

Figure 2.7a. Kallikrein 5 expression level. The error bars represent standard deviations; all the measures are statistically significant (*$p < .05$; **$p < .01$; ***$p < .001$)

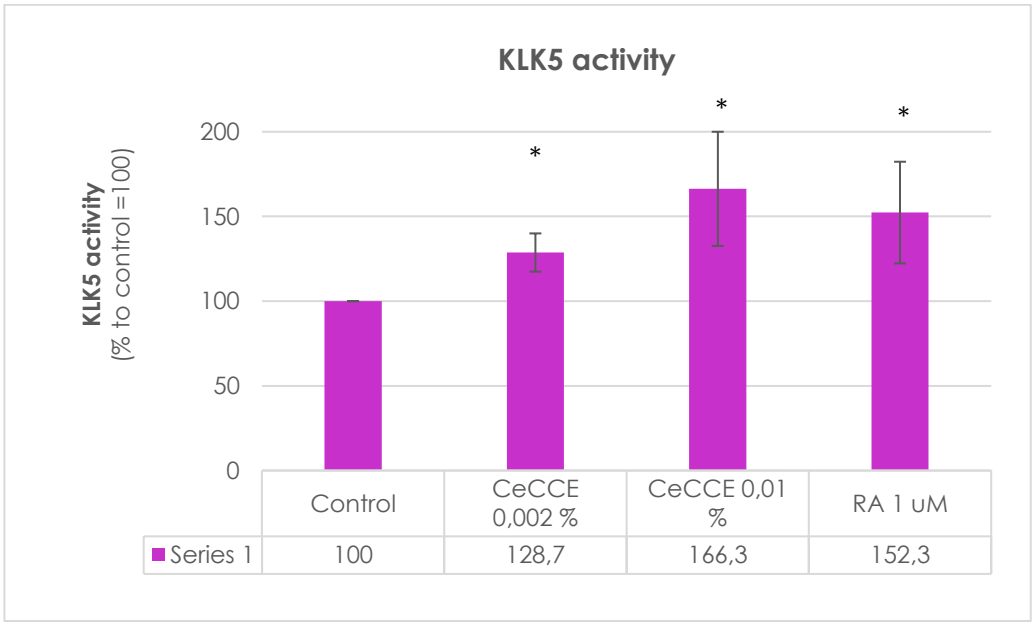

Figure 2.7b. Kallikrein 5 activity. The error bars represent standard deviations, and all the measures are statistically significant (*$p < .05$; **$p < .01$; ***$p < .001$)

2.5.2.3 Anti-inflammatory activity

The capacity of CeCCE to inhibit the release of inflammatory mediators by skin cells was evaluated. Epidermal keratinocytes were challenged with an excess of the bacteria Staphylococcus epidermidis [31], mimicking a skin

bacteria dysbiosis in vitro, and the expression levels of the inflammatory cytokines interleukin-1α (IL-1α), interleukin-1β (IL-1β) interleukin-8 (IL-8), and Tumor Necrosis Factor-α (TNF-α) were measured by RT-PCR.

The results, shown in Figure 2.8, indicated that the treatment with CeCCE, at both concentrations, led to significant inhibitions of all the analyzed cytokines.

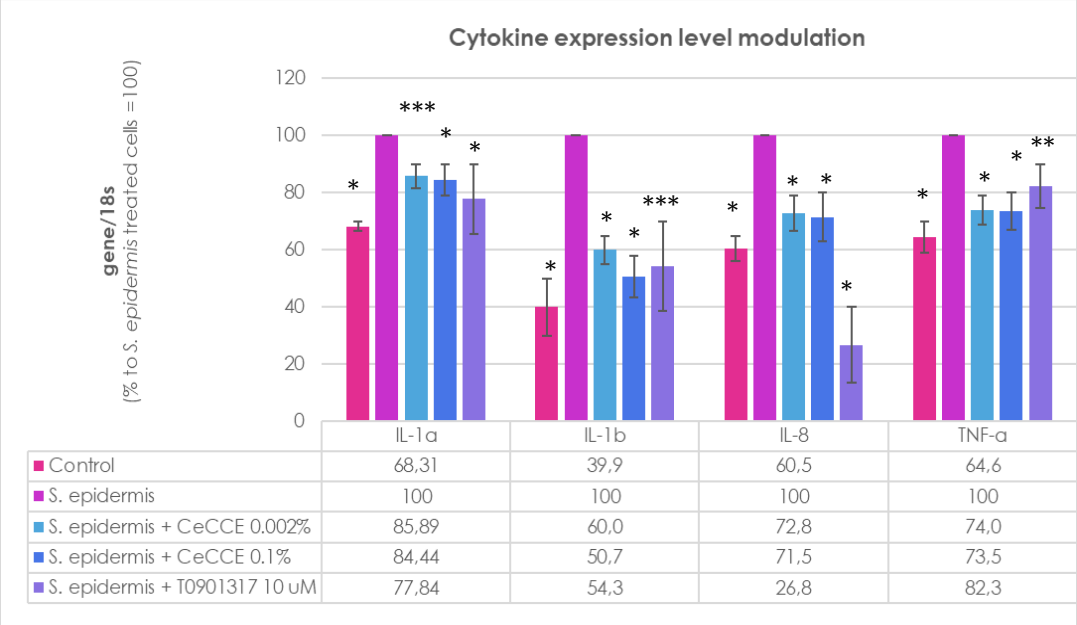

	IL-1a	IL-1b	IL-8	TNF-a
Control	68,31	39,9	60,5	64,6
S. epidermis	100	100	100	100
S. epidermis + CeCCE 0.002%	85,89	60,0	72,8	74,0
S. epidermis + CeCCE 0.1%	84,44	50,7	71,5	73,5
S. epidermis + T0901317 10 uM	77,84	54,3	26,8	82,3

Figure 2.8. Cytokine expression level modulation. The values ± standard deviations are expressed as relative % to the S. epidermidis treated samples, set as 100% (*p < .05; **p < .01; ***p < .001)

2.5.2.4 Collagen I production

We analyzed CeCCE ability to induce collagen I production in skin fibroblasts since this essential protein is responsible for keeping the skin firm around the pores.

The analysis results indicated that CeCCE significantly stimulated Pro-Collagen I production in ELISA assay, analogously to the positive control TGFβ [32], suggesting a positive role of the extract in maintaining a correct dermis tone (Figure 2.9).

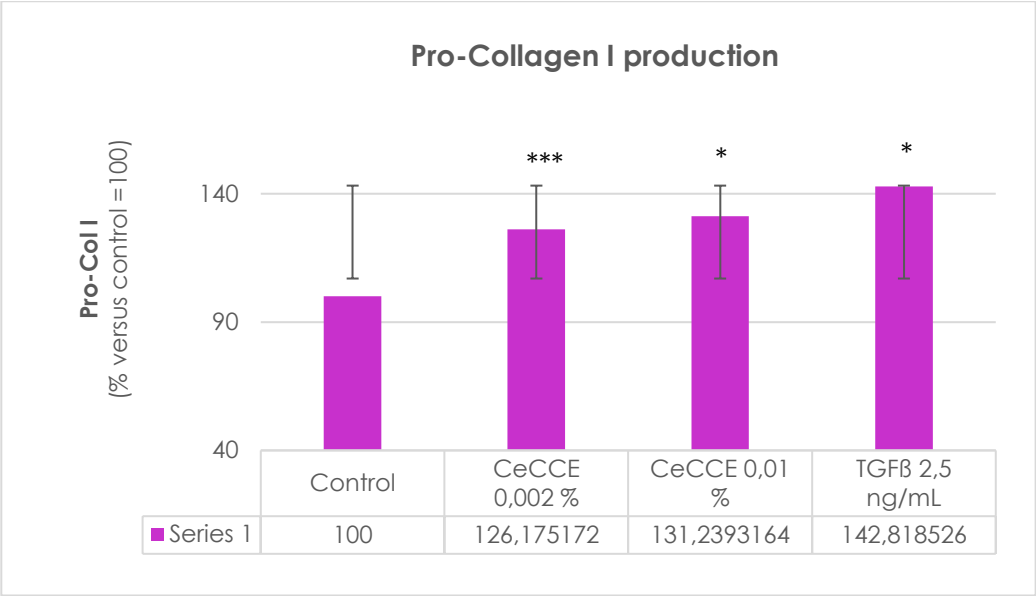

Figure 2.9. Pro-Collagen I production measure. The error bars represent standard deviations. All the measures are statistically significant (*p < .05; ***p < .001)

2.5.3 In vivo studies

Twenty volunteers (healthy female and male individuals with oily or acne-prone skin) were treated on the face with a cream containing 0.5 % w/w of CeCCE, twice a day for 28 days, and the effects on sebum production, pore size, and skin hydration were compared to those of 20 volunteers who were treated with a placebo cream.

2.5.3.1 Activity on sebum production

The results of the sebum production test showed that CeCCE containing cream reduced the sebum production by 34.9 % after two weeks and 46.5 % after four weeks, significantly more than the placebo cream, which inhibited sebum production of 10.5 and 10.1 % after 14 and 28 days, respectively (Figure 2.10).

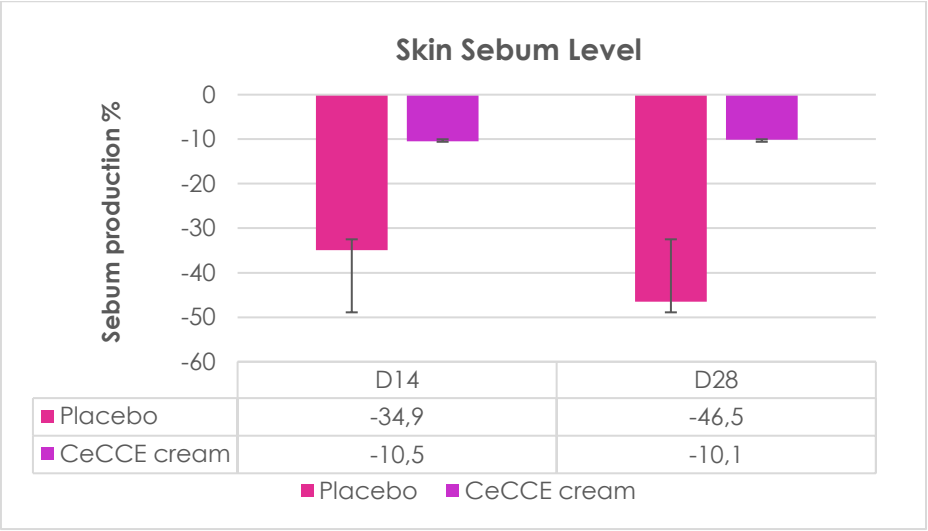

Figure 2.10. Sebum level measure. D14: 14 days of treatment; D28: 28 days of treatment. All the measures are statistically significant ($p < .05$)

2.5.3.2 Activity on pore size

The second parameter measured was the reduction in visible pores, indicating a decrease in the pore orifice size.

The CeCCE containing cream reduced the number of visible pores by 40.0 and 37.9 % after 14 and 28 days of treatment, respectively, differently from the placebo cream, whose effect on pore size was not significant (Figure 2.11). Photographs of some volunteers treated face area, taken before and after four weeks of treatment, are reported (Figure 2.12a, b, c, d).

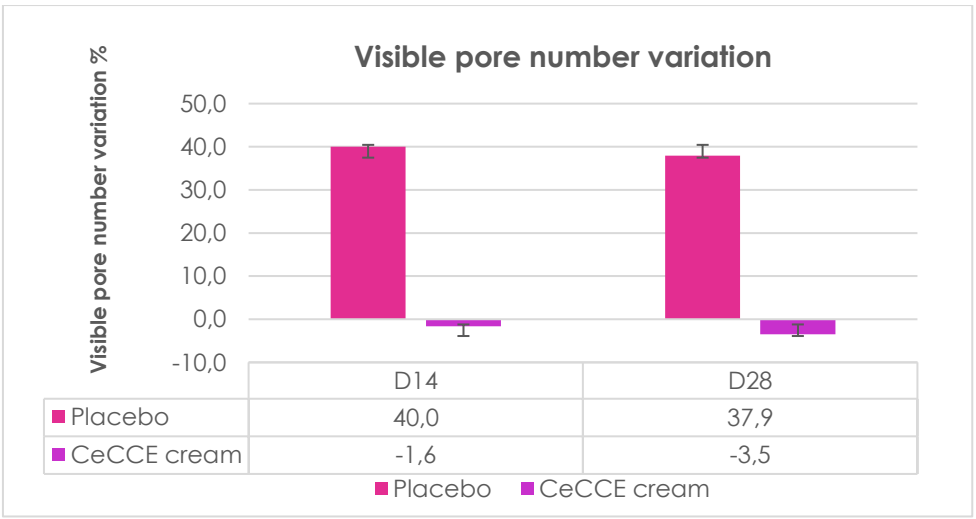

Figure 2.11. Measures of visible pores on the cheek. D14: 14 days of treatment; D28: 28 days of treatment. All the measures are statistically significant ($p < .05$)

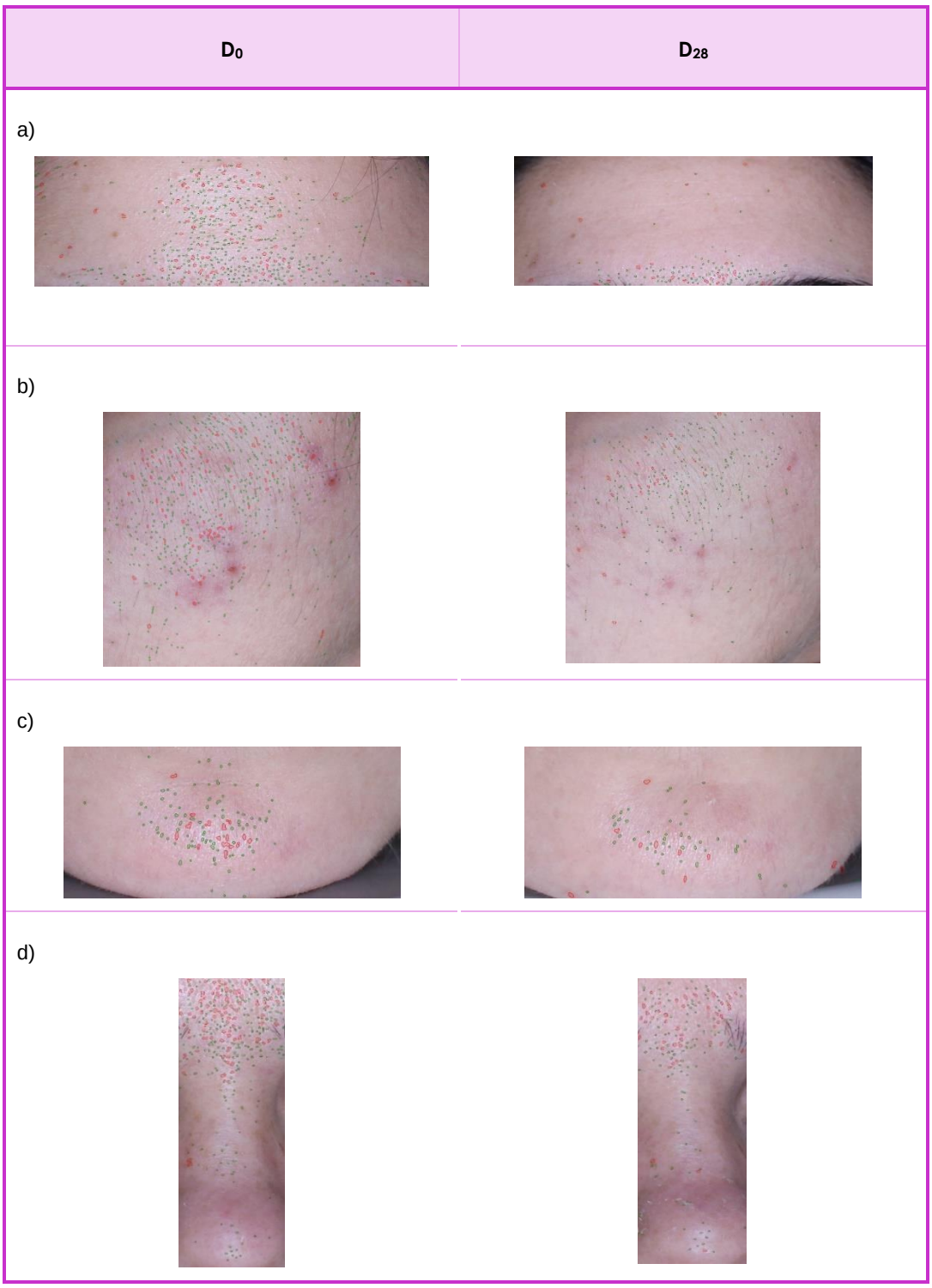

Figure 2.12. Photographs of different face areas before and after treatment. D0: baseline; D28: 28 days of treatment; a) forehead, b) cheeks, c) thin, d) nose. The red and green dots indicate the number of large and small pores, respectively.

2.5.3.3 Skin hydration

Pore enlargement can be associated with a poor skin hydration level [33]. We compared the transepidermal water loss (TEWL) produced by the active cream with the Placebo.

The CeCCE cream reduced TEWL values by 20.3 % after 14 days and 18.0 % after 28 days, while the placebo cream reduced it only by 12.2 and 12.5 %, after 2 and 4 weeks, respectively (Figure 2.13a).

Moreover, the cream containing CeCCE enhanced epidermal moisture level, measured by Corneometer CM 825, by 19.5 and 20.0 % after 2 and 4 weeks of treatment, while the placebo cream produced only a modest effect of 4.5 % after four weeks (Figure 2.13b).

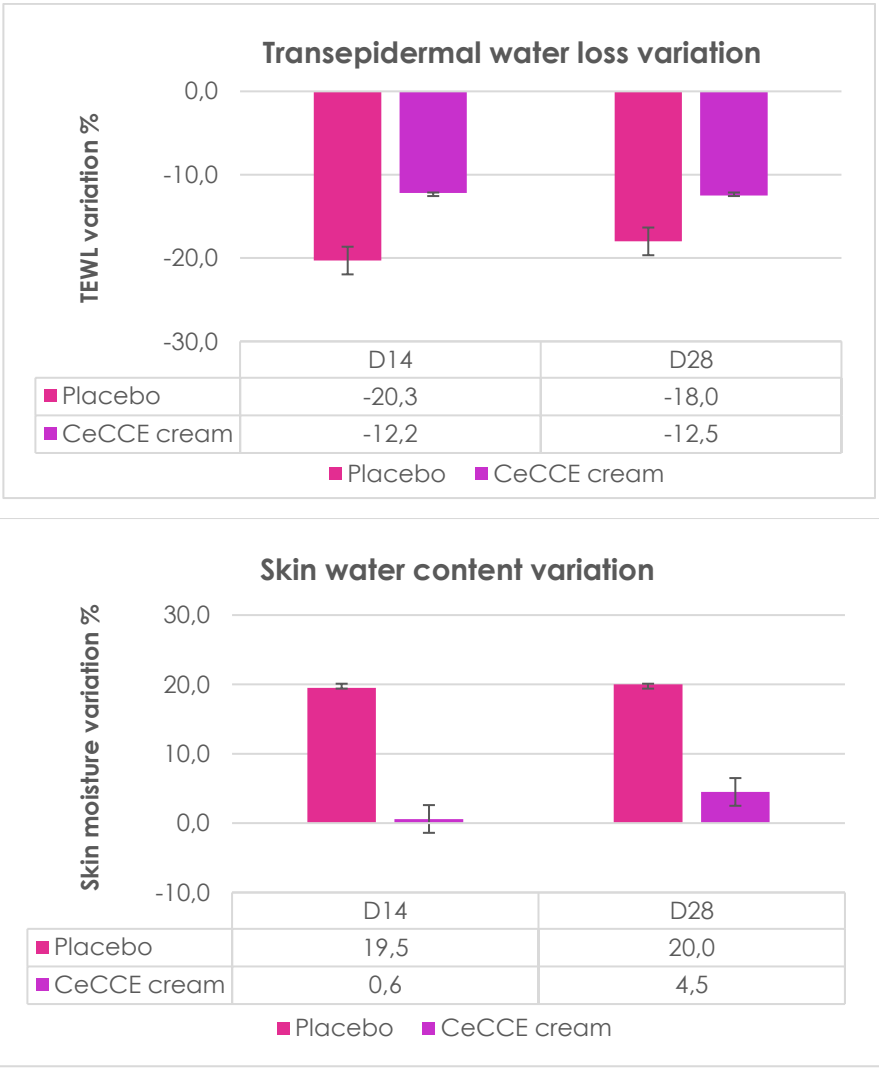

Figure 2.13. Effect on skin hydration. D14: 14 days of treatment; D28: 28 days of treatment; a) TEWL, b) Corneometry variation. All the measures are statistically significant ($p < .05$)

2.6 Discussion

As suggested by the phenolic profile and dosage investigated using an UHPLC-Orbitrap platform in MS and MS/MS levels results, *C. eriophorum* cell cultures are promising sources of bioactive molecules.

The linearity, precision and sensitivity validated the MS methods as following:

- correlation factor established the linearity of the calibration curve,

-the precision was validated by the relative standard deviation (RSD) values <15 % in the inter and intra-day repeatability.

-the range of LODs and the LOQs confirmed method sensitivity.

Comparison of the retention time, mass spectra, accurate mass measurements, and MS2 analyses with standards and with literature data allowed for Phenolic identification [34-36]. chlorogenic acid showed to be the most concentrated compound in the most representative class of phenolics in the CeCCE that was the class of Caffeoylquinic acid derivatives.

This study suggests the potential role of sebum regulation and skin stratum corneum exfoliation by a water-soluble C. eriophorum cell cultures extract since it could increase Kallikrein 5 and inhibit 5α-Reductase activity expression when tested on skin cells in vitro. Due to their activity in reducing the desquamation impairment and helping anti-acne therapeutic drugs, respectively, both KLK5 inducers and 5α-R inhibitors have recently drawn much interest in Cosmetics and Dermatology[37-39].

Indeed, in the pore enlargement with loss of dermis structural components and alterations in the thickness of epidermis the infundibulum hyper-keratinization plays its role. Thus, when treating skin desquamation a key issue is played by KLK5 role in reducing this type of dysfunction[17].

Increased collagen synthesis and negative modulation of pro- inflammatory cytokines IL-1α, IL-1β, IL-8, and TNF-α over-expression in keratinocytes are shown by CeCCE datas. the dermal skin properties, which get compromised in the skin areas around enlarged pores may be improved CeCCE as indicated by its effect on collagen I stimulation[40]. Indeed, resulting in an enlargement of the pore orifice diameter, collapse of the pore duct and dermis relaxation is also associated with alteration of stability and of production collagen in aged skin[41].

Confirmed by clinical studies this study provides results on the effect of phenolic compounds contained in a *Cirsium* cell culture extract on the regulation of four main

skin activities which all translate into a pore refining and moisturizing effect: sebum production, desquamation, inflammatory response, and collagen synthesis.

Indeed, confirming the ability of the extract in attenuating the signs of seborrheic and acne-prone skins, CeCCE has effectively shown to reduce sebum secretion and the number of visible pores in the study on human skin in vivo.

Exhibiting a higher TEWL value and a lower water content within the stratum corneum, leads to dry skin conditions and more frequent irritations as shown by people with dysfunctional pores[42,43].

Reducing TEWL and opposing pore widening the application effects of CeCCE containing cream, suggests its capacity to recover the skin barrier.

The upper skin layers' ameliorated hydration in volunteers treated with CeCCE extract was indicated by the increased registered conductance values (corneometry).

By decreasing pore size, modulating sebum production and improving skin barrier properties without side effects and with long-term efficacy the CeCCE extract studied in this work showed that it could effectively improve the skin appearance.

This rich in phenolic compounds natural active ingredient can be used in all skincare products claiming targeting the cutaneous imperfections to improve skin texture and pore minimizing refining effect.

2.7 Conclusions

C. eriophorum cell culture extract has shown to be responsible for inhibiting expression of pro-inflammatory cytokines in skin cells and reducing expression and activity of essential markers, like 5α-Reductase and Kallikrein 5, that associated with pore enlargements and sebum production. Moreover, its epidermal barrier functionality amelioration, average sebum level restoring and pore size reducing suggests it as a dermo-cosmetic ingredient in agreement with its potential effect in alleviating critical conditions related to seborrheic and acne-prone skins since.

CHAPTER 3

Phenylalanine butyramide is a promising soothing and anti-reddening cosmetic ingredient

3.1 Introduction

The most significant interface between environment and the human body is represented by the skin. Exposure of the biological tissue to oxidative stress [44], lipid peroxidation, chronic inflammation [45], and DNA damage [46-49] can generate in the skin from reactive oxygen species (ROS) after exposure to UV B (wavelength of 280–320 nm), and in turn, can result in erythema, edema, and epidermal hyperplasia [50-52].

Several bacteria, fungi, viruses, archaea, and mites which are known as commensal microbes colonized the skin as a part of a network that is defined as skin microbiota (SM) contributing to the skin barrier function ensuring its homeostasis [53-54] mediating essential physiological and pathological processes [55].

Enzymes responsible for urea degradation (ureases), lipidic film surface breakdown (lipases) and involved in the SC renewal and desquamation process (proteases), are released by skin microbes. Moreover, indoles that inhibit many molds and yeasts [56], antimicrobial peptides by commensal bacteria [57], bacteriocins and microbiota biofilms [58-59] are produced by the microbiota.

Most microbial metabolites (i.e., short-chain fatty acids including butyric acid) are responsible for the beneficial effects produced by the SM, including those made to improve dysbiosis (imbalances in the SM composition) due to various skin conditions, both pathological (i.e., dermatological diseases) and non-pathological

(i.e., aging) [60]. Acidification of the skin's pH (it varies between 4.2 and 7.9) [61] and improve the epithelial barrier function by decreasing its permeability, eliciting the eutrophic effect on the skin, and suppressing cutaneous inflammatory reactions are due to fatty acids secreted by the sebaceous glands. [54,62]

Therefore, for skincare a novel strategy in cosmetic formulations could consist of short-chain fatty acids (SCFAs).

Previous studies have shown that the major metabolite of Staphylococcus epidermidis fermentation, the butyric acid has a significant role in inflammatory skin diseases. It provokes secretion of inflammatory cytokines by interaction with receptors expressed by keratinocytes [63]. Strongly limiting its dermatologic use, unfortunately, are unfavorable physicochemical and sensorial properties. Therefore, the idea of synthetic analogs to allow its use in the cosmetic and dermatological fields.

Among the synthesized derivatives for the topical use of butyrate the phenylalanine butyramide, FBA (Figure 3.1), proved to be particularly noteworthy as a valid alternative. It is able to release butyric acid quickly, with no smell, having however the same pharmacokinetic and safety profiles as butyric acid [64]. in vitro it also does not show any genotoxicity.

No mutagenic properties are showed by the Ames test and at the same time it cannot induce chromosomal breaks as attested by the micronucleus test that [64].

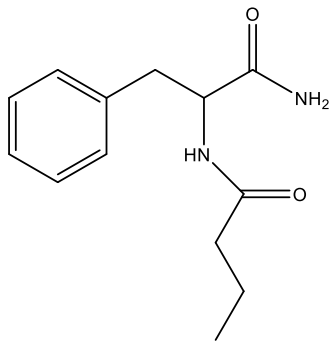

Figure 3.1. Phenylalanine butyramide

Potential permeation through the skin, in vitro experiments for the presence in the bloodstream, and in vivo tests for the soothing and anti-reddening effects, were estimated in this study for the potential cosmetic applications of FBA.

3.2 Study Design

The FBA logP value was evaluated using a pig model, and results were validated with two software to predict logP (XLOGP and ADMET).

Since the experimental results suggested that the FBA is a lipophilic substance, thus it was hypothesized that the transepidermal penetration pathway was the most probable; moreover, the low molecular weight made FBA a good candidate for skin application.

Therefore, it was necessary to carry out the test of Franz cells to study the permeation and diffusion of FBA through selective biological membranes to determine the skin affinity and the characteristics of diffusion of this substance in the skin.

The standard Franz diffusion cells were then used to study the diffusion and penetration kinetics of the labeled molecule. The protocol consisted in applying a known quantity of the FBA solution on the skin surface and analyzing the amount distributed in the various skin layers (stratum corneum, epidermis, and dermis); furthermore, the amount of peptide recovered in the Franz cell receptor fluid (transcutaneous flow).

The sample collection occurred at various times (1, 2, 4h) on intact skin, and its concentration was determined by a new validated chromatographic method, according to AOAC Guideline [65].

The recovery of 95 % was considered optimal for experimental purposes. The dosage method was validated by a correlation coefficient (R^2) higher than 0.999, a sensitivity tested by measures of the LLOQ (lowest concentration of the calibration curve) and LOD (limit of detection) that can be quantified with precision (RSD %) < 20 %, and an accuracy (RE %) lower than 15 %.

Finally, the soothing and anti-reddening effects of a w/o emulsion containing 1.5 % FBA were tested in vivo in a skin area Sodium Laureth Sulfate (SLES)-induced erythema.

A single-blind trial was set. The test provided the identification of 3 zones, each one with an area of about 4 cm^2 on the upper volunteers' forearm where erythema is induced rubbing a high-concentrated SLES solution (5 mL of Sodium Laureth Sulfate at 30 %) for 1 minute and successively gently rinsed with water and dabbed with absorbent paper.

The erythema's area was divided into three portions: Placebo, FBA emulsion-treated-area, and control.
The erythema index was quantified using the Colorimeter CL 400 (C+ K electronic GmbH) probe.
Parameter a* was measured at the erythema induction (T_0), after 30 and 60 minutes from the application on two of the three test site areas of the Placebo and FBA cream.
The instrumental measurements occurred in an air-conditioned room at T = 20 ± 5°C and controlled humidity (50 ± 5 % RH) after an acclimatization period of about 30 minutes.
The Student t-test assesses if the difference between averages is significant. The values are significant for values of $p \leq 0.05$.

3.3 Materials and Methods

3.3.1 In Vitro Studies

3.3.1.1 Reagent and Chemicals

Phenylalanine butyramide (FBA) ($C_{13}H_{18}N_2O_2$) (234.29 g/mol) (US patent US 2011 00983.19A1; 28 April 2011) by ChiroBlock® (Wolfen, Germany). Phosphate buffered saline (PBS) was provided by Sigma Aldrich (St. Louis, MO, USA). The analytical grade pure water (DW), acetonitrile (ACN), and ethanol (EtOH) were purchased from Exacta+Optech (S. Prospero, MO, ITALY).

3.3.1.2 Determination of Octanol/Water Partition Coefficient

Octanol−water partition coefficients of FBA were determined using a shake-flask approach following the guidelines of the European Chemical Bureau. Briefly, n-octanol−water mixtures were first vortexed for 1 min and then shaken overnight at room temperature (22 ± 2 °C) to reach the equilibrium and phase distribution. The phase ratio was water/n octanol: 4/1. FBA was dissolved in a water-saturated organic solution at a concentration of 200

µg/mL. This solution (8 mL) was transferred to 15 mL centrifuge tubes and added to 2 mL of pre-saturated octanol. The tubes were shaken for one hour (a time window enough to reach equilibrium as demonstrated by preliminary experiments). After equilibration and phase separation, FBA was analyzed by liquid chromatography (LC) in both phases. 10 µL of the organic phase was sampled and added to 1 mL of mobile phase while the sampled aqueous phase was analyzed straight by liquid chromatography. The partition coefficient was calculated as the organic phase ratio and water concentration of FBA at equilibrium. Experiments were performed in triplicate.

3.3.1.3 Validation of Octanol/Water Partition Coefficient

The XLOGP (Atomistic and knowledge-based method calculated by XLOGP program, version 3.2.2, courtesy of CCBG, Shanghai Institute of Organic Chemistry) and ADMET (Simulation Plus, West Lancaster, USA) programs predicted the octanol/water partition coefficient (log $P_{oct/w}$).
ADMET software result was given as log K_p* K_p (cm/h) defined below:

$$\mathbf{K_p = (K_m * D)/h}$$

K_m is the distribution coefficient between stratum corneum and vehicle.

D is the average diffusion coefficient (cm^2/h),

h is the skin thickness (cm).

3.3.1.4 Tissue preparation

For permeation analysis, porcine skin, coming from the outer part of the ear, was used. The skin was excised post-sacrifice from female and male animals (age 10 - 12 months, weight 150 - 190 kg) from a local slaughterhouse (Avellino, Italy) within three hours from animal death.
Subcutaneous fat was removed, and skin samples were maintained at 4°C until the experiment, performed within 24 hours. The skin was put on a filter paper (Fisherbrand™ Grade 601, Fisher Scientific, Leicestershire, UK) and cut into pieces of appropriate size before assembly in the Franz cells.
The integrity of porcine skin was examined by measuring the impedance of

the skin.

3.3.1.5 Chromatographic analysis for skin permeation study

The quantitative determination of FBA was performed with a chromatographic system consisted of a high-performance liquid chromatographic system (LC-20 AD VP; Shimadzu Corp., Kyoto, Japan), equipped with a 7725 Rheodyne injection valve fitted with a 20 µL loop, and an ultraviolet (UV)–visible detector (Shimadzu Model SPD10 AV) set at λ 200 nm.

The chromatographic condition was reported in Table 3.1. The mobile phase solvents were vacuum-filtered through 0.45 µm nylon membranes (Millipore, Burlington, MA USA).

Data acquisition and integration were accomplished by Cromatoplus 2011 software. Each sample was injected three times to test the instrument repeatability.

Table 3.1. Chromatographic conditions

Column	**Phenyl Hexyl (250 × 4.6 mm, 100 Å) (Kinetex, USA)**
Precolumn	4 × 3.0 mm; Phenomenex, CA, USA
Mobile phase	ACN: DW (30:70)
UV detection λ	200 nm
Flow rate	0.5 mL/min
Retention time	5.90 ±0.5 min

3.3.1.6 Validation of FBA extraction method and HPLC analysis

The method validation was performed according to AOAC Guideline [66].

3.3.1.6.1 Selectivity

Blank samples of epidermis and dermis were Blank. They were extracted at room temperature with 1 mL of EtOH. The solutions were analyzed to verify the presence of interfering peaks eluting at the retention time of FBA.

The receptor solution of a blank permeation experiment was analyzed, too. Blanks samples were spiked with known amounts of FBA (25, 10, and 5 µl of standard solution in ethanol 200 µg/mL). The dried specimens were extracted with 1 ml of EtOH in various conditions. The samples were centrifuged at 15.000 rpm for 10 min and sonicated for 6 min. The recovery of FBA from skin layers was assessed compared to the amount applied, evaluated by injection of spiked concentrations without skin layers samples.

The HPLC system was calibrated using standard synthetic solutions prepared by diluting the FBA in EtOH to four different concentration values ranging from 0.625 to 10 µg/ml. A stock solution of FBA with a 2 mg/mL concentration was prepared by dissolving 2 mg of FBA in 1mL of ACN. Each concentration level was analyzed in triplicates. Linearity was assessed by inspecting the detection signals as a function of analyte concentrations by a regression line by the method of the least-squares.

Quantitative analyses were performed on matrix-matched calibration curves, peak area vs. concentration (µg/mL). The matrix-matched calibration curves were obtained from the analyses of blank sample extracts spiked FBA at the same range concentrations above reported.

3.3.1.6.2 Sensitivity

The analytical sensitivity defines the minor concentration of a measure and that an analytical procedure can reliably measure. This validation parameter explains the lower limit of quantification (LLOQ) and the lower detection limit (LOD).

- LLOQ : the method's LLOQ was the concentrations of the analytes that provided signals equal to 10 times the noise signal of the analysis. It was evaluated on the synthetic standards and calculated on the standard deviation of the response (SD_a) of the curve and the slope of the calibration curve (S). The standard deviation of the response was determined based on the standard deviation of y-intercepts of regression lines [80].

$$\mathbf{LOQ = (SD_a * 10)/S}$$

- LOD : the method's LOD was assumed as the concentrations of the analytes that provided signals equal to 3 times the noise signal of the analysis [81].

$$\mathbf{LOQ = (SD_a * 3)/S}$$

3.3.1.6.3 Precision and accuracy :

The method's precision was evaluated by running three replicate samples at four different concentration levels. The analyses were repeated along the two different days to cover both intra-day and inter-day precision.

The accuracy (relative error RE %) was measured as the difference between the theoretical amounts and the approximation, divided by the magnitude of the exact value. The precision (RSD %) was calculated as the coefficient of variation of the back-calculated concentrations.

3.3.1.6.4 Matrix effect

Matrix effect was calculated as follows:

$$\textbf{Matrix effect (\%)} = \frac{\textbf{Peak area of analyte in a standard solution-peak area of the analyte in a sample}}{\textbf{Peak area of analyte in a standard solution}}$$

All the analyses were expressed as the mean of the three analyses.

3.3.1.7 Skin Permeation and Retention

The FBA diffusion tests were undertaken on Franz-type vertical diffusion cells (Ø 9 mm, 5-ml receptor compartment, SES GmbH-Analyse System, Bechenheim, Germany) with an effective diffusion area of 0.6 cm^2 and receptor volume of 4 mL. The total thickness of the skin was washed three times with 1 mL of water and mounted between the two halves of the cell with the stratum corneum facing the donor compartment. The receptor

compartment was filled with 4 mL of degassed saline solution (NaCl 0.9% w/v), while in the donor compartment, was put 1 mL of a solution composed of 1 mg FBA dissolved in 1 mL of PBS/EtOH (70:30).

The Franz Cell system was maintained at a constant temperature of 37 ± 0.5 °C through thermostatic bath circulation, while the receptor medium was constantly kept under magnetic stirring through the experiments. At the end of the application time (1, 2, and 4 h), the skin was removed from the cell. Some donor chamber aliquots were collected and analyzed by HPLC to quantify the FBA amounts. The skin was wiped three times with paper soaked in distilled water, and the epidermis and dermis separated. The skin was cut according to the permeation area (1 cm^2) and heated at 50 °C with an air dryer for 30 s.

Then epidermis was separated from the dermis by scraping with a scalpel. Experiments were performed in triplicate. Epidermis and dermis samples were placed in glass vials and extracted with 1mL of EtOH. The samples were centrifuged at 15.000 rpm for 10 min and sonicated for 6 min. One mL of the samples was filtered using a 0.45 µm polyamide (PA) filter (Sartorius AG, Goettingen, Germany) [82].

3.3.1.7.1 Permeability calculation

The skin permeability was calculated by dividing the amount of FBA present in the SKIN (epidermis and dermis) by skin surface area using the following formula:

D(µg/cm) = (Amount receptor fluid + Amount skin) / SSA (skin surface area)

The ratio of the total amount of PP in the receptor fluid and skin to the amount of FBA applied was calculated to determine the total absorption rate :

Total absorption (%) = (Amount receptor fluid + Amount skin) / (Amount total) x 100

3.3.2 In vivo study

The study accords to the Helsinki Declaration (1964) principles and revisions

recognized by the European Community [83], and according to the Colipa Guidelines for evaluating the efficiency of cosmetic products (May 2008) [84].

3.3.2.1 Clinical Trial

An active cream with 1.5 $\%_{w/w}$ FBA (1.5 *10 µg/mL) and a Placebo cream were compared to treat skin-induced erythema. Results were also compared with a non-treated area (Control).

The selected test site is the upper forearms of 20 healthy volunteers. Three areas of about 4 cm^2 were identified. In all of them, erythema was induced rubbing 5 mL of 30 % SLES solution, then two were treated respectively with the Placebo and the FBA cream, and one was not treated.

After 30 and 60 minutes of the cream application, skin redness was detected through Skin Colorimeter® CL 400.

The device detects minor color changes in the skin, therefore ideal for comparison measurements. The probe features a large illumination area so that enough light reaches the skin surface for measurement while keeping the measurement area small enough to ensure that only the surface color is measured and not the more profound layers' color. The probe emits white LED light arranged circularly to illuminate the skin evenly. The light emitted is diffused in all directions. Some parts pass through the different skin layers; others reflect. The light reflected from the skin is measured in the probe and expressed accordingly. The probe's raw data (XYZ values) are corrected with a unique color matrix close to the standardized values. The measured color can be calculated in different color spaces.

The CIELAB color space (Fig. 3.2), also known as L * a * b *, is defined by the International Commission for Illumination (CIE). Each letter represents an axis:

- L* value (brightness) is inversely proportional to the pigmentation. The higher the L * value, the less pigmented the skin
- a* refers to the red-green axis and is proportional to the erythema (microcirculation/redness of the skin). Positive values of a * indicate red, negative values green
- b * shows the position of the color on the blue-yellow axis; in the literature, it often describes the pigmentation

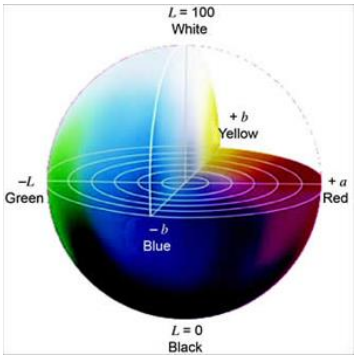

Figure 3.2. CIELAB color space system

3.3.2.2 Study population

Twenty healthy female volunteers (caucasian ethnicity), from all social categories, aged 20-60 years, skin phototype: II-IV Fitzpatrick scale, who had no systemic pathologies, and who had not applied any product on the test site in the previous seven days, were enrolled. Instead, were excluded pregnant or breastfeeding women, women with cutaneous hyper-reactivity or intolerance reactions to cosmetic products/ingredients, topical or systemic treatment with any drug that may interfere with the outcome of the test, women affected by skin diseases (eczema, psoriasis, lesions), topical use of retinoids in the previous six months the start of the study or with systemic retinoids in the previous 12 months, topical use of products based on alpha and beta-hydroxy acids in the 30 days before the start of the study.

The volunteers subscribed an informed consent to permit the process of the personal data and images taken during the in vivo tests for the uses permitted by D.Legs n. 196 of June 30, 2003, and in which they declared to know the composition of the active/formulation and no allergy to its components.

For each volunteer, a detailed form was prepared to use the samples provided by the RD Cosmetics center of the Pharmacy Department.

3.3.2.3 Cream composition

The Emulsion with FBA contained two phases: phase O (oil phase) polyglyceryl-3 methyl glucose 5.0%, cetyl alcohol 2%, and cetearyl alcohol 3%, and phase W (water phase) containing water (88.8 %), FBA (1.5 %), sodium benzoate 0.5 %, potassium sorbate, and perfume (0.1 %).

The placebo cream contained all the ingredients without the FBA. The creams' components were bought at ACEF Spa (Fiorenzuola D'Arda, Italy) and Parfum by Farotti Srl (Rimini, Italy).

The two creams were made, homogenizing the two phases energetically at 70 °C using a Silverson L5M-A Laboratory Mixer (SBL, Shanghai, China), cooling in an ice bath, and adding the remaining components at room temperature. Finally, the pH (5.4–5.5) and viscosity (30.203 – 30.406 mPa; L4, 20 rpm) were tested using a Crison GPL 20 pH-Meter (Crison, Barcelona, Spain) and a Visco Basic Plus rheometer (Fungilab Sa, Barcelona, Spain).

3.4 Statistical analysis

Descriptive statistics were reported as means and standard deviations (SDs) for continuous variables. The independent sample t-test was performed to evaluate the differences among continuous variables. The level of significance for all statistical tests was two-sided, $p < 0.05$. All data were collected in a dedicated database and analyzed by a statistician using the QSPR model implemented by Potts and Guy, 1992 Pharm. Res Swissadme® (Swiss Institute of bioinformatics) [85] and ADME® (Simulation Plus, West Lancaster, USA) predictor software was used.

3.5 Results

FBA is a 1-carbamoyl-2-phenyl-ethyl derivative of butyric acid (Figure 1). In this study, its lipophilic potential was evaluated by in vitro studies validated by silicon studies.

3.5.1 In vitro studies

In vitro studies were performed to determine the FBA's ability to permeate the skin and its soothing and anti-reddening potential. The FBA levels were evaluated after 1, 2, and 4 hours.

3.5.1.1 Partition coefficient and in silico parameters

The experimental Log P o/w, estimated by the shake-flask method, was 0.79 ± 0.12.
The calculated Log P o/w obtained by the XLOGP program was 0.79. Instead, the calculated Log P o/w found by the ADMET® program was 0.74.
The value found experimentally was in line with those determined statistically. ADMET® program calculated FBA Log Kp (skin permeation) too, which resulted in 1,919 cm/h.

3.5.1.2 Dosage method used to determine FBA levels

A new chromatographic method was used to determine the FBA concentration in the epidermis, dermis, and receptor compartment by time. The results, expressed in µg/ml, were reported in Table 3.2.

Table 3.2. FBA concentration in epidermis, dermis, and receptor compartment by time (µg/ml).

Time (h)	Conc. FBA in epidermis (µg/ml)	Conc. FBA In dermis for PBs donor (µg/ml)	Conc. FBA in the receptor compartment (µg/ml)
1	1.49 ± 0.40	0.30 ± 0.07	0
2	0.37 ± 0.06	0.71 ± 0.11	0
4	1.73 ± 0.31	3.18 ± 0.49	0

The amount permeated in the skin was 0.2 % at 60' and 0.4 % after 4 hours.

The FBA chromatograms used to dosage the FBA in the epidermis and dermis are shown in Figure 3.3

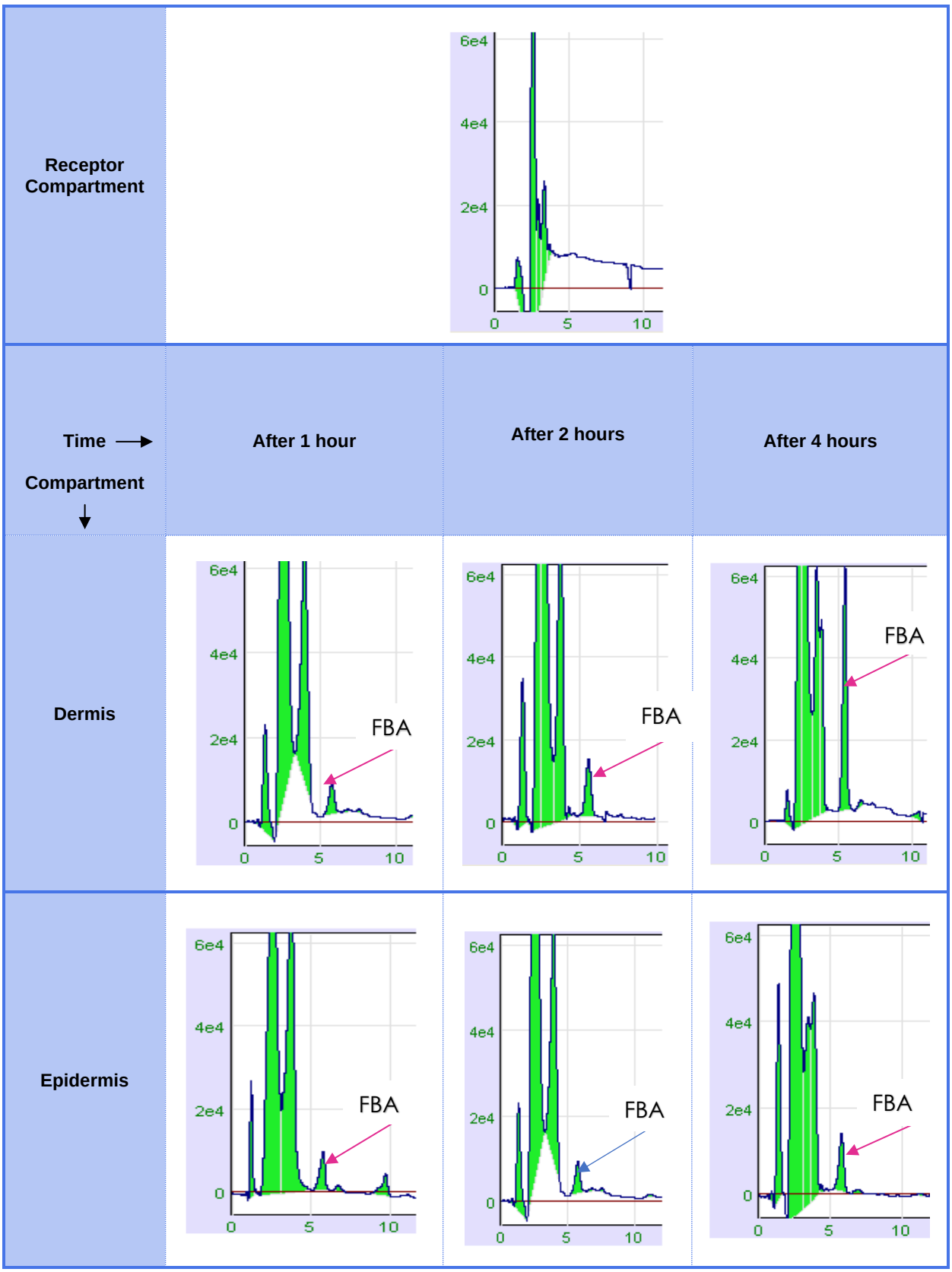

Figure 3.3. Chromatograms related to the determination of FBA levels in the skin. Y assis reports the absorbance in mAU in function of the time expressed in minutes (x assis)

3.5.1.3 Validation of the analytical method

The dosage method was validated to confirm the validity of the results as required by the AOAC guideline [66]. Recovery was tested at different ultrasonication times.

Ultrasonication time of 6 minutes was used for experimental purposes since it gave a reproducible average recovery of 95 %. The matrix-matched calibration curve accomplished in the receptor phase supported a negligible (~ 95 %) matrix effect, assessed as the ratio between the slopes of the calibration curve achieved in EtOH and measured in the receptor phase (saline solution, NaCl 0.9 % w/v). Each concentration level used to determine the calibration curve was analyzed in triplicates.

The validation parameters are summarized in Table 3.3.

Table 3.3. Validation parameters for the quantitative analysis of FBA

Calibration parameters	
Linear range (µg/mL)	0.5 - 10
Slope	13178
Intercept	2195.5
R^2	0.9995
Chromatographic system precision and accuracy	
Repeatability (n = 5); RSD (%)	4.80
Intermediate precision (n = 10); RSD (%)	8.70
LOQ (ng mL^{-1})	0.020
LOD (ng mL^{-1})	0.00991
Matrix effect	95.0

The proposed method was sensitive and straightforward to quantify the FBA in skin layers at the end of a permeation experiment.

3.5.1.4 Skin permeation

The product was applied at various times (1, 2, 4 h) on healthy skin, and its concentration was determined in the epidermis and dermis and the receptor compartment (Table 3.2).
The amount permeated across the skin was 0.2 % at 60' and 0.4 % after 4 hours.

3.5.2. In vivo study

3.5.2.1. Erythema Index

The erythema index, calculated as a*(skin redness), was measured after 30 minutes and 1 hour from the application of the w/o emulsion containing 1.5 % FBA (A), the Placebo emulsion (P), and on the control site (Control).
The results are reported in Table 3.4 and Figures 3.4 – 3.6.

Table 3.4. Average of Erythema Index (a* average values) at T_0, $T_{30'}$ and $T_{60'}$ and average of decrease in erythema (%) after 30' and 60' for emulsion with FBA (site A), Placebo (site P), and control site.

Site	Product	a* average values			Erythema index variation (%)	Erythema index variation (%)
		T_0	$T_{30'}$	$T_{60'}$	$T_{30'} - T_0$	$T_{60'} - T_0$
A Area	FBA Emulsion	9.63 ± 2.48	8.04 ± 1.63	7.63 ± 1.46	**- 15.7 %** *p = 0.0013*	- **17.8 %** *p = 0.0037*
P Area	Placebo cream	9.68 ± 2.19	8.61 ± 1.36	8.32 ± 1.34	**- 8.6 %** *p > 0.05*	**- 10.5 %** *p > 0.05*
Control Area	Not treated	8.98 **±** 2.26	8.04 ± 1.53	7.84 **±** 1.41	**- 8.8 %** *p > 0.05*	**- 11.8 %** *p > 0.05*

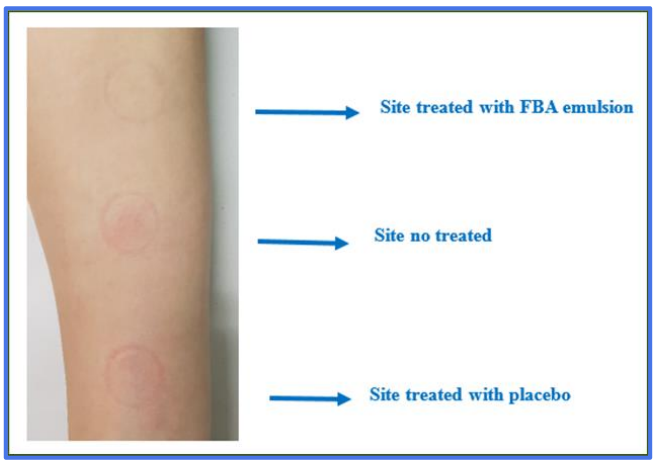

Figure 3.4 Image of the three test sites identified on the volunteer's forearm at T1h

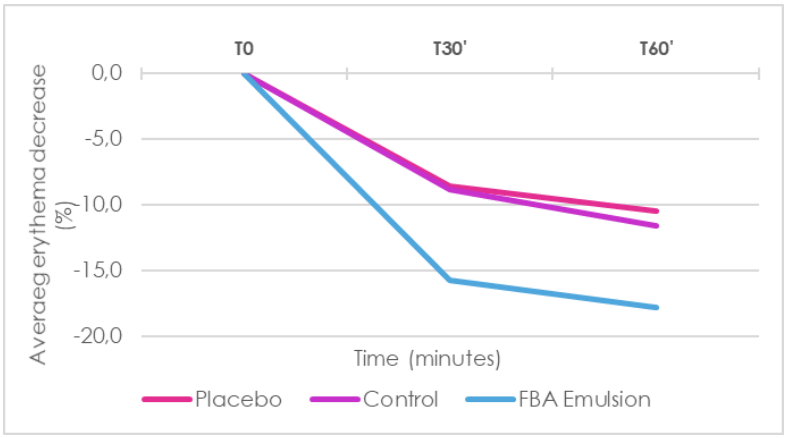

Figure 3.5. Average of decrease in erythema (%) after 30'and 60' for emulsion with FBA (A area), Placebo (P area), and control site.

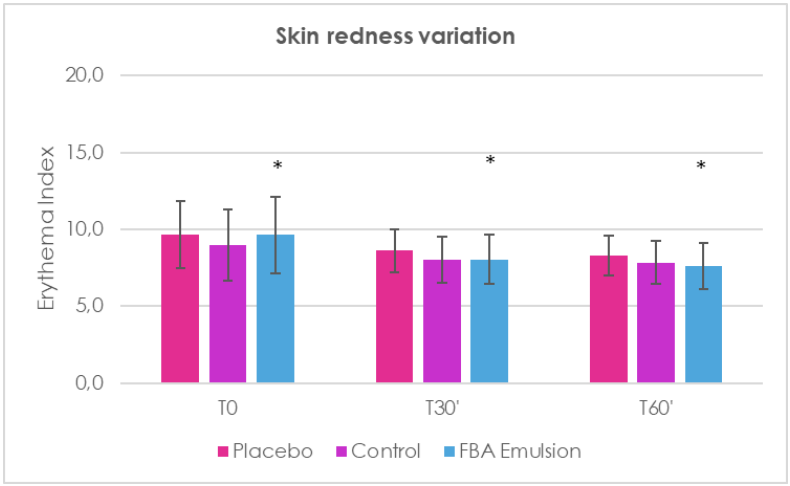

Figure 3.6 Average values of erythema index at T0, T30', and 60' for emulsion with FBA (site A), Placebo (site P), and control site. (*$p < .05$)

There was a decrease in skin redness values on the control site (- 8.6 % after 30' and - 10.5 % after 60'), and on the placebo site (- 8.8 % after 30' and - 11.8 % after 60'). Moreover, a significative erythema index' decrease (- 15.7 % after 30' and - 17.8 % after 60') was detected after applying the emulsion containing FBA (Table 3.4, Figures 3.4 – 3.6).

3.6 Discussion

Relevant anti-inflammatory, anti-redness, and lightening properties is shown to be possessed by butyric acid[64]. However, its use in the cosmetic field is limited by unpleasant organoleptic properties. Therefore, to eliminate this unfavourable characteristic and test the potential cosmetic properties a butyrate (FBA) phenyl derivative, which can release butyric acid on the skin surface, was used. A feature that differentiates the cosmetic from the pharmaceutical product is that the cosmetic product must not enter the bloodstream as stated by Regulation (EC) No 1223/2009 of the European Union [4] which defines a cosmetic product as "any substance or mixture intended to be placed in contact with the external parts of the human body (epidermis, hair system, nails, lips, and external genital organs) or with the teeth and the mucous membranes of the oral cavity with a view exclusively or mainly to cleaning them, perfuming them, changing their appearance, protecting them, keeping them in good condition or correcting body odors." This has to be respected for any substance to be defined as cosmetic, but topically applied compounds can enter the body through sweat ducts and hair follicles or diffusing across the skin layers (transepidermal pathway). In this last case, the solute's molecular properties determine the access route in permeating the skin intracellularly or transcellularly. Intercellular route is preferred by lipophilic molecules prefer[67]. Therefore, to establish which was the pathway of skin permeation FBA's lipophilicity was evaluated. The skin's permeability to the permeant (Kp) and the gradient of permeant concentration across the skin·(Δc) determine the substance's amount permeated per unit area and unit time (J). In the case of passive diffusion Kp depends on the partition coefficient P[68]. Using in vitro models, including pig, rat, rabbit, mouse, and synthetic membranes previous studies evaluated skin permeation [69.70].

In this study, results were validated with two software to predict logP (XLOGP and ADMET) evaluating the FBA logP value using a pig model. Experimental results suggested, in a similar way to those determined statistically, that the FBA is a lipophilic substance. Thus, it was hypothesized that the most probable pathway of penetration was the transepidermal. Moreover, FBA showed to be a good candidate for skin application according to its log P value and low molecular weight. Therefore, on intact skin FBA was applied at various times (1, 2, 4h), and its concentration was evaluated in the epidermis and dermis, and the receptor compartment by a new validated chromatographic method establishing the correctness of the results. According to AOAC Guideline, selectivity, linearity, precision, and accuracy were estimated for the method validation[66]. By obtaining FBA without interfering peaks the selectivity was tested by changing the organic solvents[71]. Different ultrasonication times instead were used for testing recovery. Recovery of 95 % was considered optimal for experimental purposes. Then by mean of a correlation coefficient (R^2) higher than 0.999, a sensitivity tested by measures of the LLOQ (lowest concentration of the calibration curve) and LOD (limit of detection) that can be quantified with accuracy (RE %) and precision (RSD %) < 20 %, and an accuracy (RE %) lower than 15 % the dosage method was validated.

Our study's results suggested that the cosmetic properties of FBA could be attributable to butyric acid since FBA was not able to access the bloodstream. Moreover, in the skin the low dosage of FBA implies that butyric acid is quickly generate by FBA's transformation. Lower than those found at 1 h and 4 h, 2 hours FBA level, could more probably depend on the right conditions to degrade it almost wholly into butyric acid while, the higher concentrations of FBA accumulated after 4 hours shows failure in doing the same. The produced by skin microbiome enzymes (amidases) or the skin's pH could be responsible for transformation of the FBA into butyrate[72]. The acid group of L-phenylalanine and a second one between the butyric acid and the amino group of L-phenylalanine shows that FBA has two carboxylamine bonds that in an acidic environment, amidases could break by cleaving of the amide bond, and as consequence the butyric acid can be released. In an acid environment FBA releases phenylalanine and butyric acid in a time-dependent manner as shown by in vitro studies [65]. Thus, the FBA releases of butyrate is plausible at the acid skin's pH. Finally, an emulsion containing 1.5 % FBA for the soothing and anti-reddening effects was used for testing in vivo a treated with

Sodium Laureth Sulfate (SLES)-induced erythema skin area and results were compared to a placebo cream. Because active ingredients used in cosmetics at a variable concentration range from 1 to 2 % the concentration of FBA was settled at 1.5% as the most appropriate for the formulation.

After applying the containing FBA emulsion, a significant decrease in the erythema index was detected. Since FBA does not cross the skin, and previous studies have shown that butyrate regulates immune/inflammatory reactions in the skin [73] via binding to its receptor, GPR43 [64,74,] which modulate the production of pro-inflammatory cytokines induced by skin injuries [75-77] the soothing and anti-reddening effects of the emulsion containing 1.5 % FBA were ascribable to butyrate.

3.7 Conclusions

In this study for the first time a new odorless and rapid skin absorbed butyrate-derivative able to release butyric acid (the FBA), in the skin was tested, together with its skin permeation and the soothing and anti-reddening effect.

The results suggest cosmetic benefits could be attributable to butyric acid and that FBA does not reach the bloodstream.

Therefore, without organoleptic limits of butyric acid FBA represents instead, in the cosmetic field, an innovative way to exploit the benefits of butyric acid.

CHAPTER 4

Ficus carica cell cultures extract works as an anti-stress ingredient for the skin

4.1 Introduction

The skin is the most exposed organ of our body such that its health is threatened by a large variety of environmental factors (temperature shifts, sun radiation, tobacco smoke, ozone, chemical pollutants), which is known as the "exposome." The exposome concept includes the totality of factors to which an individual gets exposed from conception to death; this term entered our vocabulary quite recently [78].

Besides the exposome, additional factors have been recognized as skin-aging potentiators, acting separately or in combination with the exposome [79], such as psychological stress, lack of sleep, and inappropriate nutrition. Among these, psychological stress represents one of the most occurring issues nowadays. It can be defined as the condition in which environmental demands exceed the individual's ability to cope, resulting in behavioral and mood changes [80]. Psychological stress determines the deliverance of corticotropin-releasing hormone (CRH), adrenocorticotropin (ACTH), glucocorticoids, catecholamines, epinephrine (adrenaline), and norepinephrine (noradrenaline) into the bloodstream in response to the unfavorable conditions [81]. If the stress response is persistent, those hormones may trigger adverse physiological events and exacerbate the stressful condition [82]. The skin and brain are strictly connected: the brain delivers signals to the skin that influences its stress response, mainly through the hypothalamic-pituitary-adrenal

(HPA) axis, while the skin cells, in turn, produce a CRH, ACTH, epinephrine, and their receptors, triggering autocrine pathways and regulating the endocrine and immune systems [83]. Catecholamines stimulate keratinocyte differentiation by inducing keratin, involucrin, and transglutaminase [84] and exacerbate atopic dermatitis in an inflamed state via the continuous induction of a cytokine cascade [85].

Moreover, catecholamines, which are overproduced during psychological stress, impair the skin barrier's recovery, reducing the accumulation of epidermal lipids—mainly cholesterol, fatty acids, and ceramides—by suppressing their synthetic pathways [86]. Chronic psychological stress strongly increases reactive oxygen species in mice skin, which dramatically accelerates skin aging [87]. Oxidative stress in the skin is strictly related to the formation of age spots too. The accumulation of oxidized lipids and proteins culminates in the formation of lipofuscin particles responsible, together with melanin, for dark spots [88] that the hydrolase enzymes hardly degrade.

Plant cell cultures are becoming a popular source of cosmetic ingredients with proven efficacy [89], where their safety and sustainability have been very much requested by the skincare market [90].

This study evaluated the activity of an extract from *Ficus carica* cell suspension cultures to alleviate skin damage caused by psychological stress using in vitro and in vivo analyses.

4.1.1 *Ficus carica*

Moraceae is an angiosperm plant family rich in edible species characterized by milky latex in all parenchymatous tissue, unisexual flowers, anatropous ovules, and aggregated drupes or achenes. Moraceae are divided into five tribes; between them, Ficeae are monotypic with a pantropical distribution and ~750 species [91]. Ficus is one of the thirty-seven genera of this family, and its distribution in America consists of over 100 species divided into two subgenera: Ficus subg. *Urostigma* (Gasparrini) Miq. sect. *Americana* Miq. and *Ficus* subg. *Pharmacosycea* (Miq.) Miq. sect. *Pharmacosycea* [92]. *Ficus* spp. represents an ancient source of food and health; its importance is as remarkable as to be named in several chapters of Christian sacred texts, the Gospels [93].

The fig species of most significant commercial importance is *Ficus carica* L. (syn. *Ficus kopetdagensis* Pachom.), also known as the common fig, which consists of numerous varieties with significant genetic diversity [94,95] (Figure 4.1).

Common fig tree originated in the Middle East and is one of the first humans cultivated plants; nevertheless, several Ficus spp. are used as food and medicinal properties in ayurvedic and traditional Chinese medicine, especially amongst people who live where these species grow [96].

Figure 4.1. *Ficus carica*

The plants are shrubs or small trees; the foliage is single, alternate, and large, deeply lobed with three or seven lobes, rough and hairy on the upper surface and soft, hairy on the underside; the bark is smooth and grey.

Various biological activities, such as antibacterial [97], antiviral and antioxidant, have been evaluated and confirmed on *F. carica* organic extracts.

Thus, *F. carica* has been included in occidental Pharmacopoeias (i.e., Spanish Pharmacopoeia, British Pharmacopoeia) and therapeutic guides of herbal medicines, as crucial as the PDR for Herbal Medicines (2000).

F. carica represents an extraordinary and ancient source of medicines and food in the human culture, and appreciated now and extremely promising in the future, *F. carica* illustrates an exciting example of cosmetic ingredient.

4.1.1.1 *Ficus carica* : chemical properties

Several secondary metabolites have been isolated from different parts of *F. carica* (leaves, fruits, roots, latex) and their biosynthetic origins.

Nevertheless, a generalization can be made: flavonoids have been isolated mostly from fruits and leaves, coumarins from leaves and roots, sterols from leaves, and triterpenoids from latex (mainly as steryl derivatives) and roots.

Most compounds characterized and reported in essential oils are monoterpenes and sesquiterpenoids, showing different oxidation patterns.

No reports were found about the isolation of alkaloids from *F. carica*, except for indole [98].

4.1.1.2 *Ficus carica* : functional properties

The importance of *F. carica* as an alternative to cure some illnesses has been recognized through the centuries, and nowadays, it is included in several pharmacopeias and books dedicated to herbal medicines.

A recent revision performed with plants used as medicines at the central region of Córdoba province in Argentina reported that heated, dried fruits of the 'higuera' are used to facilitate the maturation of skin pustules and furuncles with its direct application.

In addition, latex is usually applied locally to treat warts [99].

Some biological activities of *F. carica*, namely, antioxidant, acetylcholinesterase inhibition, antifungal [100], anti-helminthic [101], and anticarcinogenic [102], have been reported. Parts (fruits leaves, twigs) of *F. carica* are reported, either fresh or dry, to treat tumors and inflammatory syndromes.

In the European Union, pulverized *F. carica* fruit is authorized for use in cosmetic products as a skin conditioning agent, fruit extract as a humectant (a substance capable of retaining moisture), juice of fruits as an astringent, and fig water (aqueous solution of the steam distillate obtained from the fruit) with a masking function (to reduce or inhibit the primary odor of a cosmetic).

4.2 Study Design

Ficus carica cell suspension culture extract (FcHEx) was tested in vitro (on keratinocytes cells) and in vivo to evaluate its ability to manage the stress-hormone-induced damage in the skin.

The FcHEx action on reducing the primary stress mediator was tested in vitro with several essays:

- The activity of the FcHEx on Epinephrine Signaling
- The activity of the FcHEx on the Inflammatory Cytokine IL-6
- Lipid Peroxide Measurements
- Carbonylated Protein Determination
- The activity of the FcHEx on the Ceramide Production

Stress induces the release of catecholamines through the sympathetic-adrenal medullary (SAM) axes. The inner layer of the adrenal medulla releases epinephrine (adrenaline) and norepinephrine (noradrenaline) upon activation by stress.

They are the critical components of the “fight or flight response”: acceleration of heart rate and respiration, constriction of blood vessels except in the muscles, increased perspiration, and dilation of the pupil.

Epinephrine acts by binding to various adrenergic receptors, leading to decreased skin blood flow and altered immune and inflammation functions, including lymphocyte trafficking, circulation, proliferation, and cytokine production [103-105]

In monocytes and dendritic cells, adrenergic signaling can inhibit IL-12 production via increasing cAMP, thus blunting TH1 response and promoting TH2 differentiation [106]. It also has an impact on the production of various cytokines in dendritic cells [107].

The skin also holds a peripheral catecholamine system where epinephrine is synthesized in keratinocytes while the adrenergic receptors are present in both epidermal keratinocytes and melanocytes [108]. In keratinocytes, after epinephrine activates the β_2-adrenoceptor, it induces a significant increase in cAMP, which in turn increases calcium concentration through protein kinase C (PKC) activation [109-110]. Since calcium levels can regulate both epidermal proliferation and differentiation, epinephrine can affect epidermal health.

Here the importance to investigate the capacity of the FcHEx to affect the epinephrine signal cascade in the skin cells through the first essay.

Consequently, the synthesis of inflammatory cytokines through cAMP is less activated to ensure that the IL-6 gene expression in stimulated cells treated with FcHEx was monitored.

Stress prompts the body to produce internal free radicals that target cells for destruction and cause oxidative stress. When free radicals target lipids, it leads to dehydration and skin barrier damage, and acne. The FcHEx's ability to reduce the oxidative stress induced by epinephrine was investigated by measuring the lipid peroxide production in keratinocytes.

On the same line, reducing carbonylated protein levels in stressed keratinocytes is associated with reducing protein oxidation.

In the end, ceramides are necessary elements for the lipid barrier performance, so to investigate the FcHEx's ability to preserve the epidermal skin barrier against epinephrine stress, the extract's ability to induce its production was monitored.

The relationship between psychological stress and skin parameters, such as TEWL, exfoliation, sebum, pH, and skin color, was investigated in 40 pharmacy students without coexistent skin disease.

In this way, the in vitro test results were confirmed by a double bind clinical trial performed at the RD Cosmetic of the Federico II University (Naples, Italy).

All skin parameters were assessed at an initial period of presumed lower stress, after return from winter vacation (January 2020 = T_0), approximately 2 weeks later, during examination week (February 2020 = T_{2w} acute stress time), and at a lower stress occasion, approximately two weeks after examinations (T_{4w} = recovery stress time).

The study subjects, who ranged in age from 22 to 27 years, were 38 F and 2 M.

Vitalab Srl commissioned the study to evaluate the ability of the FcHEx, inserted in an o/w emulsion, to protect the skin during acute stress.

The test site identified was the students' cheeks. Measurements of TEWL, Sebum quantity, Desquamation, Skin Colour, and pH were carried out (T_0).

Twenty volunteers received the active product (with 0.5 % of FcHEx), whereas the other twenty the Placebo, randomly, in double-blind.

The first product application was conducted at the Research Lab to show volunteers the correct conditions of the test product use. The treatment was carried out for four consecutive weeks with a twice-per-day application (morning and evening). Skin control parameters were re-measured reliably after 2 (T_{2w} = Acute stress Time) and

4 weeks (T_{4w} = Recovery Stress Time) to evaluate the antistress effects of the tested products.
Analysis of skin parameters (Figure 4.2) was carried using :

- Tewameter® TM300
- Sebufix® F16 and Corneofix® F20 applied to a Visioscan® camera
- Colorimeter CL400®
- Skin-pH-Meter PH 905

All the instruments were by C+K electronic GmbH, recognized as a standard in cosmetology studies.

Figure 4.2. Skin parameters analyzed

4.3 Materials and Methods

4.3.1. In Vitro Studies

4.3.1.1. Plant Cell Culturing and Extract Preparation

A certified fig plant (*Ficus carica*) was obtained from a local nursery ("Vivai Milone," Lamezia Terme, Calabria Region, Italy). The leaves were surface sterilized with 70% (v/v) EtOH (Sigma Aldrich, St. Louis, MO, USA), followed by a treatment with 1 % bleach (supplemented with Tween 20 (Sigma Aldrich, St. Louis, MO, USA)), and finally rinsed with sterile distilled water.
Then, the leaves were excised into 0.5 – 1.0 cm segments and cultured on solidified Gamborg B5 medium (Merk, Darmstadt, Germany) containing 500 mg/L myo-inositol, 30 g/L sucrose, phytohormones, and 8 g/L phytoagar.

The explants were subcultured every four weeks onto a fresh medium for three months. Once a compact and friable callus was obtained, the cells were transferred to the liquid Gamborg B5 medium, supplemented with 500 mg/L myo-inositol, 30 g/L sucrose, 1 mg/L adenine, and phytohormones.
The suspensions were shaken on a rotary shaker at 27 °C, with a 16-h daily photoperiod. Once the liquid suspension cultures of about 200 g/L were obtained, the cells were collected, lysed in a water-based buffer, and lyophilized to prepare a water-soluble extract. The powder (*Ficus carica* hydrosoluble extract (FcHEx)) was dissolved in water or cell culture media at appropriate testing concentrations.

4.3.1.2. Skin Cells and Explants

Immortalized Human Keratinocytes (HaCaT), purchased from Addexbio Technologies (San Diego, CA, USA), were maintained in Dulbecco's Modified Eagle Medium (DMEM; Sigma Aldrich, St. Louis, MO, USA) that was supplemented with 10 % fetal bovine serum (FBS; Sigma Aldrich, St. Louis, MO, USA) in 95 % air, 5 % CO_2, and humidified atmosphere at 37 °C.
Skin explants were obtained from the skin of healthy female donors (aged 35 – 49) following mastectomy or breast reduction procedures at the Villa Cinzia surgery center (Naples, IT).
The use of skin tissue was done according to the Declaration of Helsinki, and all patients had given their written informed consent.
Skin punch biopsies (8 mm) were obtained from skin explants and cultured in 24-transwell plates in DMEM/FBS plus antibiotics in air-liquid conditions at 37 °C in 5 % CO_2 humidified air.

4.3.1.3. Gene Expression Analysis

A total of 2×10^5 HaCaT were seeded in six-well plates, incubated for 16 h, and then treated with the FcHEx or ICI-118,551 (Sigma Aldrich, St. Louis, MO, USA) for 4 h in the presence of 10 µM of epinephrine (Sigma Aldrich, St. Louis, MO, USA).
At the end of the incubation, total RNA was extracted with the GenElute Mammalian Total RNA Purification Kit (Sigma Aldrich, St. Louis, MO, USA) and treated with DNAse I (Sigma Aldrich, St. Louis, MO, USA) at 37 °C for

30 min. Reverse transcription was performed using the RevertAid™ First Strand cDNA Synthesis Kit (Thermo Fisher Scientific, Dallas, TX, USA).

RT-PCR was performed with the Quantum RNA™ kit (Thermo Fisher, Waltham, MA, USA) containing specific primers to amplify 18S rRNA and competimers that reduced the amplified 18S rRNA product within the range to be used as an endogenous standard. The amplification reactions were performed using the Mastercycler™ ProS (Eppendorf, Milan, Italy) with the following general scheme: 2 min at 94 °C, followed by 35 cycles of 94 °C for 30 s, 50 °C for 30 s, and 72 °C for 30 s, with a 10 min final extension at 72 °C.

The PCR products were loaded onto 1.5 % agarose gel (Merk, Darmstadt, Germany), and the amplification bands were visualized and quantified with the Geliance 200 Imaging system (Perkin Elmer, Waltham, MA, USA). The amplification band corresponding to the analyzed gene was normalized relative to the amplification band corresponding to the 18s and reported as a percentage of untreated controls (fixed at 100 %).

The RT-PCRs were done in triplicate, where the average results are reported in the graphs.

The sequences of the used primers were as follows:

- interleukin 6 (IL-6) forward (Fw)—GTCCTGATCCAGTTCCTGCAG
- IL-6 reverse (Rv)—CTACACTTTCCAAGAAATGATC (gene ID: 3569)
- β-glucocerebrosidase (GBA) Fw—AGTTGCACAACTTCAGC
- GBA Rv—GTCCAGGTACCAATGTAC (gene ID: 2629)

4.3.1.4. Determination of the Lipid Peroxides

A total of 1.8×10^4 HaCaT were seeded in 96-well plates and then treated with the FcHEx or ICI-118,551 for 24 h. After incubation, the cells were washed in phosphate-buffered saline (PBS; Sigma Aldrich, St. Louis, MO, USA) and then incubated with the dye C11-Bodipy (Thermo Fisher, Waltham, MA, USA) at 37 °C for 30 min. A total of 50 µM of epinephrine was used to induce lipid peroxidation, and the fluorescence was read at 510/580 using the Victor3 plate reader system (Perkin Elmer, Waltham, MA, USA).

4.3.1.5. Lipofuscin Measurements

A total of 8×10^3 HaCaT were seeded in a 96-well plate and then treated with the FcHEx for 24 h. A total of 50 nM of epinephrine was added to the cells and incubated for an additional 48 h. The cells were then washed in PBS and incubated with Sudan Black (Sigma Aldrich, St. Louis, MO, USA) (0.7% dilution in EtOH 70 %) for 5 min.

After that, they were lysed in 1 M of NaOH (Sigma Aldrich, St. Louis, MO, USA) for 20 min at 70 °C to solubilize the dye.

The quantity of solubilized dye was determined by reading the absorbance at 595 nm in the Victor3 plate reader system.

4.3.1.6. Epidermal Lipid Measurements

A total of 1.0×10^4 HaCaT were seeded in 96-well plates, grown for 48 h, and then treated with the FcHEx or ICI-118,551 as a positive control for an additional 24 h. The cells were incubated with 10 µM of epinephrine for 24 h, and the lipid accumulation was detected via the addition of the AdipoRed assay Reagent (Lonza, Basel, Switzerland).

The fluorescence at 485 nm was read using the Victor3 plate reader system, and the content of the epidermal lipid was normalized relative to the cell density determined by crystal violet staining.

4.3.1.7. Measuring of Carbonylated Proteins in Cells and Skin Explants

1.5×10^4 HaCaT were seeded in 96-well plates and then incubated with the FcHEx or ICI-118,551 in the presence of epinephrine 50 µM for 24 h.

The cells were washed in PBS and fixed in 4 % paraformaldehyde (PFA; Sigma Aldrich, St. Louis, MO, USA). After washing in PBS + 0.05 % Tween 20, the samples were incubated with 5 mM 2,4-Dinitrophenyl-hydrazine (DNPH; Sigma Aldrich, St. Louis, MO, USA) in 2N HCl (Sigma Aldrich, St. Louis, MO, USA) for 1 h at room temperature. The carbonylated products were detected via ELISA using a specific antibody against DNP (sc69697, Santa Cruz Biotechnology, Heidelberg, Germany).

The skin punches were treated with the FcHEx in the presence of 56 nM of epinephrine for 24 h. After incubation, the punches were fixed with PFA for 6

h, washed in PBS, and then incubated in 15 % and 30 % sucrose (Sigma Aldrich, St. Louis, MO, USA).

The punches were embedded in optimal cutting temperature (OCT) medium (Tissue Tek, Sakura Finetek USA, Inc., Torrance, CA, USA), frozen in dry ice, and stored at − 80 °C. Cryosections (10 µm) were obtained using the CM1520 cryostat (Leica Microsystems, Wetzlar, Germany). The slides were incubated with 5 mM DNPH in 2 N HCl for one hour at room temperature, washed in PBS/EtOH (1:1), and then in PBS/Tween 20. The slides were incubated in a blocking buffer (3 % bovine serum albumin (BSA) in PBS) for 30 min, washed with PBS/Tween 20, incubated with the primary antibody anti-DNP (1 : 50 dilution), and then with the secondary conjugated antibody Alexa Fluor 488 (Life Technologies, Carlsbad, CA, USA). Nuclei of the cells were stained using 4′,6-Diamidino-2-phenylindole (DAPI; Sigma Aldrich, St. Louis, MO, USA). The signals were detected using fluorescent microscopy.

4.3.1.8. cAMP Measurements

The HaCaT cells were washed in PBS, detached from the flask with a non-enzymatic dissociation solution (Sigma-Aldrich, St. Louis, MO, USA), and resuspended at the concentration of 106/mL in a stimulation buffer (BSA 0.1 %, isobutylmethylxanthine (IBMX) 0.5 % in PBS) containing Alexa Fluor 647-labeled anti-cAMP antibody (Thermo Fisher Scientific, Dallas, TX, USA). The procedure accords to the protocol described by the provider of the Lance Kit (Perkin Elmer, Waltham, MA, USA).

1.2×10^4 cells were distributed in 384-well plates and treated with either the FcHEx or ICI-118,551 in the presence of 10 µM of epinephrine. In parallel, a standard curve for cAMP (Thermo Fisher Scientific, Dallas, TX, USA) was prepared by diluting known cAMP concentrations in the stimulation buffer in the presence of an anti-cAMP antibody. The cells were incubated for 1 h at room temperature, and then a detection mix containing Europium-W8044-labeled streptavidin and biotin-labeled cAMP (Thermo Fisher Scientific, Dallas, TX, USA) was added to each well.

The cAMP concentration was measured by exciting at 320 nm and recording at 615 and 665 nm using an EnVision instrument (Perkin Elmer, Waltham, MA, USA).

4.3.1.9. Determination of Ficin Amount and Activity

The ficin amount was determined using ELISA: scalar dilutions of the extract were incubated on a 96-well plate at 4 °C for 16 h, the quantity of ficin was calculated using a specific antibody (AS09550, Agrisera, Vännäs, Sweden). Scalar dilutions of the extract were incubated with 0.43 mM of the substrate pGLU-PHE-LEU-pNitroanilide (Sigma Aldrich, St. Louis, MO, USA) in a pH 6.5 phosphate buffer (Sigma Aldrich, St. Louis, MO, USA) to measure the ficin activity. Purified ficin was used as standard starting from 0.015 enzymatic units. The color developed was measured by reading the absorbance at 405nm with the Victor3 multiplate reader system.

4.3.2. In Vivo Studies

An active cream with 0.5 % w/w FcHEx and a Placebo cream were compared to treat volunteers in acute stress skin conditions.
They were examined in a room with controlled temperature and humidity (20 ± 2 °C, 40 ± 5 % RH) at the same time of day after a stationing time of about 30 minutes.
Measurements of the skin parameters were carried out with pre-calibrated devices at pre-established times :

- T_0 = No stress period after the return from winter vacation
- T_{2w} = Acute stress time during examination week
- T_{4w} = Recovery time, approximately 2 weeks after examinations

Panelists had to apply about 2 mg/cm^2 of cream on the face, avoiding direct contact with the eyes and gently massaging until completely absorbed.
The skin parameters were monitored through worldwide recognized cosmetic tools, like Tewameter® TM300.
Sebufix® F 16 and Corneofix® F 20 were applied to a Visioscope PC35® that measured the sebum secretion and skin desquamation.
The Sebufix® F 16 is a special foil that absorbs the skin surface's sebum due to its micropores and shows them as spots of different sizes. The Visioscope® PC35 camera monitored the qualitative sebum production in real-time. The number, size, and area covered with spots (mm^2) were evaluated for five increasing spot sizes,

together with the slope of the sebum development during the measurement time on the cheeks and foreheads.

Corneofix® F 20 special adhesive tapes collected flakes of dead cells, known as corneocytes. The number, size, and thickness of the corneocytes are correlated with the exfoliation of the stratum corneum. When mounted on the Visioscope® PC35 camera, the exfoliation rate can be evaluated.

Finally, Visioface 1000 D was used for the skin pore counting.

The skin lightness evaluation was undertaken using the Colorimeter® CL 400, previously described (Cap. XX Par. XX)

The Skin-pH-Meter PH 905 measured the skin surface pH. The measurement is based on a high-quality combined electrode, where both glass H+ ion-sensitive electrode and additional reference electrode are placed in one housing. It is connected to a probe handle containing the measurement electronics (Figure 4.3).

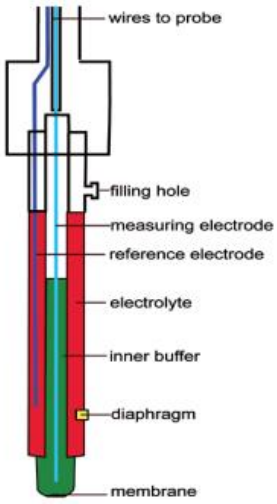

Figure 4.3. Skin pH-meter measurement principle

The data analyses were carried out using CK-MPA-Multi-Probe-Adapter FBQ (C+K Electronic GmbH, Cologne, Germany) software version for Windows® 10.

4.3.2.1. Study Population

Forty healthy volunteers, female (n = 38) and male (n = 2), from all social categories, were enrolled according to these inclusion criteria:

- Healthy Caucasian subjects

- Aged between 20 and 27 years and going through a period of psychological stress two weeks before the examination T_0, the day of the examination (T_{2w} — acute stress time), and two weeks after the examination (T_{4w} — recovery time)
- Sex: female and male
- Phototype: II-IV Fitzpatrick scale
- Subjects who have read and signed the informed consent form written by the investigators
- Subjects with stressed skin, as assessed via CSI analysis
- Subjects who did not apply products other than the one studied on the test area and no product within seven days before the test
- Subjects who agreed to follow the study rules and the planned check-ups
- Subjects who agreed not to expose themselves to UV for the duration of the study

Exclusion criteria:

- Pregnant or breastfeeding women
- Subjects with anamnesis of cutaneous hyper-reactivity or intolerance reactions to cosmetic products/ingredients
- Subjects with diseases in the period immediately preceding the current study
- Subjects undergoing topical or systemic treatment with any drug that may affect the outcome of the test or subjects affected by skin diseases (eczema, psoriasis, lesions)
- Subjects treated with topical retinoids in the previous six months at the start of the study or with systemic retinoids in the previous 12 months
- Subjects who performed treatments with topical products based on alpha and beta-hydroxy acids in the 45 days before the start of the study

4.3.2.2. Cream Composition

The cream with *Ficus carica* cell suspension culture extract (FcHEx) contained two phases:

- **Phase O** (oil phase) polyglyceryl-3 methyl glucose 5.0 %, cetyl alcohol 2 %, and cetearyl alcohol 3 %
- **Phase W** (water phase) containing water (88.8 %), the FcHEx (0.5 %), sodium benzoate 0.5 %, potassium sorbate, and perfume (0.1 %)

The placebo cream contained all the components without the FcHEx.

All components used to produce the creams were bought from ACEF Spa (Fiorenzuola D'Arda, Italy) and Parfum by Farotti Srl (Rimini, Italy).

The two creams were produced by energetically shaking the two phases at 70 °C using a Silverson L5M-A Laboratory Mixer (SBL, Shanghai, China), cooled in an ice bath, and adding the remaining components at room temperature.

Finally, the pH (5.1–5.2) and viscosity (28.179–29.287 mPa; L4, 20 rpm) were tested using a Crison GPL20 pH-Meter (Crison, Barcelona, Spain) and a Visco Basic Plus rheometer (Fungilab, Barcelona, Spain).

4.4 Statistical analysis

The in vitro experiments were performed in triplicates and repeated at least three times. The data are expressed as mean ± standard deviation (SD) of three independent experiments. The statistical tests were performed with the GraphPad Prism version 9 software (GraphPad Software, San Diego, CA, USA). A two-way analysis of variance (ANOVA) was used, followed by a Tukey's multiple comparisons post-test; a p-value lower than 0.05 was considered statistically significant. The number of asterisks in the graphs indicate the level of significance (*** p-value < 0.001; ** 0.001 < p < 0.01; * 0.01 < p < 0.05).

The in vivo measured average parameters were considered at times T_0, T_{2w}, and T_{4w}. The student's t-test was used to assess whether the differences between the averages were significant, where the significance level was set to $p \leq 0.05$. The

mean value and standard deviation were calculated for the initial, intermediate, and final instrumental data using a spreadsheet by setting:

T_0 = average baseline values, measured in the no stress period

T_{2w} = average acute stress time detected values

T_{4w} = average recovery time detected values

$T_{2w} - T_0$ = average variation value after 2 weeks of treatment

$T_{4w} - T_0$ = average variation value variation after 4 weeks of treatment

This difference is also reported as a relative percentage of variation (Δ%).

4.5 Results

4.5.1. In Vitro Studies

4.5.1.1. Extract Preparation

A hydrosoluble extract was obtained from the *Ficus carica* liquid suspension culture by disrupting the cells in a saline buffer and taking the water-soluble supernatant (FcHEx). *Ficus carica* cell cultures are rich in polyphenols (flavones, flavanones, catechins, anthocyanidins, and phenolic acids) [111]. The concentration of ficin, a sulfhydryl protease with a papain-like activity abundant in the fig latex [112], was measured in the FcHEx using a specific antibody in ELISA presence was already reported in F. carica cell cultures [113]. The concentration of ficin was about 1.48 µg/mg of dried extract, which was higher than that previously reported. The ficin activity was measured using an enzymatic assay and was found to be 0.9 enzymatic units/µg of extract. The extract concentrations to be used in the cellular tests were calculated via the MTT (3-(4,5-dimethylthiazol-2-yl)-2,5-diphenyltetrazolium bromide) cytotoxicity assay on the keratinocyte cell lines (HaCaT), treated with increasing concentrations of the FcHEx (from 0.01 to 0.0002 % w/v). No significant cytotoxicity was recorded at all for the used concentrations (data

not shown). For convenience, the two doses of 0.006 % and 0.002 % of the extract were chosen for all the following experiments.

4.5.1.2. Activity of the FcHEx on Epinephrine Signaling

Keratinocytes were stimulated with epinephrine alone or in the presence of the FcHEx at the two concentrations, and the level of the second messenger cAMP was measured to investigate the capacity of the FcHEx to affect the epinephrine signal cascade in the skin cells. The ICI-118,551 was used as a positive control, inhibiting the β_2 adrenergic receptors [114]. Figure 4.4 shows that FcHEx attenuated epinephrine-stimulated cAMP synthesis by about 40-fold, respectively about 43 % and 24 % at the concentrations of 0.002 % and 0.006 %. As expected, at a concentration of 10 µM, the ICI-118,551 abolished the epinephrine stimulation.

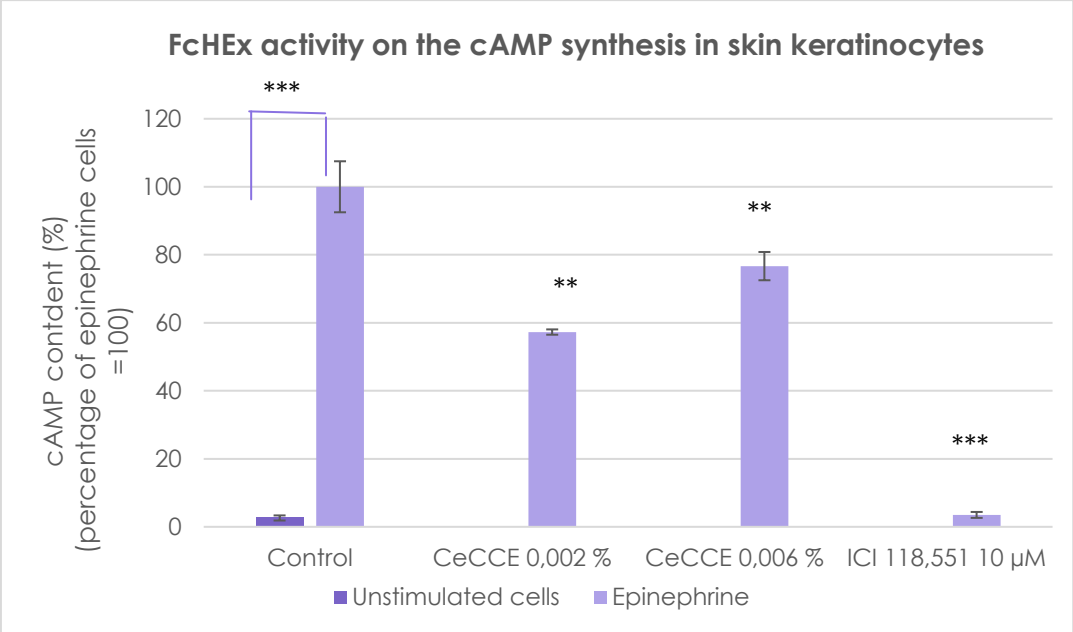

Figure 4.4. Effect of the FcHEx on the cAMP synthesis in skin keratinocytes. The keratinocytes were stimulated with 10 µM of epinephrine alone or with the FcHEx or with a positive control for 30 min and then processed to determine the cAMP content. The reported values represent the averages of three independent experiments and are expressed as the percentages of cells treated with epinephrine only, set to 100 %. The asterisks indicate statistically significant values (*** p-value was between 0.0001 and 0.001; ** p-value was between 0.001 and 0.01).

4.5.1.3. Activity of the FcHEx on the Inflammatory Cytokine IL-6

The IL-6 gene expression was measured in keratinocytes treated with the FcHEx after stimulation with 10 µM of epinephrine, as it activates the synthesis of inflammatory cytokines through cAMP [115].

Figure 4.5 shows that IL-6 gene expression in stimulated cells significantly reduced after treatment with the extract (38.3 % and 35.6 % at 0.002 and 0.006 % concentration, respectively), and the positive control ICI-118,551.

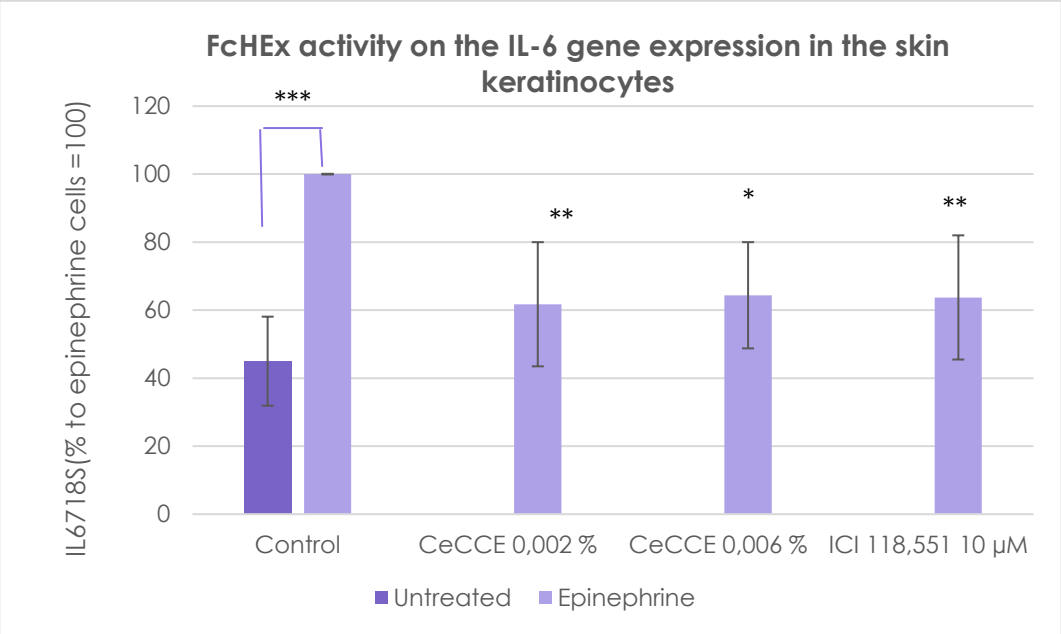

Figure 4.5. Effect of the FcHEx on the IL-6 gene expression in the skin keratinocytes. The keratinocytes were stimulated with 10 µM of epinephrine alone or with the FcHEx or the positive control for 4 h and then processed for RT-PCR analysis. The reported values represent the averages of three independent experiments and are expressed as the percentages of cells treated with epinephrine only, set to 100 %. The asterisks indicate statistically significant values (*** p-value was between 0.0001 and 0.001; ** p-value was between 0.001 and 0.01; * p-value was between 0.01 and 0.05).

4.5.1.4. Lipid Peroxide Measurements

The FcHEx's ability to reduce the oxidative stress induced by epinephrine was investigated by measuring the lipid peroxide production in keratinocytes. As shown in Figure 4.6, 50 µM of epinephrine increased lipid peroxide production by 50 %. Pretreatment with the FcHEx (at both the used concentrations) decreased this event by 25 %.

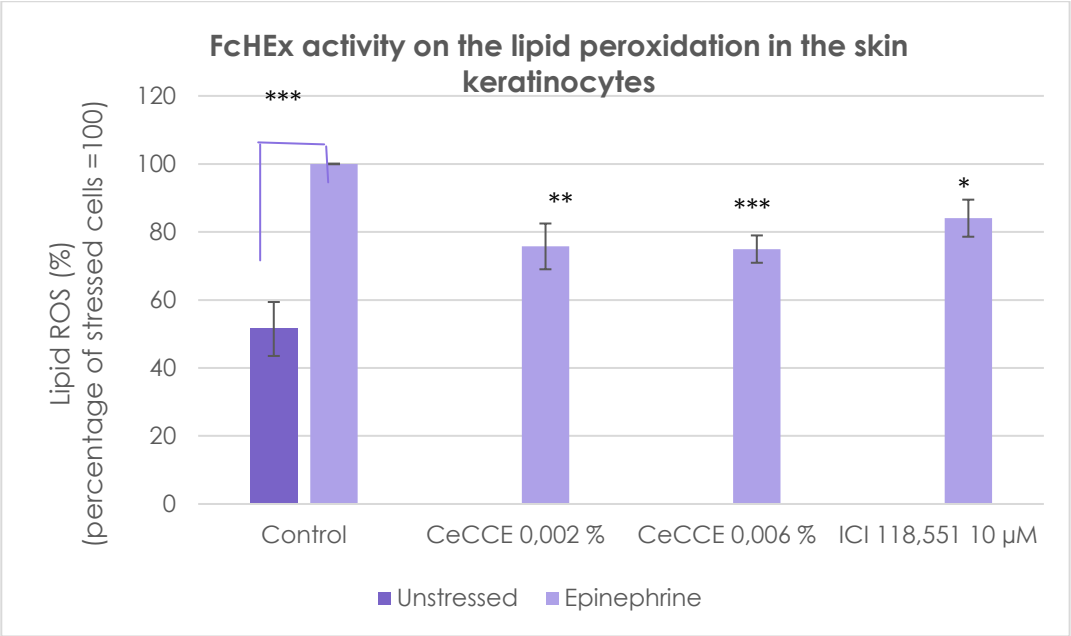

Figure 4.6. Effect of the FcHEx on the lipid peroxidation in skin keratinocytes. The keratinocytes were treated with the FcHEX or the positive control for 24 h, stressed with 50 µM of epinephrine, and then analyzed for lipid peroxide content using C11-Bodipy dye. The reported values represent the average of three independent experiments and are expressed as the percentages of cells treated with epinephrine only, set to 100%. The asterisks indicate statistically significant values (*** p-value was between 0.0001 and 0.001; ** p-value was between 0.001 and 0.01; * p-value was between 0.01 and 0.05).

4.5.1.5. Carbonylated Proteins Determination

The concentration of carbonylated proteins was measured in the keratinocytes stressed with epinephrine 50 µM and then treated with the FcHEx using a specific antibody to verify whether the lipid peroxide inhibition was associated with a reduction in protein oxidation. Epinephrine increased protein carbonylation by 40 %, significantly inhibited by the extract (about 50 %) and the inhibitor ICI-118,551 (Figure 4.7).

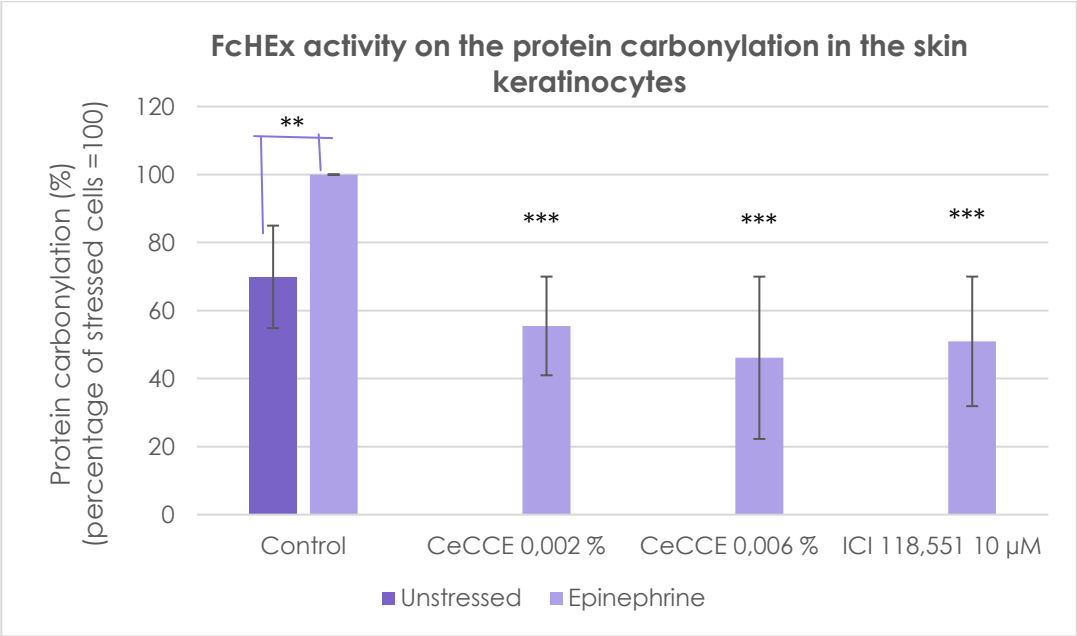

Figure 4.7. Effect of the FcHEx on the protein carbonylation in the skin keratinocytes. The keratinocytes were treated with the FcHEx or the positive control in the presence of 50 µM epinephrine for 24 h, fixed with formaldehyde, stained with DNPH (2,4-dinitrophenylhydrazine), and incubated with the specific antibody. The reported values represent the averages of three independent experiments and are expressed as the percentages of cells treated with epinephrine only, set to 100%. The asterisks indicate statistically significant values (*** p-value was between 0.0001 and 0.001; ** p-value was between 0.001 and 0.01).

The protection against protein carbonylation of the FcHEx was evaluated in the skin explants as well. Three punches from biopsy explants were topically treated for each condition. The induction of protein carbonylation was achieved with 56 nM of epinephrine, corresponding to the hormone dose found in psychologically stressed individuals' blood plasma [116]. After epinephrine treatment, the level of carbonylated proteins increased by about 45 %, while the treatment with the FcHEx 0.002 % reduced this effect by 50 %, analogously to the inhibitor drug (Figure 4.8).

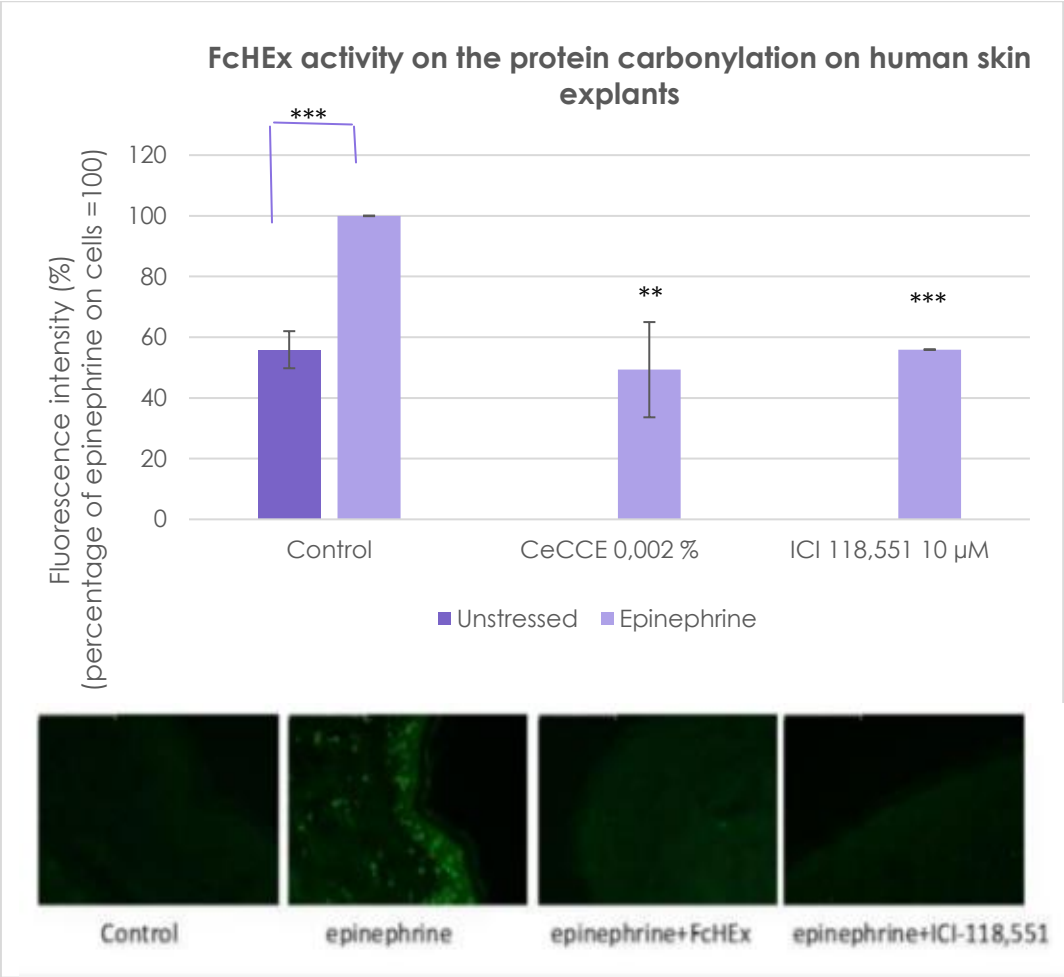

Figure 4.8. Effect of the FcHEx on the protein carbonylation in the human skin explants. Human skin punches, derived from aesthetic surgical biopsies, were treated with the FcHEx or the positive control in the presence of 56 nM of epinephrine. The reported values represent the averages of three independent experiments and are expressed as the percentages of skin explants treated with epinephrine only, set to 100 %. The asterisks indicate statistically significant values (*** p-value was between 0.0001 and 0.001; ** p-value was between 0.001 and 0.01).

4.5.1.6. Lipofuscin Measurements

The cells were stressed with epinephrine in the absence and presence of the extract, and the concentration of lipofuscin particles was measured as the accumulation of oxidated compounds, either lipids or proteins, which can often determine lipofuscin production. The treatment with epinephrine significantly increased the lipofuscin accumulation; in contrast, the treatment with both concentrations of the FcHEx decreased significantly (Figure 4.9).

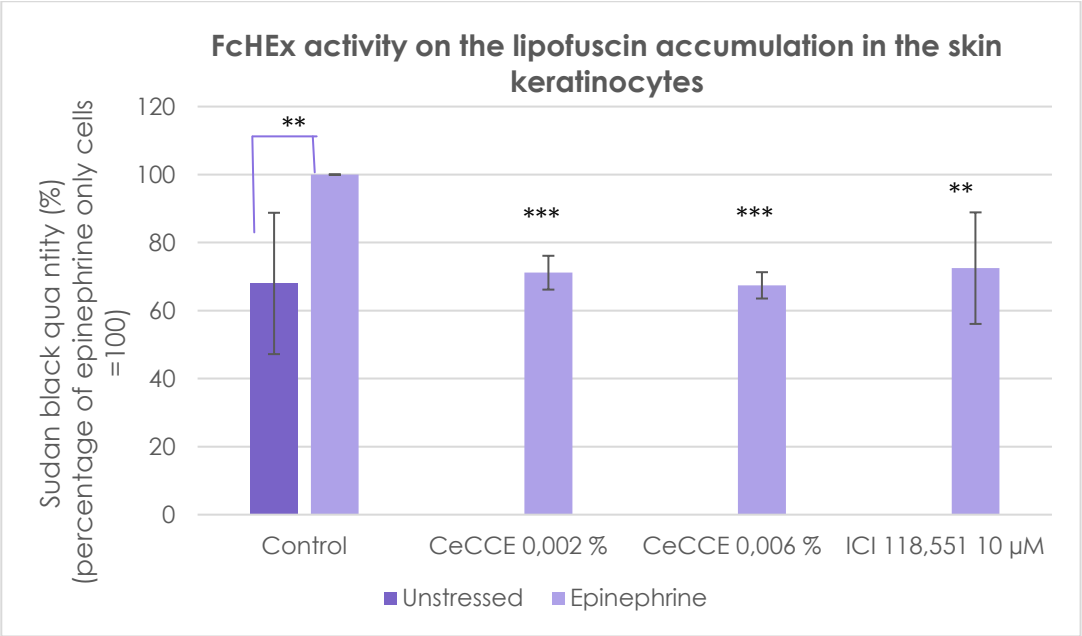

Figure 4.9. Effect of the FcHEx on the lipofuscin accumulation in the skin keratinocytes. The keratinocytes were treated with the FcHEx or the positive control for 24 h, 50 nM of epinephrine was added to the cells incubated for 48 h. At the end of the incubation, the cells were stained, and the absorbance at 595 nM was measured. The obtained values were normalized relative to the protein content determined using a Bradford assay. The reported values represent the averages of three independent experiments and are expressed as the percentages of cells treated with epinephrine only, set to 100 %. The asterisks indicate statistically significant values (*** p-value was between 0.0001 and 0.001; ** p-value was between 0.001 and 0.01).

4.5.1.7. Activity of the FcHEx on the Ceramide Production

The gene expression of the GBA enzyme, which is responsible for the hydrolysis of glucocerebrosides into ceramides, and the amount of newly synthesized ceramides were measured to investigate the FcHEx's ability to preserve the epidermal skin barrier against epinephrine stress. The treatment with the FcHEx increased the GBA expression by almost 150 % in cells stressed with epinephrine (Figure 4.10).

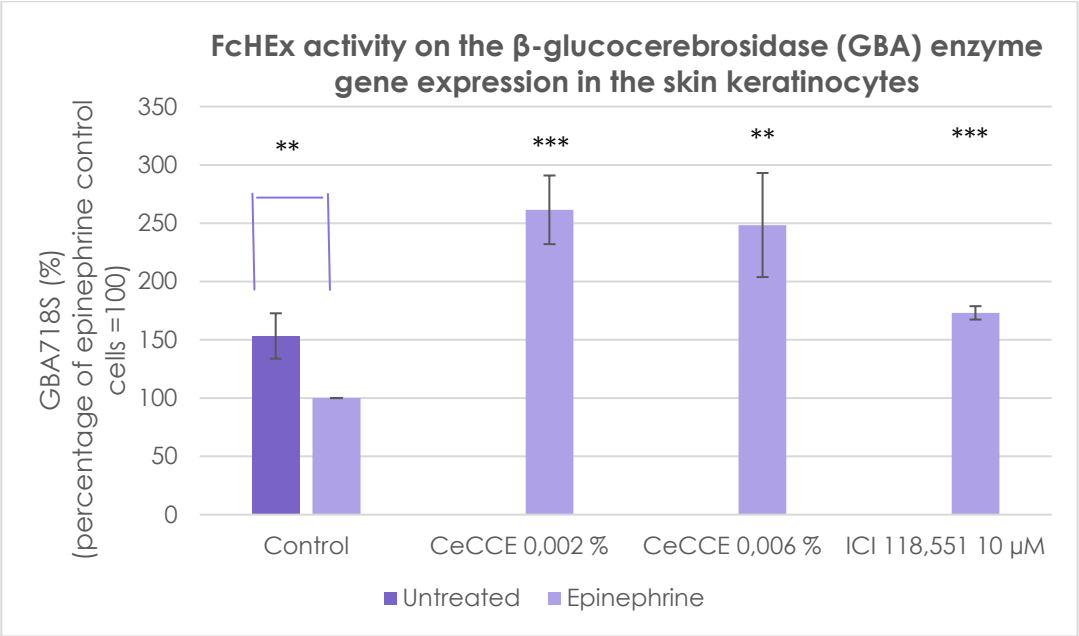

Figure 4.10. Effect of the FcHEx on the β-glucocerebrosidase (GBA) enzyme gene expression in the skin keratinocytes. The keratinocytes were stimulated with 10 µM of epinephrine alone or with the FcHEx or the positive control for 4 h and then processed for RT-PCR analysis. The reported values represent the averages of three independent experiments and are expressed as the percentages of cells treated with epinephrine only, set to 100 %. The asterisks indicate statistically significant values (*** p-value was between 0.0001 to 0.001; ** p-value was between 0.001 to 0.01).

The concentration of ceramides was measured using Nile red staining in cells stressed with epinephrine and treated with the FcHEx. The ceramide content decreased in the epinephrine-treated keratocytes. In contrast, it significantly increased when the FcHEx was administered at both the used concentrations (Figure 4.11).

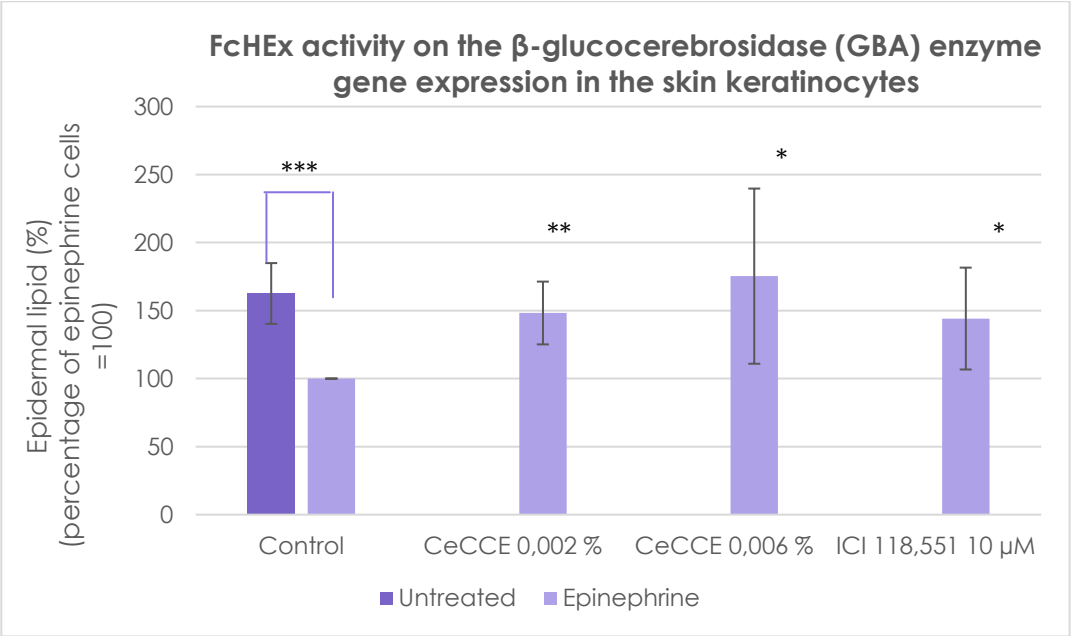

Figure 4.11. Effect of the FcHEx on the epidermal lipid content in the skin keratinocytes. The HaCaT cells were treated with the FcHEx or the positive control for 24 h, then incubated with epinephrine 10 µM for an additional 24 h. The lipid content was measured using an Adipored assay. The values were normalized relative to the cell density determined using crystal violet staining. The reported values represent the averages of three independent experiments and are expressed as the percentages of cells treated with epinephrine only, set to 100 %. The asterisks indicate statistically significant values (*** p-value was between 0.0001 and 0.001; ** p-value was between 0.001 and 0.01; * p-value was between 0.01 and 0.05).

4.5.2. In Vivo Studies

4.5.2.1. Trans Epidermal Water Loss Evaluation

The loss of trans Epidermal water (TEWL) is an indicator of the integrity of the skin barrier; there is a water concentration gradient inside the SC, which is continuously spread from the body to the skin surface and the environment. TEWL refers to the total amount of water lost from the dermal and epidermal tissues to the external environment through the horny state.

TEWL was evaluated by an evaporimeter which measures the water vapor released from a surface, based on the Fick diffusion law, in which the diffusion current provides the quantity of water vapor (g / m^2) which is transported in the time unit (h), so the measurement values will be expressed

in g / hm^2. The smaller is the TEWL, the more the skin barrier remains unaltered.

It is well known that a “Psychological stress perturbs epidermal permeability barrier homeostasis” [117]. Stress is known to affect skin barrier permeability and negatively alter TEWL values.

As shown in Figure 4.12 (a,b), the FcHEx cream counteracted the TEWL increase. During acute stress, i.e., after two weeks of treatment (T_{2w}), a peak in the TEWL values of the placebo group was observed, while the FcHEx cream abolished this increase.

After further two weeks, during the recovery time (T_{4w}), TEWL in the FcHEx group reduced by 12.2 %, showing barrier recovery efficacy and epidermal barrier function reinforcement, while the placebo showed no significant effect.

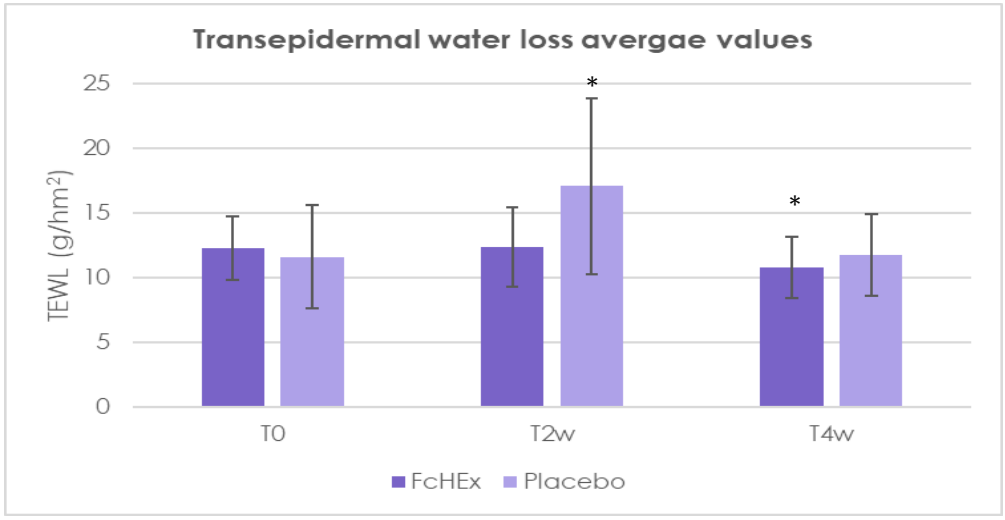

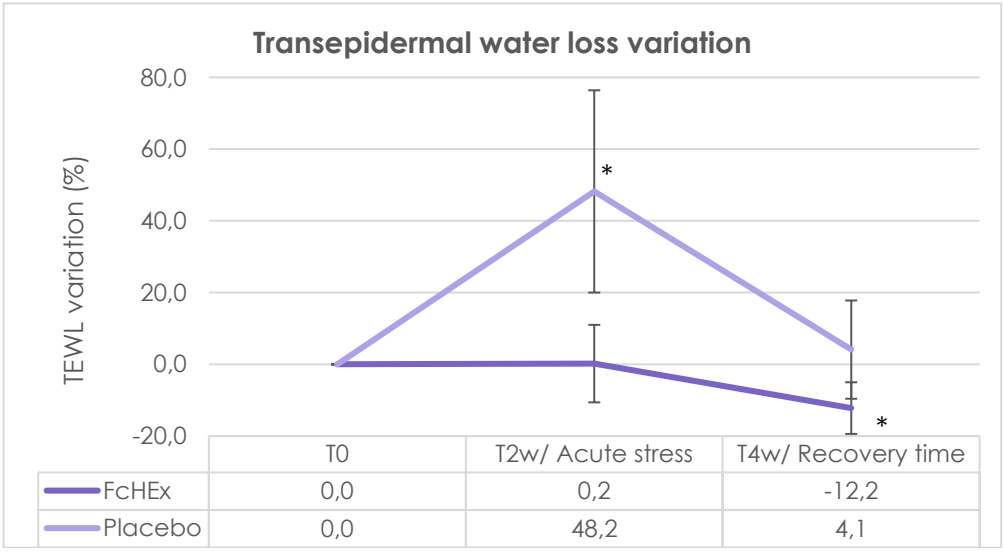

	T0	T2w/ Acute stress	T4w/ Recovery time
FcHEx	0,0	0,2	-12,2
Placebo	0,0	48,2	4,1

Figure 4.12. Transepidermal water loss evaluation. a) TEWL average values, b) TEWL average percentage variation, at time T_0 (baseline), T_{2w} (after two weeks treatment—acute

stress), and T_{4w} (after four weeks treatment—recovery time). Asterisks indicate statistically significant values (* p-value was between 0.01 and 0.05).

4.5.2.2. Skin Sebum and desquamation level detection

Students face several skin concerns during the examination period, like increased acne severity that is significantly associated with stress levels [118]. Moreover, an acute stress response triggered by an exam situation can cause an acceleration of cellular turnover [119].

The sebum and exfoliation rates were assessed using a Sebufix® F 16, and a Corneofix® F 20 applied to a Visioscope® PC35 camera.

After two and four weeks of treatment, a statistically significant decrease in the sebum face concentration in the FcHEx cream group was recorded.

More precisely, sebum production on the cheek decreased by 46.6 % after two weeks (during the acute stress) and 73.8 % after four weeks (recovery time). On the same line, the skin exfoliation underwent a significant decrease in volunteers treated with the FcHEx cream (T_{2w} = − 13.0 %, T_{4w} = − 45.7 %). Placebo cream did not show action on the sebum production and skin cell renewal control. (Figure 4.13 a, b).

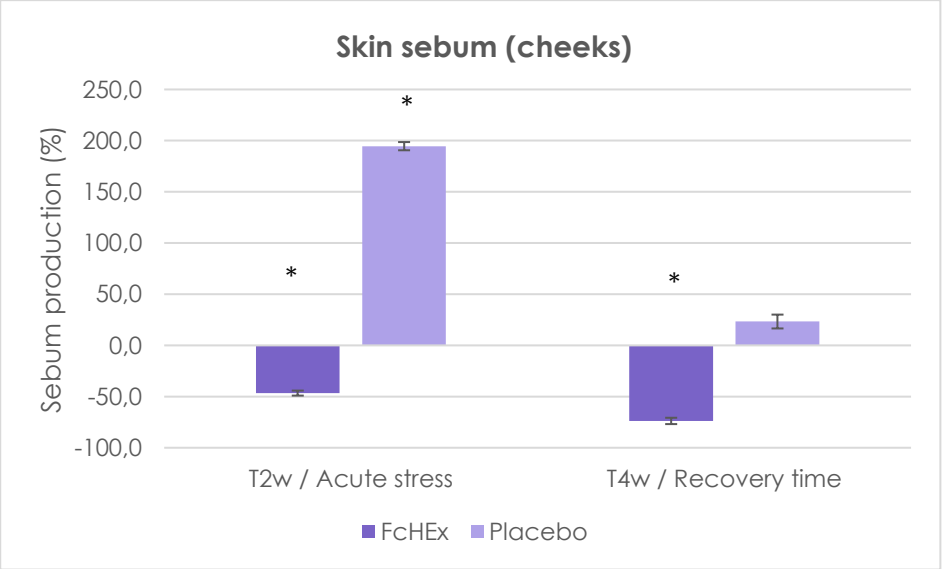

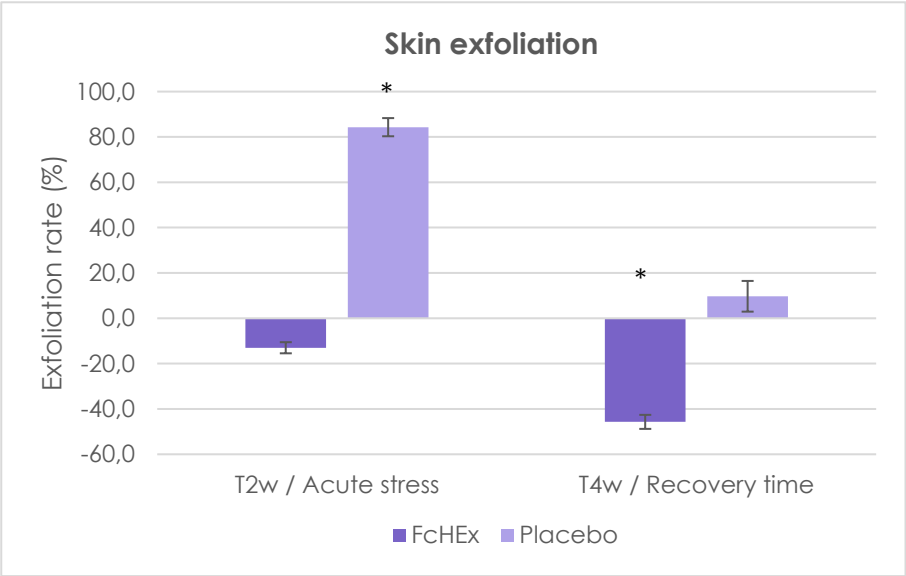

Figure 4.13. a) Sebum production and b) skin exfoliation average percentage variation after 2 and 4 weeks of treatment (T_{2w} - acute stress and T_{4w} – recovery time). Asterisks indicate statistically significant values (* p-value was between 0.01 and 0.05).

4.5.2.3. Skin Lightness

Literature reports that during acute stress, the sympathetic axis, with its mediators' adrenaline and noradrenaline, is responsible for the startle response, that is: increased blood pressure and heart rate; blood vessel dilation in heart, lungs, muscles; blood vessel constriction in bowels, kidneys, skin; sweat secretion; and catabolic metabolism with increased glycogenolysis, lipolysis, and protein metabolism. The activation of this axis is easily visible on the skin by its turning pale [119].

Colorimeter® CL 400 measured the skin lightness, L* value can range from 0 (= black colors) to 100 (= white). The recorded L* values increased both in the FcHEx group (T2w = 1.9 %, T4w = 2.7 %) and in the placebo users (T2w = 4.3 %, T4w = 0.8 %), but the volunteers that used the placebo showed paler faces during the acute stress (T2w) than the group used the active cream (Figure 4.14 a). Then this parameter is valid to assess the paleness of the skin undergoing a biological stress condition.

Although the skin paleness triggered by periods of stress is known, it is equally common in literature; it is also reported that the skin manifests an evident redness [119].

Anxiety can also cause the skin to be redder/pinker - especially around the face and head. This condition is caused by capillaries in the face dilating, which allows more blood and makes a face noticeably red.

The detection of skin redness is possible through the Colorimeter a*-value proportional to the erythema (microcirculation/redness of the skin). FcHEx cream can decrease the a* value in the treated group, so volunteers' skin is less red during stress time (- 3.2 % and - 4.2 %, respectively, at T_{2w} and T_{4w}). The Placebo cream could not fight the acute stress skin disease showing a significant skin redness on volunteers + 14.1 % (T_{2w}), especially around the face. The skin redness decreased (+ 2.5 %) in the recovery time, demonstrating its correlation with the stressing period. (Figure 4.14 b)

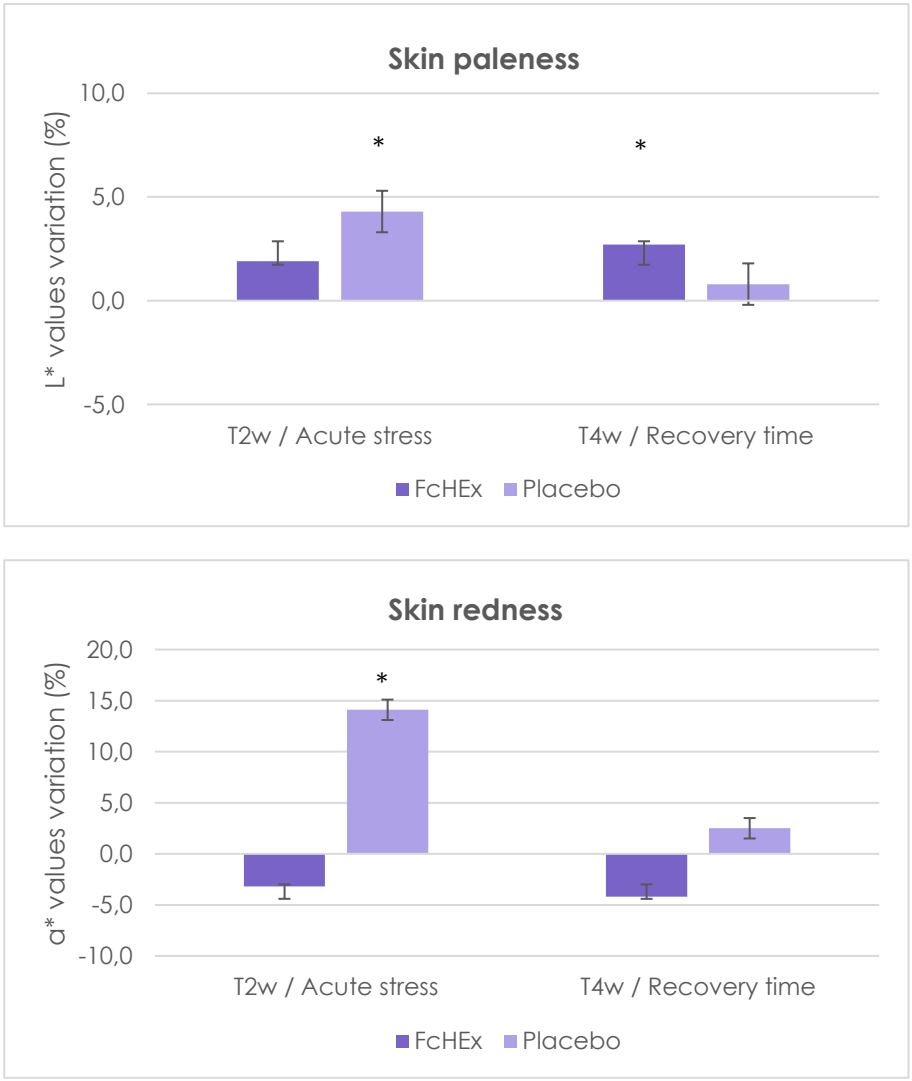

Figure 4.14. Skin paleness evaluation. Skin lightness values average variation after two and four weeks of treatment (acute stress time and recovery time, respectively. (* p-value was between 0.01 and 0.05).

4.5.2.4. Skin pH

A skin pH meter measured the pH on the skin surface. The FcHEx cream normalized and maintained the volunteers' face pH in a normal range (5.5 – 6) during the acute stress. In contrast, the placebo could not counteract the increasing skin pH during acute stress (at T_{2w} pH = 6.05; Figure 4.15).

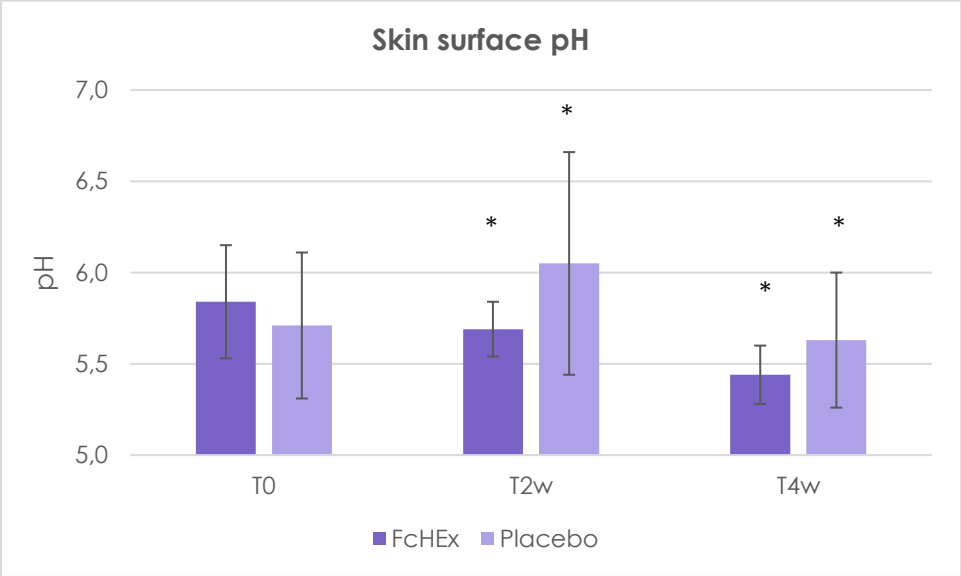

Figure 4.15. Skin pH evaluation. The skin pH values at baseline (T_0), T_{2w} (2-week-treatment, acute stress time), and T_{4w} (4-week-treatment, recovery time). Asterisks indicate statistically significant values (* p-value was between 0.01 and 0.05).

4.6 Discussion

Psychological stress is the process by which the environmental requirements exceed a person's capacity to adapt, leading to emotional, behavioral, and physiological changes 80. Chronic stress-induced augmentation in glucocorticoids, epinephrine, and norepinephrine release can accelerate aging [120], bacterial colonization, and human peptide protection [121,122]. Stressful conditions, such as those of a chronically ill patient undergoing treatment, might decrease the leukocyte telomere length and telomerase activity, accelerating cellular senescence and decreasing life expectancy [123]. These changes depend on β_2-adrenoceptor activation by catecholamines, causing DNA damage and p53 suppression [124]. Oxidation and inflammation processes enhance neutrophil elastase and matrix

metalloproteinase-8 (MMP-8) production, which leads to collagen and elastic fiber degradation and wrinkle formation [125]. Research on new cosmetic materials to relieve psychological stress diseases of the skin has been actively pursued. Natural ingredients are generally safer to use than synthetic materials [126]. In this study, a hydrosoluble extract of Ficus carica cell suspension cultures (FcHEx), a known source of ficin and phenolic compounds [127], was characterized for its capacity to protect skin cells against the oxidative damage caused by psychological stress.

In vitro and in vivo experiments were performed to demonstrate the positive action of the FcHEx that can revert oxidative damage on lipids and proteins due to epinephrine's stress-induced effect. Skin cells and neurons share a common embryonic origin, as both express proteins involved in conserved signaling pathways. Psychological stress triggers the autonomic nervous system to release catecholamines, such as epinephrine and norepinephrine, significantly affecting many cell metabolisms and functions, including skin [128]. Epinephrine interacts directly with neutrophils, reducing these cell responses to various cAMP-mediated proinflammatory stimuli [129]. The activation of the epinephrine downstream signals was measured in keratinocytes cells to investigate the capacity of the FcHEx to affect the epinephrine signal cascade in skin cells. The inflammatory process was induced via epinephrine administration in keratinocytes, and the FcHEx significantly reduced the epinephrine stimulation. The cAMP-mediated inflammatory cytokine gene expression was analyzed, and the FcHEx administration reduced the interleukin 6 productions by 50 %.

Moreover, the lipid peroxides production in the keratinocytes was used to test the antioxidant properties of the FcHEx, which showed a significant antioxidant property, decreasing ROS production by 25 %. The lipofuscin test confirmed these data as the treatment with both the FcHEx doses entirely abolished the production of the lipofuscin that was mediated by epinephrine. Carbonylated protein concentration reduction by 50 % in keratinocytes showed that the antioxidant properties of the FcHEx are also linked to an inhibition of the protein oxidation. Experiments conducted in skin explants confirmed the protective effect of the FcHEx against protein carbonylation, suggesting that the antioxidant action of the FcHEx was mainly linked to an inhibition of protein oxidation, which is the main threat to skin functionality and integrity [130]. These results encouraged studying the potential role of the FcHEx in the recovery of the hydrolipidic skin film, which can moisturize

and stop excessive water loss of the skin [131] and protect the epidermal lipid barrier from microbe attacks and physical injuries, supporting skin integrity. HaCaT cells were treated with the FcHEx to verify its action on GBA gene expression, an enzyme that can catalyze ceramide production [132]. The results showed that the GBA expression increased dose-dependent (50 % and 75 % at the concentrations of 0.002 % and 0.006 %, respectively). Furthermore, the content of ceramides by Nile red staining in cells stressed with epinephrine and treated with the FcHEx was measured to confirm the gene expression results.

The biological activity of the FcHEx was confirmed via a clinical evaluation on a group of 40 human volunteers aged between 20 and 27 years, going through a period of psychological stress. For 28 days, twice daily, volunteers had to apply either a cream containing the FcHEx at the concentration of 0.5 % or a placebo cream on the whole face. Parameters such as TEWL, sebum flow, skin exfoliation, skin paleness and redness, and skin surface pH were evaluated. The measurements were carried out during a high-stress condition, namely, a mid-year examination, and after two weeks from the high-stress condition (recovery time).

The TEWL value in the volunteers treated with placebo was higher (48.8 %) than the volunteers treated with the cream containing the FcHEx (active cream − 0.2 %), indicating that the extract restored the regular epidermal permeability barrier homeostasis, which was perturbed by the psychological stress.

Generally, during a student's psychological stress period due to an approaching examination, acne-related symptoms increase [133], and cellular turnover accelerates, depending on the stress levels [134].

The cream containing the Ficus carica extract decreased sebum production and inhibited exfoliation in the clinical tests. Desquamation involves the degradation of corneodesmosomes by enzymes that depend on water and pH for their activity. In the skin, the exfoliation is highest at neutral-to-low alkaline pH levels and decreases at acidic pH levels [135]. The active cream normalized and maintained all volunteers' face pH normal during acute stress, which usually rises in stress conditions. A neutral pH impedes the secretion of polar lipids (glucosylceramides) into mature lamellar bilayers (ceramides), enhancing proteolytic activities and increasing corneodesmolysis aberrations in corneocyte cohesion [136].

Moreover, the skin pH influences the peroxidase activity of the ficin, which is one of the components of the FcHEx that is responsible for the antioxidant activity of the extract [137]. The ficin peroxidase activity was around 60 % or higher at a pH of 4.5–5.0, the pH of normal skin [138]. Finally, whether the skin turned pale was evaluated to test the cream's effect on the sympathetic axis (adrenaline and noradrenaline) activated by the acute stress [134]. A slight increase in L* was observed in volunteers to whom the cream was applied, suggesting a good efficacy of the extract to prevent the facial skin from turning to a pale color due to psychological stress. On the same line, the skin redness (a* values) results higher in the placebo group volunteers, demonstrating the ability of the FcHEx in soothing stressed skins conditions and preventing hives and other types of skin rashes.

4.7 Conclusions

In vitro and in vivo tests demonstrated that the extract from Ficus carica cell cultures alleviated skin damage caused by psychological stress. The FcHEx worked as an anti-stress ingredient that alleviated the negative consequences of stress hormone activity on the skin, such as inflammation, oxidation, alteration of the skin barrier, and skin turning pale. All the data support the conclusion that the Ficus carica cell culture extract has good potential to be employed in skincare products, particularly those formulated for dry and stressed skins.

CHAPTER 5

Mask-proof: the new make-up concept

5.1 Introduction

The COVID-19 disease, spread worldwide since December 2019, has made it necessary to use personal protective equipment (PPE), especially face masks, due to the high transmission rate of COVID -19 [139] and propensity to airborne infection [140].

Wearing masks is essential to prevent the transmission of infectious diseases, but this condition has made it extremely difficult to wear makeup products.

The Japanese market research firm Intage [141] ranked products that had poor sales in 2020. Lipsticks and lip products in general, are at the top of the list due to the widespread use of masks. The decrease recorded is equal to more than half (44 %) compared to the previous year.

Along with lipstick, four other cosmetics are among the top ten products with reduced sales, compared to 2020: blush, foundation, makeup base, and white powder foundation; with the reduced opportunity to exit since the state of emergency was declared in April 2020 and the spread of smart working, makeup has taken on a lower priority in people's lives.

Uneven foundation, smudged lipstick, and blush, smudged and messy masks are the most common discomforts people face when wearing such protective gear.

The manufacturing companies have tried to compensate for this inconvenience by developing new No Transfer products, whereby No Transfer means the ability of a cosmetic product to completely resist the "transfer" from one surface to another, and therefore to remain adhered to the area of original application without "transferring" to the surface with which it comes into contact.

This claim, already popular in the past, has been made more relevant than ever by the COVID-19 [142] pandemic, making it necessary to formulate cosmetics that can meet this performance, now better known as mask-proof.

Figure 5.1. Mask proof make-up

Consumers are looking for companies they can trust to buy products in total safety and keep the promises of product performance by supporting claims through effectiveness tests. This situation is crucial since the implementation of homemade tests that do not provide reliable scientific results, whose implementation methods are almost always contestable and unsubstantiated, and which are misleading for the consumer's choice, appears increasingly widespread on the web.

In light of these factors, it is necessary to subject cosmetic products to reliable, reproducible study protocols, with objective scientific evidence, compliant with European guidelines (Colipa Efficacy Guidelines), which can only be conducted by trained and qualified technical personnel, and with advanced scientific instruments.

In this study the no transfer ability on surgical mask was tested on no-transfer-foundations sold in common beauty shops. The in vivo measurements are conducted with calibrated devices, inside a closed room, maintained at controlled temperature and humidity, on a panel of volunteers selected respecting defined acceptance criteria, functional to the proper conduct of the test. These tools allow

the quantification of parameters of interest, in this case, the entity of the color applied, and the comparison of high-resolution images with lighting conditions, and positioning of the subjects, fixed and reproducible; necessary to obtain clear and indisputable results on the performance of the product.

5.2 Study Design

In determining the mask-proof claim, the study protocol provided for an in vivo no transfer test; for this purpose, we selected transfer and no-transfer foundations and then carried out a colorimetric efficacy test by comparing them.
The selected cosmetic product was subjected to a transfer test, the **mask test**, since the surgical masks were used as a contact surface.
Twenty female volunteers, regular users of cosmetic products, were enrolled in the study. They provided informed consent and underwent objective examinations in a closed room, maintained at controlled temperature and humidity (20 ± 2 ° C, 40 ± 5 % RH) at the same time of day, after a dwell time of approximately 30 minutes.
The study was conducted at the RD Cosmetics – University of Naples Federico II, Pharmacy Department, supervised by Prof. Sonia Laneri.
The measurements with a calibrated colorimetric device occurred in pre-established times, at the baseline (C_i), at the product's application (C_0), and at the end of the test (C_f).
Investigators applied the products on the volunteers' faces distributing them evenly; more precisely, they had to apply an amount of product to form a thin uniform layer that completely covers the skin.
The drying time evaluation was followed by determining the amount of pigmentation of the treated area, expressed by the parameter L * provided by the Colorimeter® CL 400.

Subsequently, a double test occurred to evaluate products' ability not to transfer to the surgical mask it comes into contact, by subsequent touches.
After the mask tests, the color difference (ΔL *) was calculated for each volunteer participating in the study; the collected data are analyzed and statistically compared by Student's t-test and considered reliable when the statistical probability was p ≤

0.05. The percentage decrease in color intensity and the amount of pigmentation ran. If it is less than 50 % (internal standard), the product can be considered mask-proof.
Besides, at the end of the test, the volunteers are subjected to a self-assessment questionnaire to evaluate the user's final perception of the tested product, which helps complete and validate the objective instrumental data obtained.

The purpose of this work, which is to strengthen conventional instrumental measures for No Transfer, is the application of surgical masks for the Mask-proof claim.

5.3 Materials and Methods

As appropriate, the study was conducted following the intent and purpose of good clinical practice regulations (GCP) and the Declaration of Helsinki. All participants provided written informed consent before the study initiation. Procedures for recruitment, selection, and inclusion of subjects in the study were established to provide the participants with clear information on the project aims.
The test was conducted on 20 volunteers using equipment that allows the comparative analysis of images and quantifies the make-up product applied, thanks to evaluating the percentage variation of specific color-related parameters.
The volunteers applied tested products on the face (Fig. 5.2), distributing them evenly and drying them to air (10 ± 2 min).

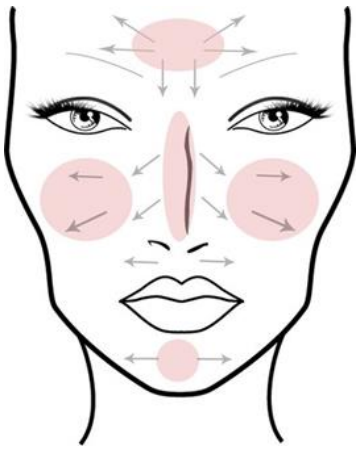

Figure 5.2. Products application area

We compared non-no-transfer and no-transfer foundations to demonstrate that the methods fit the evaluations. The products were selected from currently marketed foundations (1 non-no transfer and one no transfer). The comparative products are listed in Table 5.1.

Table 5.1. Comparative foundation product

Manufacturer	Product name	Type
Eurostyle Spa	Feel Perfect	No Transfer
nd	Fresh & Fit	Non-No-transfer

Readings are conducted for each enrolled volunteer in pre-established times: before applying the product to calculate the Individual Color (Ci), after its application and drying (C_0), and at the end of the test C_f.

Two different standardized 2x2 cm^2 areas are defined for each volunteer, both located on their face. The test products uniformly covered it, and after a drying time of not less than 10 minutes, the various parameters under examination are detected with the probes described above (C_0).

Subsequently, the first area is placed in contact with a Byd Care surgical mask (Byd Co., Ltd.), applying 50 repeated touches at constant pressure. Then, the L* values (C_f) are detected again.

The determination of the pigmentation rate in the treated area and the transfer of the product onto masks are expressed through L * values provided by the device used.

Where L * in the CIELAB color space system (Fig. 3.2), defined by the International Commission for Illumination (CIE), represents the black-white axis, it is inversely proportional to the pigmentation. The higher the L * value, the less pigmented is the analysis area.

Subsequently, the test site, in this case, an area of the face equal to 2x2 cm^2, is subjected to a mask test:

A surgical mask is applied to the area by repeated or prolonged touches with constant pressure, and the skin parameters are re-recorded (C_f).

Colorimetric measurements were also conducted on the masks before and after the transfer test.

5.3.1 Percentage No Transfer Removal Ratio

Brightness L * has a color scale from 0 (black) to 100 (white). Therefore, L * values decrease indicates a degree of foundation transfer on masks. The more significant the decrease in the L * values, the greater the percentage of foundation transferred. The smaller the decrease in the L * value, the smaller the percentage of product transferred.

Suppose no traces of product are found on the mask and the color difference on the test site of the volunteers, i.e., NT % (No Transfer Percentage), is on average less than 50 % (tolerance limit set internally by RD Cosmetics, according to the Colipa Guidelines and with previous papers [143]), the product can be considered "no transfer" and, more precisely, "mask-proof."

$$\textbf{No Transfer Removal Percentage} = \frac{(\mathrm{Cf}-\mathrm{C0})}{(Ci-C0)} \text{ x } 100$$

Eq. 5.1 : No Transfer Removal Percentage

C_i = individual analyzed color
C_0 = average value before product's application
C_f = average value after mask test

$$\boldsymbol{Mean\ Percentage\ No\ Transfer\ Removal\ Ratio}\ (\%\ \boldsymbol{NT}) = [\mathrm{Mean\ No\ Transfer\ Percentage\ Removal} - d]$$

Eq. 5.2 : Mean Percentage No Transfer Removal Ratio

Where *d* is calculated as :

$$d = \frac{t \text{ x SD}}{\sqrt{\mathrm{n}}}$$

SD = standard deviation
n = number of test subjects
t for n-1 degree of freedom
ex) n = 20 → *t* = 1,729

These values were subsequently aligned with consumer assessments through a consumer perception study.

5.4 Statistical analysis

The Student t-test assessed if the differences between average values at baseline C_0, and C_f are significant. The significance level sets for values of $p \leq 0.05$. The average values and standard deviations were calculated for the initial, intermediate, and final instrumental values using a spreadsheet, setting:

C_i = average individual analyzed color

C_0 = average value before the mask test

C_f = average value after 50 touches of contact with the surgical mask

$C_f - C_0$ = average variation after mask test

5.5 Results

The average No-transfer Percentage Removal Ratio results for a confidence limit of 95 % for the L * parameters are reported in Table 5.1.

Table 5.1 Average % NT for the L * values of foundation mask-proof evaluation

Product	Average % No transfer removal	SD	n	t-value	$d = \frac{t \text{ x SD}}{\sqrt{n}}$	Average % NT
No transfer	37,0	36,7	20	1,729	14,2	22,9
Non-No-Transfer	75,3	10,3	20	1,729	3,98	71,3

The L* value for non-no-transfer foundation yielded the mean % NT as 71.3% and for no transfer foundation as 22.9 % (Table 5.1, Figure 5.3).

Therefore, since the values for the claimed no-transfer foundation was < 50 %, the product respects the attributed claim and, more precisely, can be considered mask-proof.

Figure 5.4 represents the color change registered on the surgical mask. These data are essential to corroborate what is measured on volunteers' faces.

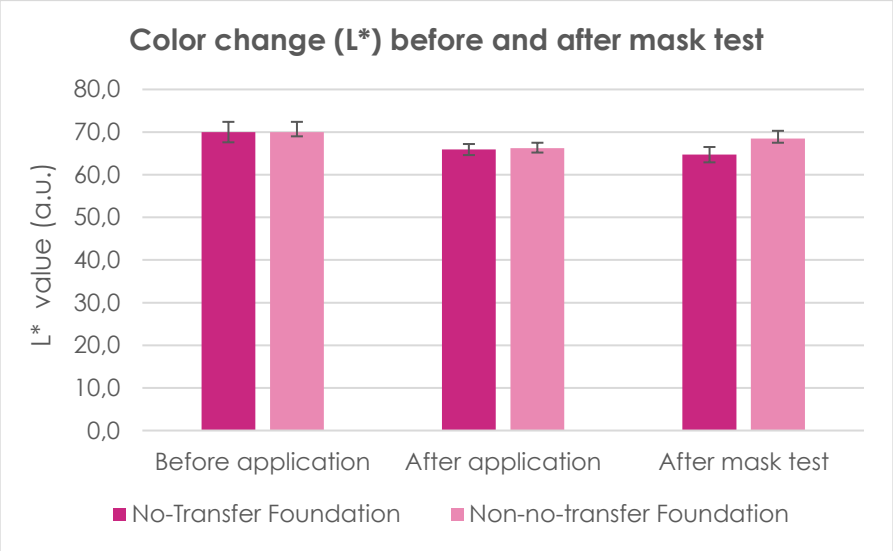

Figure 5.3. Changes of color (L* value) on volunteers' faces before, after application, and after mask test for 50 touches at constant pressure, n = 20.

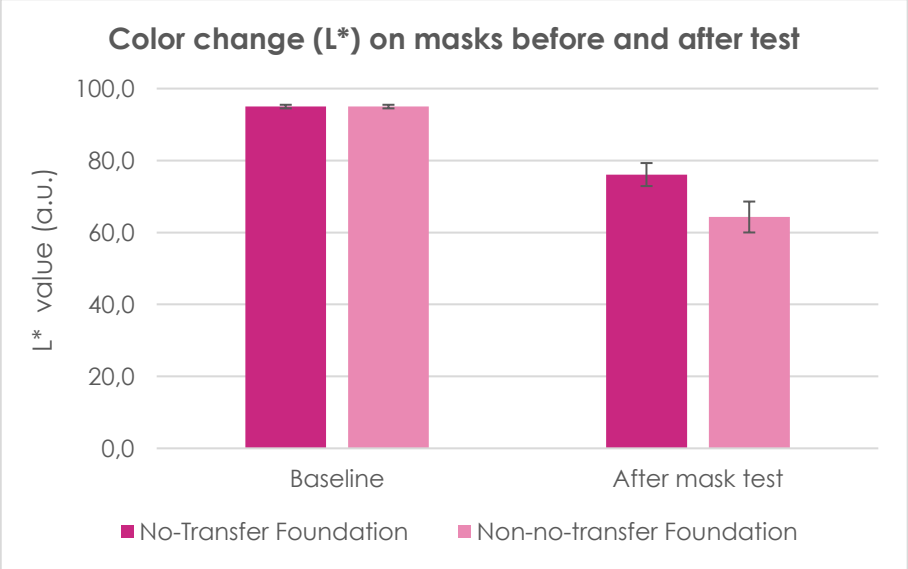

Figure 5.4. Changes of color (L* value) on surgical masks before and after mask test for 50 touches at constant pressure, n = 20.

Below (Table 5.2) are the images of some masks used during the test, and more precisely, their contact area is zoomed to highlight differences between the two tested foundations.

Table 5.2. The test employed surgical masks

After Mask Test	
No-Transfer Foundation	**Non-no-transfer foundation**
	
	

The images show that the product does not completely transfer to the surface it comes into contact with surgical masks.

5.6 Discussion

Marketing claims for make-up products are shifting from the classic "long-lasting" towards more lifestyle-related claims; similarly, trends in the beauty industry will continue to evolve under the influence of the pandemic from COVID-19.

The purpose of make-up products in beauty routines must be reinvented for the category to fit.

The creation of this test method not only fills the gap in a No-transfer-product performance evaluation but ensures that product performance is in line with consumer expectations.

This proof is possible thanks to the accuracy of the colorimetric measurements, which alas do not represent a significant change for the consumer's eye, as shown by the cut-off established by the survey.

It should be emphasized that contact with the mask is performed with a not fully standardized transfer pressure, as the study was designed to mimic the consumer's regular/own use.

The strength of the current method is allowing formulators to modify and adjust formulas based on measured performance without the need to repeat studies. The ability to report poor performance in the development phase is crucial. This method would allow formulators to tune prototypes with adequate volatile oils and film formers to improve their wear and transfer resistance capabilities, with significant savings in time, resources and costs.

The test method described paves the way for developing products with potential consumer-oriented benefits that are particularly relevant today, such as mask-proof effects.

5.7 Conclusions

In this study, a new method to evaluate the mask-proof claim for foundations was applied. According to the COLIPA Guidelines, our results indicated that the foundation sold with this claim respected a % NT lower than 50 %, while foundations that did not claim this property were removed after 50 successive touches at constant pressure with surgical masks; therefore, the efficiency of the used method was validated.

CHAPTER 6

Study on the role of lipids on the process of the hair ageing

6.1 Introduction

Aging is a process that collects progressive physiological changes in an organism that lead to senescence or a decline of biological functions and of the organism's ability to adapt to metabolic stress. Aging takes place in a cell, an organ, or the total organism over time. It is a process that goes on over the entire adult life span of any living thing.

Aging is a physiologic process, depending on intrinsic factors, and extrinsic ones can exacerbate that. It depends on the passage of time, which produces a series of involutional processes in all areas of the human body (therefore also at the skin and hair level), resulting in the complex biological event of aging. Throughout life, therefore, there is a progressive reduction in the ability of tissues to regenerate: DNA synthesis is reduced, DNA repair mechanisms become less efficient, fibroblasts, cells responsible for the synthesis of collagen and elastic fibers and glucosaminoglycans (including hyaluronic acid), decrease.
Chronological aging is normal and physiologic, and the genetic predisposition affects the skin and hair concerns that appear. During this process, dermal renewal is reduced, the skin becomes leathery and dehydrated, the cells synthesize less collagen and elastin. The result is summarized in sagging skin, signed by wrinkles and fine lines.

Even the cell metabolism and, therefore, their turnover is reduced, causing the accumulation of toxins, the skin appears thinner, poor in lipid substances, drier. In the same way, the aging process affects hairs; there is a gradual change in many aspects: hair diameter is reduced, hair density is decreased, androgenic alopecia may develop, and pigmentation may be diminished, producing a significant psychological impact. Hair aging comprises weathering of the hair shaft and aging of the hair follicle. The former involves progressive degeneration of the hair fiber from the root to the tip, while the latter manifests as a decrease in melanocyte function or graying and a decrease in hair production in androgenetic and senescent alopecia. The scalp is also subject to intrinsic or physiologic aging and extrinsic or premature aging caused by external factors. Intrinsic factors are related to individual genetic and epigenetic mechanisms with an interindividual variation. Extrinsic factors include ultraviolet radiation, air pollution, smoking, nutrition, and lifestyle. Experimental evidence supports the hypothesis that oxidative stress plays a significant role in premature skin and hair aging [144].

One of the labeled signs of hair aging is the loss of hair color or, commonly said, the appearance of grey hair. This loss of color is due to the decrease or lack of melanin in the hair fibers. The hair graying trait correlates closely with chronological aging and occurs in varying degrees in all individuals, but the rate at which graying appears depends on genetics. Although graying is related to the loss of pigment in the shaft, its cellular and molecular origins are not clear [145]. Skin and hair melanins are formed in cytoplasmic organelles called melanosomes, produced by the melanocytes, and are the product of a complex biochemical pathway (melanogenesis), with tyrosinase being the rate-limiting enzyme. It was demonstrated that there is a noticeable activity reduction in the hair follicle melanocytes in gray hair. [146] The direct result of this reduction is that fewer melanosomes are embraced into cortical keratinocytes of the hair shaft.

Gray hairs are commonly considered coarser and less manageable than pigmented hair. Moreover, gray hair often fails to hold a temporary or permanent set and is more resistant to incorporating artificial color, both of which suggest significant changes to the underlying substructure of the hair fiber. Given the very close interaction of melanin-transferring melanocytes with hair shaft-forming pre-cortical keratinocytes, it is conceivable that other functions of these cell types are affected by this activity.

Probably the hair lipid composition can also be altered, leading to modifications of the fibers. Lipids play a crucial role in keeping hair healthy, influencing shine, feel, manageability, and strength. They can be lost on exposure to external stressors, such as chemical treatments, washing, UV exposure, but it is not clear if the hair aging could also take action on this.

To date, studies of hair lipids have been performed mainly by comparing hairs derived from different ethnic groups (Caucasian, African and Asian) or by exposing hair to external damaging factors, but very few studies have focused on the processes underlying the loss of pigmentation.[147,148] It is thought that the differences in lipid content involved in the functioning of the barrier in capillary [149] fibers could explain the significant physical differences between pigmented and non-pigmented fibers.[150] During age-related changes, the hair lipid composition may also be modified at the same time that its melanin content decreases, which may lead to a modification of the fiber properties.

The main objective of this work is to study the effect of hair aging through a lipid analysis, extracting external and internal lipids separately.

Brown and white Caucasian hairs belonging to different people and brown and white Caucasian hairs belonging to the same person have been analyzed to observe whether hair lipids vary by person.

The lipid analysis and quantification were done using thin-film chromatography coupled to a flame detector (TLC-FID). Next, a study was made of the calorimetric behavior of the different lipids extracts obtained from the hair samples using thermogravimetric (TGA) and dynamic vapor sorption (DVS) analysis. Finally, their moisture content was assessed, and liposomes were formed to determine the organization of these lipids by Fourier-transform infrared spectroscopy (FTIR).

This analysis allows us to characterize the differences between white and brown Caucasian hairs and determine the role of the external and internal lipids in the aging process.

The study was conducted at the Institute for Advanced Chemistry of Catalonia (IQAC), and more precisely, with the Cosmetic and Textile innovation group managed by Prof. Luisa Coderch.

6.2 Study Design

Hair samples were obtained from white and brown Caucasian hair of the same person and different people. The lipids were extracted with several organic solvents, making two different extractions to separate the external and internal lipids. The external lipids were subjected to Soxhlet extraction then by stirring in a thermostatic bath with a stirrer swaying to collect the internal ones. Lipid analysis and quantification were performed using thin layer chromatography coupled to an automated flame ionization detector (TLC-FID). Lipid properties were also determined using thermogravimetric analysis (TGA) and their influence on the hair diffusion performance with the Dynamic vapor sorption technique (DVS). Finally, their moisture content was assessed, and liposomes were formed with capillary lipid extracts to determine the organization of these lipids through a Fourier transform infrared spectroscopy using attenuated total reflection (ATR-FTIR).

6.3 Materials and Methods

6.3.1 Hair samples

The hair samples used in this study were natural virgin brown Caucasian Hair and white Caucasian hair, both without any pretreatment, provided by the De Meo Brothers (Passaic, New Jersey, USA). On the other hand, brown Caucasian hair and white Caucasian hair from the same volunteer were also studied, both without previous treatment. These hairs were supplied by a 49 years old female volunteer (Catalonia, Spain). All hair samples were washed with 3 % diluted Pantene Pro-V commercial shampoo (Procter & Gamble, USA) at a hair/surfactant solution 1/30 bath ratio followed by a water rinse and ambient conditions drying.

6.3.2 Lipid extractions

Extractions of external and internal lipids were performed with different organic solvents. The external surface lipids were initially removed from the washed hair surface with Soxhlet extraction with t-butanol and n-hexane for 4 hours. Internal lipids were extracted with different solvent mixtures of Chloroform: Methanol (2:1 $_{v/v}$,

1:1 v/v, and 1:2 v/v). Each mixture was applied to the hair samples for 2 hours. Then, 100 % Methanol was applied to the same hair samples overnight at RT in a stirring system. The different internal lipids extracted fractions were then combined, concentrated, and dissolved in a chloroform/ methanol mixture (2:1 v/v) before analysis.

6.3.3 Lipids Analysis

Lipid analyses of the different extracts were performed with a thin-layer chromatography coupled to an automated flame ionization detector (TLC/FID) and an Iatroscan MK-5 analyzer (Iatron, Tokyo, Japan). The lipids extracts were directly spotted on a silica gel-coated Chromarods (type S-III) using a precision Hamilton 2 µL syringe coupled to an SES 3202/IS-02 sample spotter (NiederOLm, Germany). The determination of the lipid content was performed using an optimized TLC/FID protocol [151] using a methodology where rods (in a set of 10) were developed using the following mobile phases: (i) chloroform/methanol/water (57:12:0.6, v/v/v) for a distance of 2.5 cm twice, (ii) n-hexane/ethyl ether/formic acid (50:20:0.3, v/v/v) to an 8 cm and (iii) n-hexane/benzene (35:35, v/v) to a 10 cm, and finally a total scan (100 %) to quantify the most polar lipids was performed.

6.3.4 Thermogravimetric analysis

Thermogravimetric analyses were performed with a TGA instrument (Model TGA/SDTA 851; Mettler Toledo, Barcelona, Spain). Approximately 5 mg of extract was packed into an alluminum pierced pan (100 µl) and heated under a nitrogen stream from 25 to 550 °C at a heating rate of 10 °C/min.

6.3.5 Moisture content

The moisture content was evaluated from non-extracted hair samples. A hair sample of 0.5 g was maintained in a conditioned room (23 ° C, 50 % RH) for at least 24 hours before being weighed and subsequently dried in an oven at 105 ° C for 24

hours. The sample was cooled in a desiccator with a P_2O_5 atmosphere and weighed again; then, the moisture content was calculated as humidity percentage.

6.3.6 ATR-FTIR

The possible differences between different hair fibers due to their different composition and structural lipid organization can be evaluated using FTIR-ATR. This technique can determine the lipid order disposition. For example, the CH_2 symmetric stretch mode position would indicate orthorhombic, lamellar, or gel lipid order with increased permeability. Integration of CH_2 asymmetric stretching mode is also quite reliable to determine lipid content.

A Nicolet Avatar 360-FTIR spectrophotometer equipped with an attenuated total reflection (ATR) accessory with a diamond crystal (with ZnSe lens) with a 42 ° angle of incidence in horizontal orientation was used. Before analysis, the hair is placed towards the diamond crystal. To ensure reproducible contact between the sample and the glass, a pressure of 10,000 psi is applied to the samples. All the analyzed spectra represent an average of 64 scans with a resolution of 2 cm-1, and the wavenumber range used is 4200 - 650 cm-1. The maximum positions have been determined with the help of OMNIC software version 8.1.210.

6.3.7 Dynamic Water Vapour Sorption

A thermogravimetric balance, Sorption Analyzer Q5000SA (TA Instruments, New Castle, USA) with a controlled humidity chamber, was applied to determine water absorption and desorption in the hair fibers. Experiments were conducted by triplicate on each hair sample (10 ± 1 mg) with a total gas flow of 200 mL/min, at 25 ºC following the protocol described elsewhere [152,153].

To describe sorption isotherms, some mathematical models based on theoretical and empirical criteria have been published. One of the most commonly used is the Guggenheim, Anderson, de Boer model (GAB). The GAB model gives a particular value to the monolayer moisture content of the fiber. Its parameters, with a theoretical basis, provide a more physical aspect to the sorption process than other empirical models. Therefore, in this work, the sorption isotherm data were modeled

following the GAB model.[154] Description of the GAB equation (Eq. 6.1), and the parameters used to fit the experimental sorption data are listed in Table 6.1.

$$W = W_m C_g K a_w / [(1 - Ka_w + C_g Ka_w)]$$

Eq. 6.1. Guggenheim, Anderson, de Boer model (GAB)

Table 6.1. Parameters used to fit the experimental sorption data

Parameter	Definition
a_w	Water activity is expressed as vapor relative pressure p/p0, where p0 is the saturated vapor
W	The equilibrium moisture content at aw in g sorbed/100 g of sorbent on a dry basis.
W_m	Monolayer moisture content in g sorbed/100 g of sorbent on a dry basis
C_g	Energy constant is related to the difference between the free enthalpy of the water molecules in the pure liquid state and in the monolayer, which is proportional to the rate between both the attachment and the escape rate constants of the primary sites
K	The ratio between the standard vapor pressure of the liquid and the vapor pressure of the sorbate in the secondary (upper) layers. Proportional to the rate between the attachment rate constant and the escape for all higher layers.

The Vickerstaff method [156] to study the diffusion of dyes within fibers provided the diffusion coefficient. It is represented by an expression derived from Fick's equation applied to moisture diffusion. Satisfactory results for the early stages of moisture absorption were obtained with this expression, as in the case of dye diffusion. The fraction of absorbed water plotted against the square root of the absorption time should lie on a straight line in which the slope is the square root of the apparent

diffusion coefficient, D_A (Equation 6.2). The apparent diffusion coefficient is measured in min^{-1} over the sample's mass.

$$R(t)/R_f = \sqrt{D_A}\sqrt{t}$$

Eq. 6.2. Vickerstaff equation

6.4 Statistical analysis

Statistical analyses were performed with StatGraphics software (version 5.0). Differences were tested for statistical significance using non-parametric tests (Kruskal-Wallis) with $p < 0.05$ considered significant.

6.5 Results

6.5.1 Hair lipid analysis by TLC-FID

Extraction of lipids from white and brown Caucasian hair was performed after washing with shampoo. As detailed in the materials and methods section, the external surface lipids were extracted from the hair surface using Soxhlet extraction with t-butanol and n-hexane. This methodology was performed in duplicate.

It is important to note that the brown and white hair did not show significant differences in the total lipid amount of the external or sebaceous lipids, mainly apolar compounds. Divergences occur on the internals (mainly polar compounds): brown hair shows more internal lipids (+ 67 %), particularly the FFA and Polar lipids.
While internal lipids account for approximately 1.62 % of the whole fiber in the brown hair, it is essential to note that external lipids accounted for less than 1 %.
The discrepancy between external and internal lipids amount in white hairs are less evident than in brown ones. (Table 6.2).

It has to be remarked that fibers were previously washed with shampoo; previous results [156] indicate that shampooing does not remove some free lipids from the fiber's surface because an essential amount of lipids remains on the surface layers.

Table 6.2. The total amount of lipids obtained by extraction with t-butanol/hexane (external lipids) and chloroform/methanol mixtures (internal lipids) in the percentage of Black Caucasian and White hair mass.

LIPIDS	BE	WE	BI	WI
Total Lipids (%owf)	0,53 ± 0,11	0,52 ± 0,15	1,62 ± 0,39	0,85 ± 0.16
Apol. L. (%owf)	0,13 ± 0,07	0,10 ± 0,04	0,20 ± 0,07	0,11 ± 0,04
FFA (%owf)	0,28 ± 0,08	0,34 ± 0,06	0,98 ± 0,15	0,43 ± 0,15
St. (%owf)	0,04 ± 0,02	0,00 ± 0,00	0,12 ± 0,05	0,08 ± 0,01
Pol. L. (%owf)	0,08 ± 0,06	0,08 ± 0,02	0,32 ± 0,06	0,23 ± 0,08

Similar conclusions can be obtained from Figs. 6.1, 6.2. The differences in the internal lipids related to the entire fiber weight are even more pronounced and significant for Brown hair when compared with White hair.

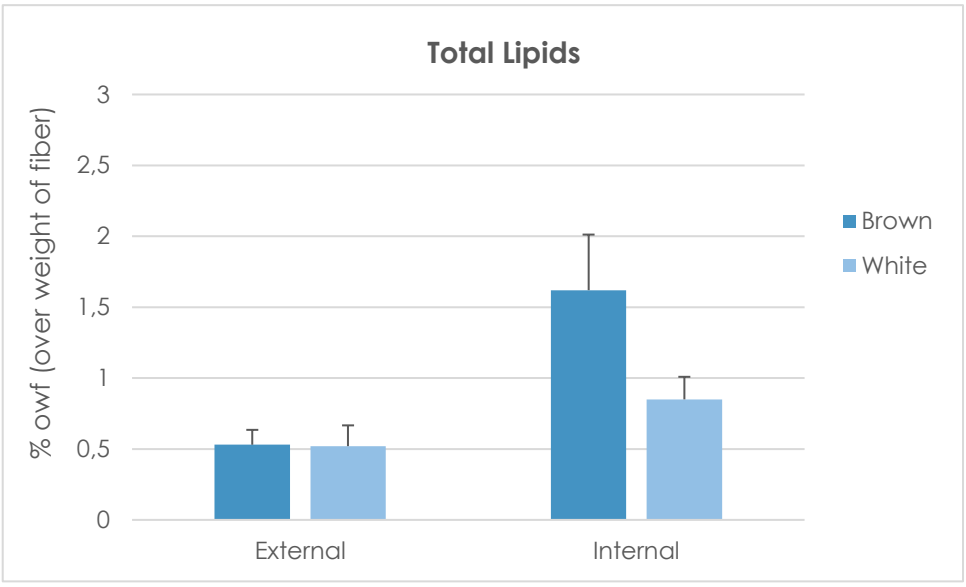

Figure 6.1. Quantify external and internal hair lipids in Brown and White Caucasian hairs using TLC/FID (percentage over the total weight of dry hair fiber [o.w.f]).

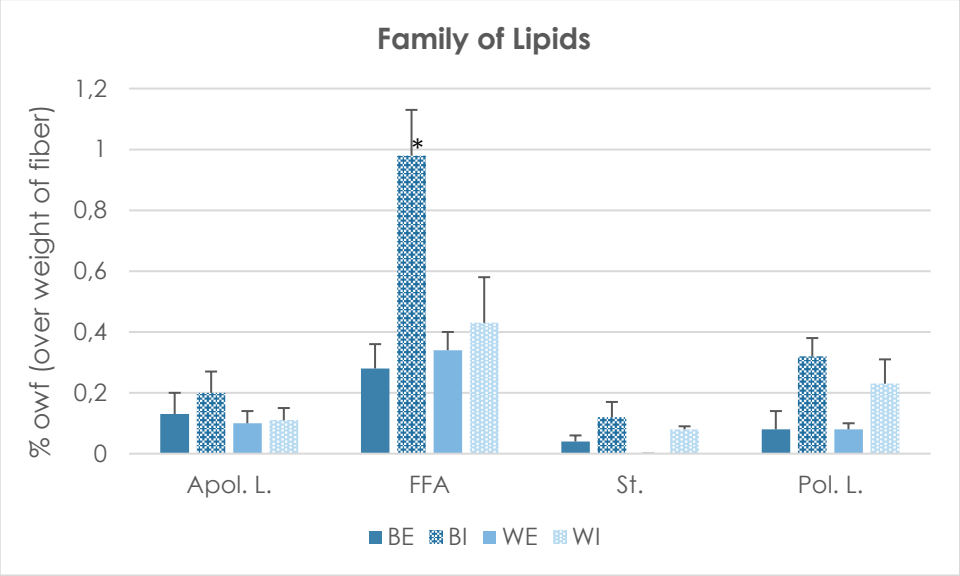

Figure 6.2. Quantify external and internal hair lipids in Brown and White Caucasian hairs using TLC/FID (percentage over the total weight of dry hair fiber [o.w.f]). Apolar lipids (Apol. Lip), free fatty acids (FFA), sterols (St.), and polar lipids (Pol. Lip) (* p >.05)

Subsequently, the lipid analysis was conducted on brown and white hair belonging to the same person to overpass inter-individual variability. Then, the same-volunteer black and white hair (vw and vb hairs) were compared with black and white commercial-hair (w and b hair). In this way, it is possible to corroborate the data for the afferent category.

The external lipids, such as squalene and sterol esters (apolar lipids), usually compose most sebaceous surface lipids. In contrast, the internal lipids, sterols, free fatty acids, and more polar compounds such as cholesterol sulfate and ceramides are mainly constitutive lipids of the hair matrix cells.

Results are expressed as percentage of lipids in the total lipid extract in Table 6.3 – 6.4 and expressed as the percentage of lipids over the whole mass of the hair fiber in Figs 6.3 – 6.4.

Table 6.3. The total amount of lipids obtained by extraction with tert-butanol/hexane (external lipids) in the percentage of total analyzed (o.t.a.) for Brown and White Caucasian commercials hairs (B and W) and from the same volunteers (VB and VW).

LIPIDS (% ota)	ECHOL	FFA	CHOL	CER3
VWE	66,62 ± 3,35	29,93 ± 2,36	n.d	6,18 ± 0,16
VBE	63,58 ± 3,65	36,79 ± 5,53	n.d	2,45 ± 2,85
WE	58,96 ± 1,22	36,87 ± 2,79	n.d	5,51 ± 2,42
BE	56,83 ± 2,69	39,30 ± 1,37	n.d	5,13 ± 0,73

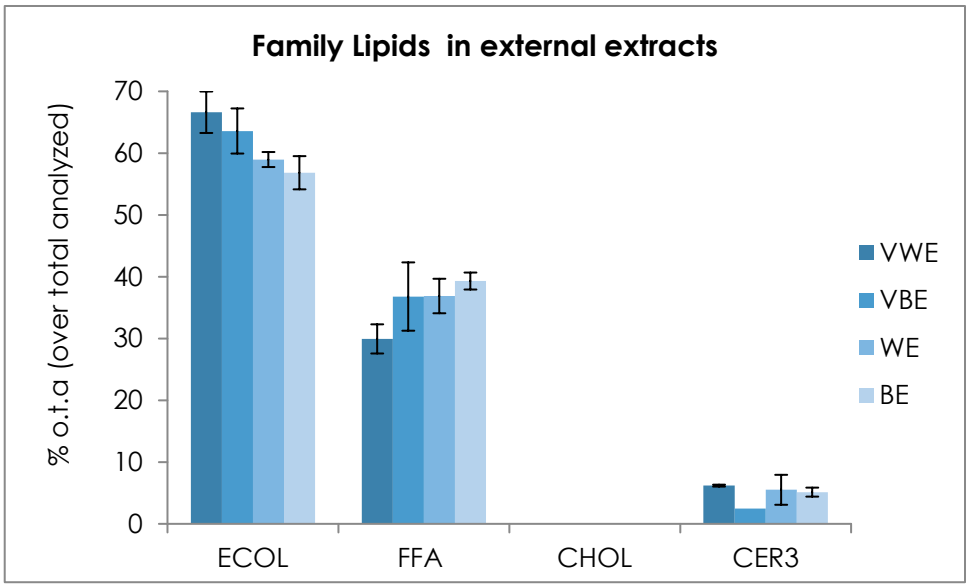

Figure 6.3. Amount of external lipids obtained by extraction with tert-butanol/hexane in the percentage of total analyzed (o.t.a.) for Brown and White Caucasian commercials hairs (B and W) and from the same volunteers (VB and VW).

Table 6.4. The total amount of lipids obtained by extraction with tert-butanol/hexane (external lipids) in the percentage of total analyzed (o.t.a.) for Brown and White Caucasian commercials hairs (B and W) and from the same volunteers (VB and VW).

LIPIDS (% sta)	ECHOL	FFA	CHOL	CER3
VWI	16,72 ± 1,30	38,69 ± 1,93	14,89 ± 0,95	29,70 ± 3,25
VBI	23,45 ± 1,70	53,68 ± 0,63	12,54 ± 2,08	10,33 ± 2,86
WI	18,33 ± 2,89	43,93 ± 4,52	8,54 ± 1,76	29,19 ± 5,17
BI	13,12 ± 1,36	62,93 ± 1,64	4,67 ± 1,17	19,61 ± 2,42

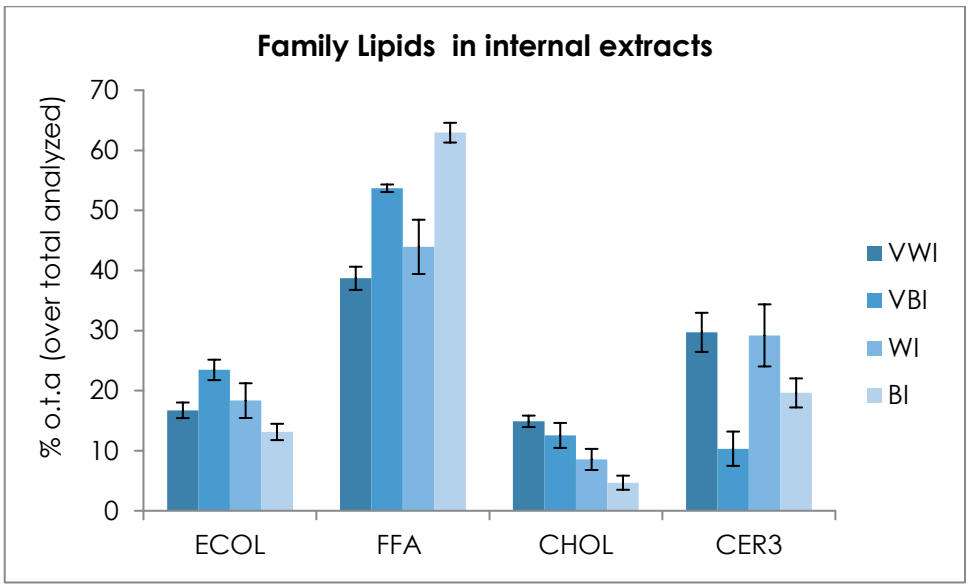

Figure 6.4. Amount of external lipids obtained by extraction with chloroform/methanol (internal lipids) in the percentage of total analyzed (o.t.a.) for Brown and White Caucasian commercials hairs (B and W) and from the same volunteers (VB and VW).

Regarding the entire fiber, Brown and White Internal lipids contains the most significant proportion of free fatty acids and sterols (CHOL). The External lipid extracted shows fractions rich in apolar lipids (ECOL) in brown and white hair. It is important to note that commercial and volunteer white and brown hair exhibit the same behavior.

6.5.2 Thermogravimetric analysis

First-derivative thermogravimetric analysis (TGA) evaluation of the four extracts presents two main degradation steps, one more important from 237 to 240 ° C and the second from 330 to 340 ° C. The caucasian Brown external and White internal lipids have a new peak at a higher temperature, 425 ° C, indicating a highly saturated fraction.

Degradation temperatures of the extracts are difficult to correlate with the number of lipids extracted or with the chemical composition of the extracts. The external lipids from Brown caucasian hair fibers possess higher degradation temperatures, indicating high saturations or less fluidity. (Figure 6.5 a, b). This data will be related to the hair permeation analysis in the following paragraphs.

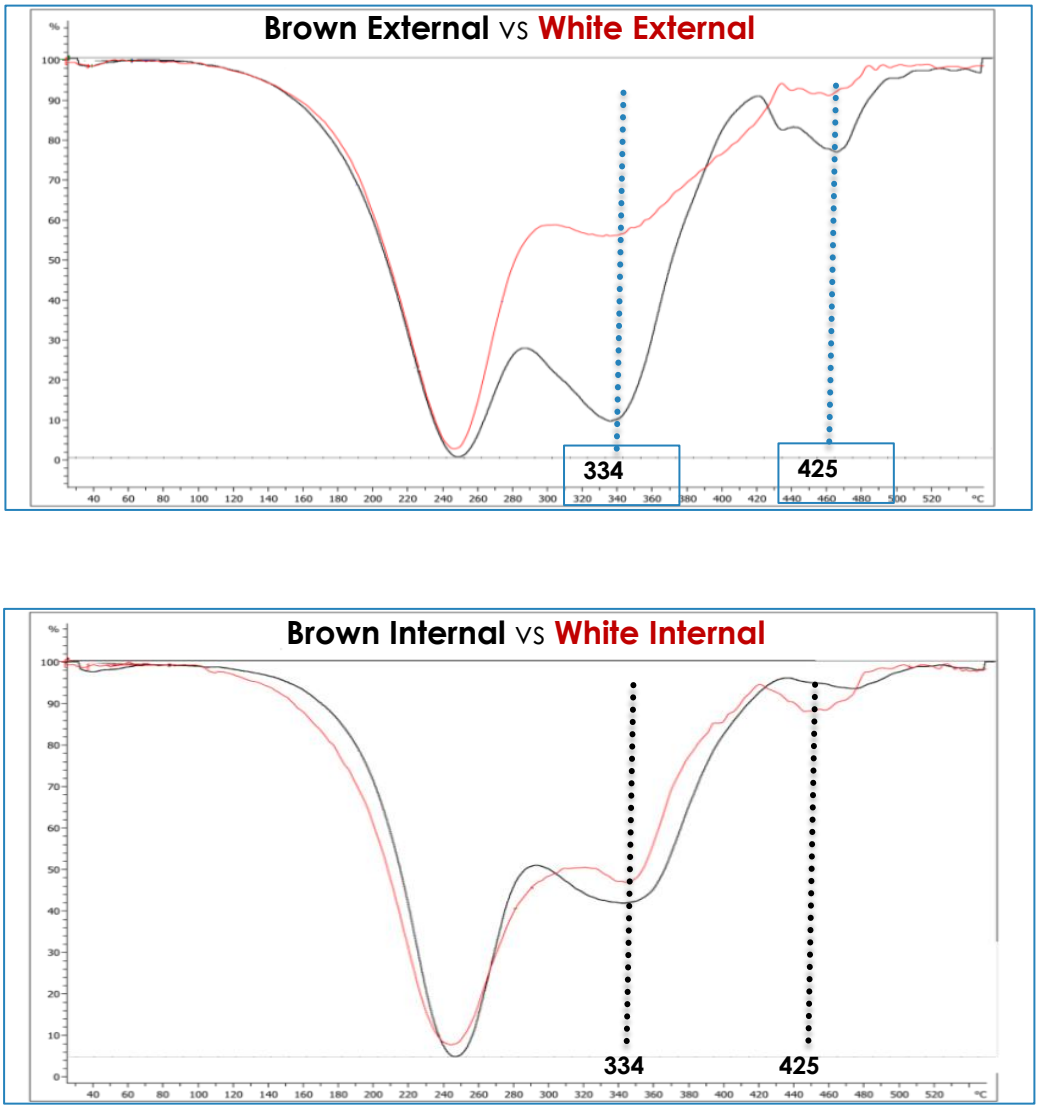

Figure 6.5. Thermogravimetric analysis (TGA) evaluation of a) external and b) internal lipids obtained by extractions of Brown and White Caucasian commercials hairs (B and W) and from the same volunteers (VB and VW).

6.5.3 Hair Moisture

Moisture (H) measured at 22 ° C and 50 % RH for native and extracted hair fibers was determined, and the results are listed in Table 6.5.

Moisture content was approximately 10.3 % in the brown native hair fibers and about 9.2 % in the white ones. When the fibers were externally extracted, there was a

significant 10.1 % decrease in humidity retention for the brown hair, but a slight increase (+ 7.5 %) occurred for the white hair after the extraction.

Remarkably, when the internal lipids were removed, the humidity retention increased to nearly the initial values for the brown hairs; the rising trend is going on for the white internal extracted fibers.

Table 6.5. Humidity of Brown and White caucasian hair fibers before and after lipid extraction

Lipids	% Humidity		Lipids	% Humidity
B	9,61		**W**	8,12
VB	10,92		**VW**	10,33
Average	10,26		**Average**	9,23
Sd	0,92		**Sd**	1,56
BE	9,97		**WE**	9,83
VBE	8,48		**VWE**	10,02
Average	9,23		**Average**	9,92
Sd	1,05		**Sd**	0,14
BI	10,99		**WI**	10,76
VBI	10,81		**VWI**	9,50
Average	10,90		**Average**	10,13
Sd	0,13		**Sd**	0,89

It is not easy to relate these results to the different amounts of lipids extracted. A diminution of the water content in the brown caucasian hairs could be related to modifying the external lipid barrier, which facilitates the loss of water content after external lipid depletion. Additionally, the extraction of internal lipids, mainly from the inner hair matrix cells, seems to facilitate water penetration, leading to more hydrated fibers.

This assumption also clarifies the growing moisture content found in the white external and internal extracted fibers because white hair presents lower internal lipids that can hinder the water molecule entrance. In conclusion, as the fiber ages, it loses water, and therefore the moisture in the hair decreases.

6.5.4 Dynamic Vapor Sorption (DVS)

Water absorption/desorption of hair is an important characteristic that can reflect damage due to aging. Therefore, water absorption and desorption behavior of caucasian brown and white hairs with and without lipids were evaluated to determine the humidity content of the fibers, the binding energies of water to the different components of the fiber, and most importantly, the water diffusion, which gives information about the integrity of the hair samples. The sorption analyzer evaluated water uptake and desorption isotherms for the native and lipid extracted brown and white hairs. The shape of the water equilibrium water sorption isotherms obtained for the three hair types is described by a type II isotherm, which shows a small amount of water at a very low RH and a significant increase at high RH (Table 6.5, Figs 6.6a, b, c).

Table 6.5. Summary of all DVS parameters. Maximum moisture regains, GAB monolayer capacity (Wm), GAB energy constant (Cg) constant (K), GAB determination coefficient (R2), and apparent diffusion coefficient (Da) and apparent diffusion coefficient only at the desorption process (Da desorb) for native, external, and internal extracted brown and white caucasian hair fibers.

	B	BE	BI	W	WE	WI
Regain at 95 % RH (%)	26,25	25,61	26,18	24,85	24,15	25,50
W_m (%)	0,0772	0,0732	0,0795	0,0789	0,0729	0,0793
C_g	5,915	5,848	5,667	5,813	6,460	5,455
K	0,7367	0,74805	0,7334	0,72095	0,7396	0,7260
R_2	0,9980	0,9977	0,9989	24,85	24,15	25,50
Da (min^{-1} $x10^{-3}$)	20,46	21,17	19,05	21,04	21,52	20,53
Da desorb (min^{-1} $x10^{-3}$)	24,96	25,35	23,72	25,24	25,28	24,93

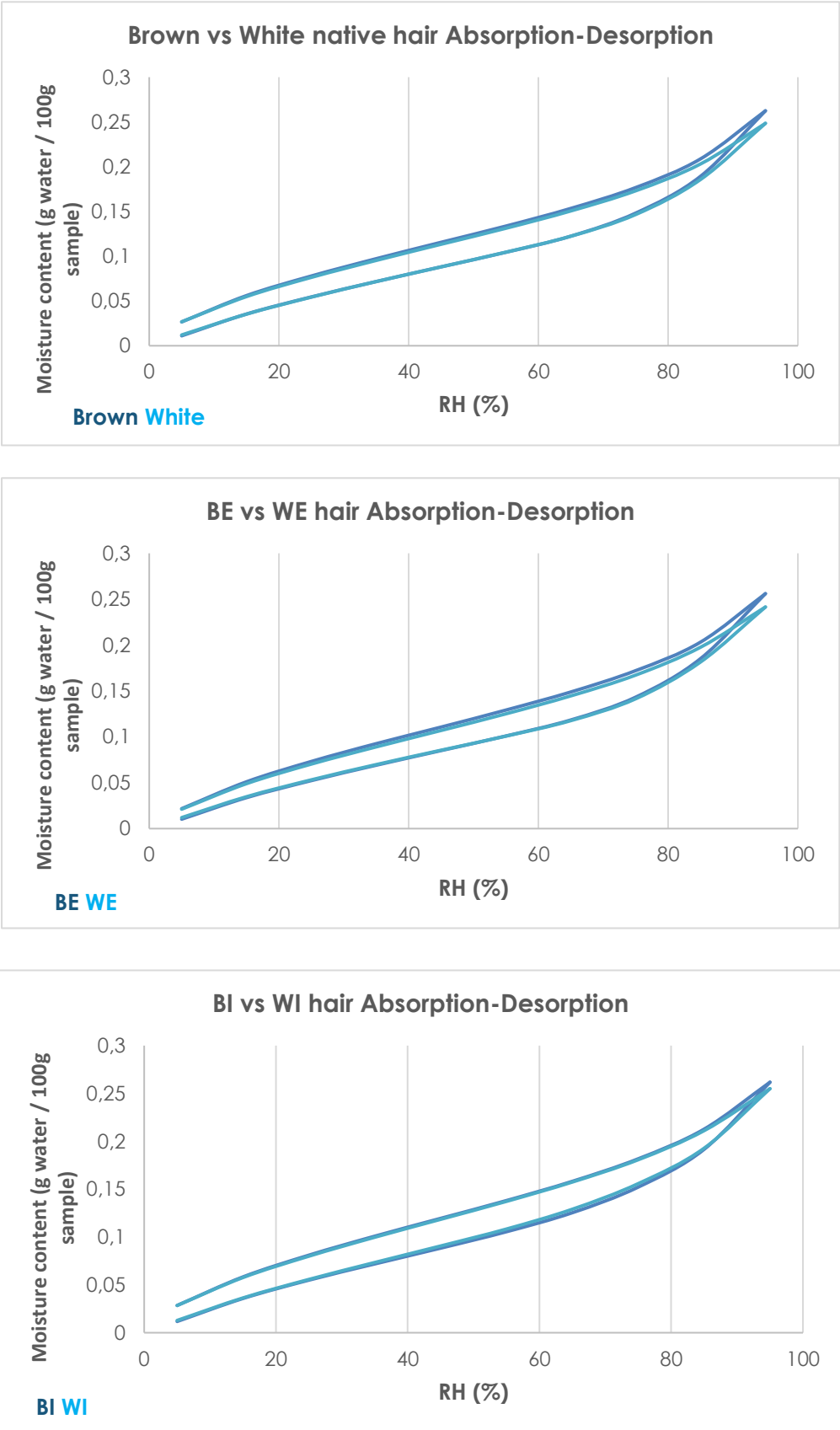

Figure 6.6. Absorption desorption Average Isotherms of Brown and White a) native hair, b) external lipid extracted, and c) internal lipid extracted hair.

Data show a lower amount of water regained in white than brown native fibers (24,85 and 26,25 %). Brown hair fibers had a lower degree of Wm or water directly bound to the structure than white fibers (0.0772 and 0.0789 %, respectively). On the other hand, the energy constants (Cg and K) reflected that the strength of water bonding was higher in the brown hair (Table 6.5). The lower Wm value and higher energy constants found for brown hair may indicate a higher degree of a water attraction, increasing the number of water layers. One possible explanation could be the presence of melanin in brown hair, which may increase the attraction of water to the entire fiber due to its hygroscopic properties [159]. After the external lipids extraction, there is a reduction of the water regain and moisture. The removal of the lipidic barrier leads to less water content in the fibers.

Unexpected results occur after the internal lipids extraction because the regain of water and the monolayer moisture content increase. The subsequent internal lipid extraction makes the inner of the fiber more polar. Hair medulla has been shown to have a rich lipid content fraction[158] which can be removed by C/M solvent extraction. This condition would increase polarity inside the fiber.

White fibers exhibit more excellent water permeability than brown ones, and the external lipids extraction exacerbates this behavior because of higher water diffusion detected in the analyzed samples. The extraction compromises the barrier properties of the external lipids. On the same line of the water moisture, after the internal lipids extraction, there is a turnabout in the registered parameters. The water diffusion (Da) decreases. Maybe the removal of the internal lipids changes the keratin structure, making the fiber more compacted. Table 6.5 reports the labeled outcomes.

6.5.5 ATR-FTIR

ATR-FTIR is a non-invasive spectroscopic technique that has been used to investigate hair structural organization. [153,158] The technique measures the amount, conformational order, and packing of the lipids on hair structure. Its importance is related to the possible correlation between lipid organization and barrier properties. The spectrum analysis focuses on the alkyl chain bands of the hair lipid vibrations: CH_2 symmetric stretching approximately 2920 cm^{-1} and CH_2 asymmetric stretching

2850 cm^{-1}. The shift to higher wavenumbers (λ) indicates an increase in lipid disorder, a λ value :

- < 2850 cm^{-1} : reveals an orthorhombic (OR) lipid chain conformation
- 2850 ≤ λ ≤ 2852 cm^{-1}: represent a hexagonal (HEX) chain conformation
- > 2852 cm^{-1} : indicates a liquid crystalline (LIQ) chain conformation

The lipid order plays an important role, as does the lipid content. The fluidity of the hair lipids can modulate the rates of penetration and departing of substances from their surface.

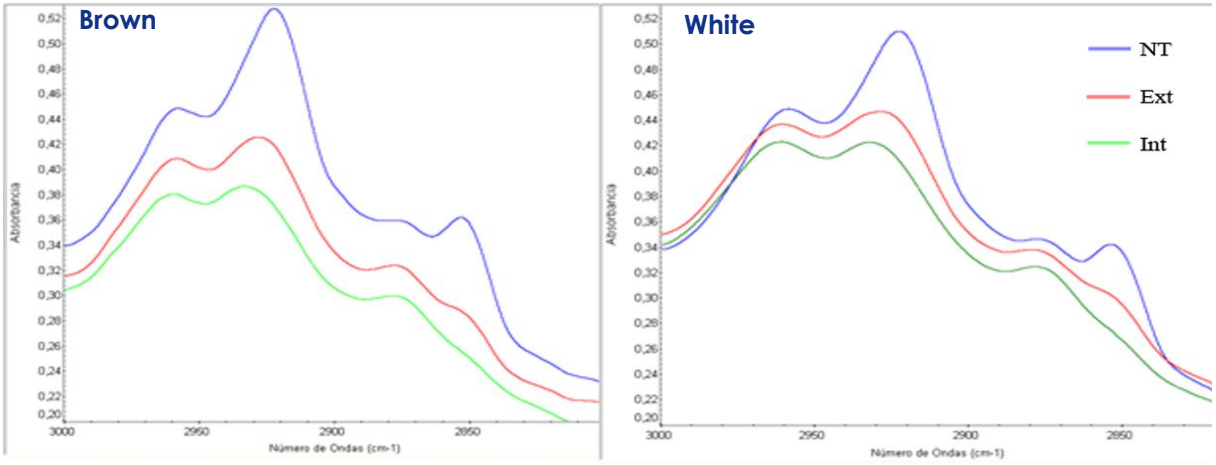

By analyzing the asymmetric CH_2 stretching of the hair samples, brown non-treated (NT) hairs indicate the presence of lipids with orthorhombic/hexagonal lamellar phases instead of the white hair that present a diminished order.

In each case, lipid extraction leads to a decrease in integration related to fewer lipids after extraction and an increase in frequency, indicating more disorder (Table 6.6), as expected.[153]

The lipid order and amount diminish in white fibers, related to DVS results that showed higher water permeability than in brown native hairs.

Table 6.6. ATR/FTIR of CH_2 symmetric and asymmetric stretching modes of native (NT), external (Ext), and internal (Int) extracted Brown and White caucasian hair fibers.

	BROWN			WHITE		
	NT	**EXT**	**INT**	**NT**	**EXT**	**INT**
λCH₂ St.Sym.	2918.9 ± 0.1	2925.9 ± 0.3	2927.6 ± 0.2	2920.9 ± 0.6	2928.7 ± 2.4	2932.2 ± 0,7
Intensity Reduction		18,5	23,85		16,57	31,73
λCH₂ St.Asym	2850.1 ± 0.3	2851.5 ± 0.4	2851.7 ± 0.3	2851.0 ± 0.8	2851.0 ± 0.8	Undetectable
Intensity Reduction		19,95	29,29		20,7	
Order	Ort	Hex	Hex	Hex	Hex	LiqC

6.6 Discussion

Hair greying or canities is one of the most evident phenotypic changes during aging, cosmetic research focuses on preventing or limiting this process, but it is essential to understand what kind of transformations occur in the hair fiber. It is well known that the gradual loss of pigmentation involves exhaustion of enzymes involved in melanogenesis, impaired DNA repair, loss of telomerase, antioxidant mechanisms, and antiapoptotic signals. Until now, the role of lipids in this process was not investigated. Our study demonstrates that pigmented hair presents more internal lipids than white one; these lipids are mainly polar, rich in free fatty acids and ceramides. The external lipids characterization exhibits a similar amount in both hair types, with an abound of apolar lipid's family.

The ATR-FTIR technique has been demonstrated to help determine differences in lipids between different hair types, which allowed for the comparison of the amounts and conformational order of lipids in different hair layers. Results showed that brown hair possesses a more significant amount of lipids. The white hair analysis reveals essential differences between it and brown hair: aged fibers showed decreased amounts of lipids. Regarding the lipid chain packing, a lower lipids order in white hair was observed. These data follow the Dynamic Vapor Sorption investigation,

where it was observed to have changed in the rate of the penetration of substances to the inner part of the fiber and to produce faster modifications to their properties upon changes in the relative humidity. DVS analysis indicated that the water dynamics of white fibers differed from those of brown fibers, resulting in a decrease in the total capacity to absorb water (lower water regain) and an increase in the water exchange rate with the environment. After the external lipids extraction, the adsorbing water capacity and the amount were sensibly reduced, how expected because of the removal of the lipidic barrier that can not face the physiological water depart from the hair fiber. The internal lipids extraction unexpectedly reverses the results: perhaps related to the inner structure modification appearing after this process, making the fiber more polar in the inner layer and with a more homogenous surface. The same attitude was observed in the diffusion parameter that increases for both fibers after the external lipid extraction and decreases after the internal lipids extraction, maybe because the removal of internal lipids changes the keratin structure, leading to a more compacted fiber that hinder the diffusion process. Both techniques demonstrated a high correlation between the characteristics of the hair lipids and the water dynamics of the fibers. They were also corroborated by the thermogravimetric test, indicating high saturations or less fluidity for the pigmented hair fibers that possess higher degradation temperatures.

6.7 Conclusions

In the last several decades, the DermoCosmetic Assessment service of the Institute for Advanced Chemistry of Catalonia (IQAC) has witnessed studies searching for the importance of lipids' role in determining the hair properties [150-153, 158]. Herein, we provide evidence that supports an indispensable role of lipids in governing the physicochemical properties of hair and how they influence the natural or environmental aging of the mature hair shaft—furnishing support in finding empirical solutions for the hair-care new-product specialists in the piecemeal hair aging sector.

CHAPTER 7

Identify key drivers of diffusion on hair and key difference of diffusion factors between Caucasian and Chinese: lipid, pH, and solvent impact

7.1 Introduction

As visiting Ph.D. Student from June to October 2021, the author of the thesis has worked at the Institute for Advanced Chemistry of Catalonia (IQAC), and more precisely, with the Cosmetic and Textile innovation group managed by Prof. Luisa Coderch. The main project on which this doctoral thesis work focused was a study on identifying the key drivers of diffusion on hair and key factors between Caucasian and Chinese diffusion differences, like lipid's impact, pH and solvent impact. The project was sponsored by the Hair Fiber Discovery Domain of L'ORÉAL Research & Innovation, 1, Avenue Eugène Schueller - 93600 Aulnay-sous-Bois – France.

Tests were conducted using scientifically recognized techniques, following the Quality System of Management following the UNE-EN ISO 9001:2008 certified by AENOR with the reference ER-0430/2012.
Hair samples were divided into three groups for each race: Untreated (U), Total (Td), and Partial delipidated (Pd).
These last two groups will be subjected to a total or partial lipid extraction with an appropriate and validated technique.

After that, the lipid fraction was analyzed by a TLC-FID, and all hair samples (Untreated and delipidated) were examined with Dynamic Vapor Sorption (DVS) and ATR-FTIR spectroscopy. Finally, a Bibliographic study had to be performed on the maintenance of solvent treatment pH on the hair fibers and the diffusion study by DVS or other techniques.

Results are covered by a non-disclosure agreement, which is why the study design and the experimental procedure are reported without the final results and their correlate comments in this chapter.

Typically, three different hair ethnicities can be categorized: African, Caucasian, and Asian (Figure 7.2). Their structural properties influence their performances, so identifying the possible differences among them can explain the different behavior of cosmetic treatment, which may interest chemists and hair-care new-product specialists.

Figure 7.1 Three main hair ethnicities

Previous morphological studies focused mainly on hair proteins, particularly on the keratin, amino-acids composition, and molecular structure [160, 161].
Nevertheless, the proteins and amino acids that constitute keratin are similar in the three ethnic groups, so that the different behavior could be due to the lipidic composition.
Several studies [162,163, 151,153] have been conducted to identify the effects of lipids on the fibers' properties with different innovative techniques, such as :

- Sorption Experiments (DVS)
- Mechanical Properties (Dynamometer)

- Moisture Content (% Humidity)
- Contact angle (Dynamic and pseudo-static)
- Synchrotron μ-FTIR and ATR-FTIR
- Thermogravimetric Analyses (TGA)
- Thermotropic studies (DSC)

They conclude that lipids play a crucial role in maintaining adequate water permeability and the hydrophobic character of the fiber surface.

The TLC/FID is a technique used to determine the lipid quali-quantitative composition differences between ethnicities. Previous studies [162,163, 151,153] show that Caucasian (C) and Asian (A) hair fibers have similar amounts of apolar lipids and sterols. AS have more Polar Lipids, but C has a significantly higher amount of FFA. The importance of lipid characterization accounts for the possible correlation between lipid amount, composition, and hair functionality.

Dynamic Vapor Sorption (DVS) is a thermogravimetric technique that evaluates how quickly a sample absorbs a solvent. This technique has application in the field of hair-care research for fiber integrity and moisture retention analysis. An absorption/desorption isotherm describes the experiment. The hair samples were exposed to different relative vapor pressure values, and the overtime weight changes were registered. Then, the isotherm shows the absorbed vapor quantity in the function of the relative vapor pressure, expressed as relative humidity (RH).

The Gab Model is the Mathematical model that describes the isotherm. (Eq. 6.1)

Previous sorption isotherms [162] show that moisture content is negligible at a very low RH, increasing with it, and Caucasian native hairs show higher maximum water regain value. (Figure 7.3).

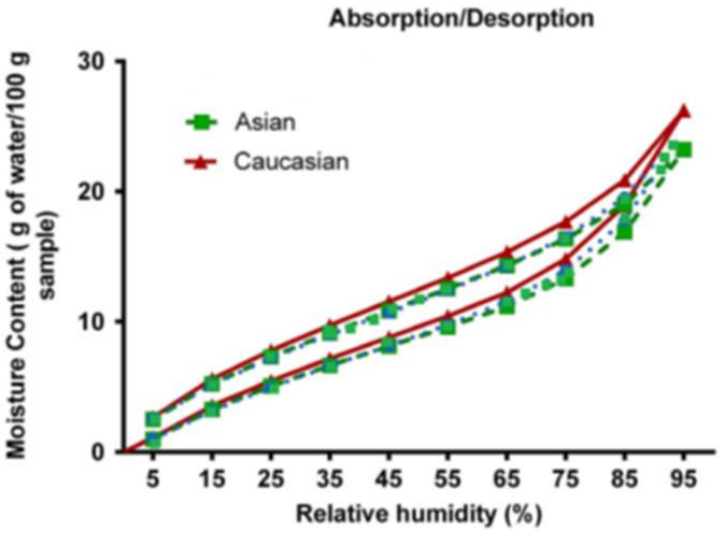

Figure 7.2 Absorption-Desorption isotherms for Caucasian (red) and Asian hair (green)

Hysteresis is the lag of the material response reacting to a change in its condition. The hysteresis amplitude is associated with the nature and state of the sample components. Hysteresis occurs because the keratin protein conformation changes with the variations of its hydration degree. Asian hair fibers have a higher degree of hysteresis, marked by their maximum value [162]. Then the AS fiber structure seems to be more resistant to hydration changes (Figure 7.4).

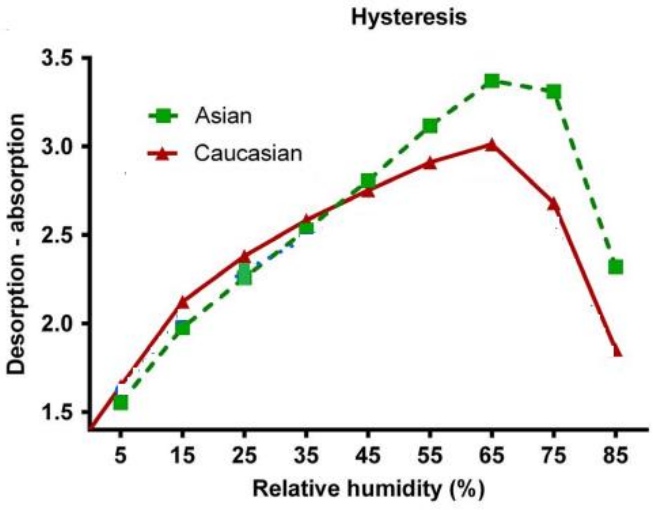

AS structure impedes the absorption of more water and looking for the hair diffusion, native C hair has more diffusion.

Permeability is believed to be managed by the cell membrane complex (CMC), which is mainly composed of internal lipids. Herein, it the importance to understand the correlation between lipid organization and barrier properties.

The IR spectra analyzed the CH_2 symmetric stretching (CH_2 sym), with maxima approximately 2850 cm^{-1}, providing information about the lipid amount, chain conformational order, and packing. The shift to higher wavenumbers indicates an increase in lipid disorder. The lipid order plays an important role, as does the lipid content because the fluidity of the lipids can modulate the rates of penetration and departing of substances.

7.2 Study Design

Virgin Caucasian and Chinese hair strands were subjected to a thermogravimetric and spectroscopic analysis, respectively, by a Dynamic Vapor Sorption (DVS) and ATR-FTIR investigations. The DVS allows the evaluation of the sample's water diffusion at different humidity levels, while the ATR-FTIR determines the possible structuration and amount of surface lipids.

7.3 Materials and Methods

7.3.1 Hair Samples

Six batches of ten 1-gram-hair strands, 3 for each race, were provided by the Sponsor.

The Hairs are virgin and did not receive any treatment, not even shampoo. They were stored in a room with controlled humidity and temperature (23,0 ± 2 ° C, 50 ± 5 % RH) and prepared to hold each strand with glue and tape to be adequately handled. Hair strands are labeled using an internal scheme reported in Table 7.1, set as follows :

- Set CH for Chinese Hair, C for Caucasian
- Set the last batch number for Chinese Hair, the first for the Caucasian
- Set a dot and after number the samples from 1 to 10

Table 7.1 Label scheme used for the hair samples

Batch Nr.	Nr of Strands	Ethnicity	Sample Name
CHIN242	10	Chinese	CH 2.1 – CH 2.10
7714-CHIN	10	Chinese	CH 4.1 – CH 4.10
7709-CHIN	10	Chinese	CH 9.1 – CH 9.10
1313CHAT	10	Caucasian	C 1.1 – C 1.10
D583	10	Caucasian	C 5.1 – C 5.10
7093HT4	10	Caucasian	C 7.1 – C7.10

7.3.1.1 Washing process

Hairs samples C1.1, C5.1, C7.1, CH2.1, CH4.1, and CH 9.1 were washed at hair/surfactant solution (ratio 1:30) with 3 % diluted commercial shampoo Pantene Pro-V for 3 minutes and then rinsed three times thoroughly with current water and dried in ambient conditions in a room with controlled humidity and temperature (23,0 ± 2 º C, 50 ± 5 % R.H). Hair samples C1.2, C5.2, C7.2, CH2.2, CH4.2, and CH 9.2 were washed with UltraDoux shampoo under the same conditions.

7.3.2 Dynamic Vapor Sorption (DVS)

The hair's water absorption/desorption kinetics was evaluated using a TA Instruments Q5000SA Sorption Analyzer, which consists of a highly sensitive thermobalance and a chamber to control relative humidity.

DVS is a thermogravimetric technique that evaluates how much and how quickly a sample absorbs a solvent. Evaluation of moisture kinetics' uptake and loss is a good strategy for obtaining more detailed information about a given sample's structural

integrity and organization. An absorption/desorption isotherm describes the process.

The sample is exposed to different relative vapor pressure values during the experiment, and the overtime weight changes are registered. The isotherm shows the absorbed vapor quantity in the function of the relative vapor pressure, expressed as relative humidity (RH). With this technique, the water diffusion coefficients are obtained.

During the tests, the weight of the analyzed hair samples was 10.002 ± 0.005 mg.

The experiments have been carried out with a gas flow of 200 mL/min, at 25 ° C and using the following methodology:

1. Stage of drying the sample at 60 ° C and 0 % RH

2. Pre-stabilization at 25 ° C and 0 % RH

3. Absorption curves: successive stages from 5 % RH to 95 % RH, in steps of 10 % RH, aborting to the following stages if weight (%) < 0.02 for 10 min, all at a constant temperature of 25 ° C

4. Desorption curves: successive stages from 95% RH to 5 % RH, in steps of 10 % RH, constant temperature of 25 ° C

The isotherms can be divided into two phases: the adsorption isotherm for increasing relative humidity stages and the desorption isotherm for decreasing relative humidity stages.

Mathematical models describe sorption isotherms, the Guggenheim-Anderson-de Boer (GAB) model being the most widely used. The GAB model allows a physical description of the sorption processes.

In our case, with the moisture content at the end of each stage, the TA Instruments software adjusted the GAB model to the experimental data.

The sorption isotherm parameters used to adjust the observed values are reported in Table 6.1.

7.3.3 IR Spectroscopy (FTIR-ATR)

The possible differences between different ethnic hair fibers due to their different composition and structural lipid organization can be evaluated using FTIR-ATR. This

technique can determine the lipid order disposition. For example, the CH_2 symmetric stretch mode position would indicate orthorhombic, lamellar, or gel lipid order with increased permeability. Integration of CH_2 asymmetric stretching mode is also quite reliable to determine lipid content.

A Nicolet Avatar 360-FTIR spectrophotometer equipped with an attenuated total reflection (ATR) accessory with a diamond crystal (with ZnSe lens) with a 42 ° angle of incidence in horizontal orientation was used. Before analysis, the hair is placed towards the diamond crystal. A pressure of 10,000 psi is applied to the samples. All the analyzed spectra represent an average of 64 scans with a resolution of 2 cm^{-1}, and the wavenumber range used is 4200 - 650 cm^{-1}. The maximum positions have been determined with the help of OMNIC software version 8.1.210.

7.3.4 Moisture content

The moisture content was evaluated from non-extracted hair samples. A hair sample of 0.5 g was maintained in a conditioned room (23 ° C, 50 % RH) for at least 24 hours before being weighed and subsequently dried in an oven at 105 ° C for 24 hours. The sample was cooled in a desiccator with a P_2O_5 atmosphere and weighed again; then, the moisture content was calculated as humidity percentage.

7.3.5 Lipid extractions

Extractions of external and internal lipids were performed with different organic solvents. The external surface lipids were initially removed from the washed hair surface with Soxhlet extraction with t-butanol and n-hexane for 4 hours. Internal lipids were extracted with different solvent mixtures of Chloroform: Methanol (2:1 $_{v/v}$, 1:1 $_{v/v}$, and 1:2 $_{v/v}$). Each mixture was applied to the hair samples for 2 hours. Then, 100 % Methanol was applied to the same hair samples overnight at RT in a stirring system. The different internal lipids extracted fractions were then combined, concentrated, and dissolved in a chloroform/ methanol mixture (2:1 $_{v/v}$) before analysis.

7.3.5.1 Lipids Analysis

Lipid analyses of the different extracts were performed with a thin-layer chromatography coupled to an automated flame ionization detector (TLC/FID) and an Iatroscan MK-5 analyzer (Iatron, Tokyo, Japan). The lipids extracts were directly spotted on a silica gel-coated Chromarods (type S-III) using a precision Hamilton 2 µL syringe coupled to an SES 3202/IS-02 sample spotter (NiederOLm, Germany). The determination of the lipid content was performed using an optimized TLC/FID protocol [151] using a methodology where rods (in a set of 10) were developed using the following mobile phases: (i) chloroform/methanol/water (57:12:0.6, v/v/v) for a distance of 2.5 cm twice, (ii) n-hexane/ethyl ether/formic acid (50:20:0.3, v/v/v) to an 8 cm and (iii) n-hexane/benzene (35:35, v/v) to a 10 cm, and finally a total scan (100 %) to quantify the most polar lipids was performed.

7.4 Results

Results are covered by a non-disclosure agreement, which is why the study design and the experimental procedure are reported without the final results and their correlate comments in this chapter.

REFERENCES

1. Cilia, G. Antimicrobial properties of terrestrial snail and Slug mucus. *J Complement Integr Med*.15(3):1-10 **2018**.

2. Conte, R. Recent advances on nano delivery of helix mucus pharmacologically active components. *Intern J Nano Dimen*. 7:181-185 **2016**.

3. Selamoglu, Z. In-vitro vitro antioxidant activities of the ethanolic extracts of some Contained-Allantoin plants. *Iran J Pharm Res*.16(Suppl):92-98 **2017**.

4. Règlement CE no 1223/2009 du Parlement européen et du Conseil du 30 novembre 2009 relatif aux produits cosmétiques [Internet. Consulté 1 oct 2016]. Disponible sur: http:// eurlex. europa. eu/ LexUriServ/ LexUriServ. do? uri= OJ: L: 2009: 342: 0059: 0209:fr:pdf

5. Thornfeldt, C. Cosmeceuticals containing herbs: fact, fiction, and future. *Dermatol Surg.* 31(7 Pt 2):873-881 **2005**.

6. Conte, R. Recent advances on nano delivery of helix mucus pharmacologically active components. *Inter J Nano Dimens*. 7(3):181-185 **2016**.

7. Kim, S.J. Increased in vivo collagen synthesis and in vitro cell proliferative effect of glycolic acid. *Dermatol Surg.* 24(10):1054-1058 **1998**.

8. Bernstein, E.F. Glycolic acid treatment increases type I collagen mRNA and hyaluronic acid content of human skin. *Dermatol Surg.* 27(5):429-433 **2001**.

9. El Mubarak, M.A.S. Simultaneous determination of allantoin and glycolic acid in snail mucus and cosmetic creams with high performance liquid chromatography and ultraviolet detection. *J Chromatogr A*.1322:49-53 **2013**.

10. World Medical Association Declaration of Helsinki: ethical principles for medical research involving human subjects. JAMA. Nov 27;310(20):2191-4. doi: 10.1001/jama **2013**.

11. Fartasch, M. Mode of action of glycolic acid on human stratum corneum: ultrastructural and functional evaluation of the epidermal barrier. *Arch Dermatol Res*. 289(7):404-409 **1997**.

12. Sugiyama-Nakagiri, Y. Ethnic differences in the structural properties of facial skin, *J of Dermatological Science*. 53, 135-139 **2009**.

13. Maia Campos, P.M.B.G. Use of Advanced Imaging Techniques for the Characterization of Oily Skin. *Front Physiol*. Mar 26;10:254 **2019**.

14. Ki, V. Bacterial skin and soft tissue infections in adults: A review of their epidemiology, pathogenesis, diagnosis, treatment and site of care. *Can J Infect Dis Med Microbiol*. Mar;19(2):173-84 **2008**.

15. Katsuta, Y. Improving the Appearance of Facial Pores. *Cosmetic & Toiletries*, 119 (10), 59-64 **2004**.

16. Sugata, K. Confocal laser microscopic imaging of conspicuous facial pores in vivo: relation between the appearance and the internal structure of skin. *Skin Research and Technology*, 14, 208-212 **2008**.

17. Murakami, M. Morphological analysis of facial pores and factors related to changes with aging in pore shape. *IFSCC Congress* **2006**.

18. Lida, T. How can we improve the appearance of conspicuous facial pores? *IFSCC Congress* **2006**.

19. Thiboutot D. New Treatments and Therapeutic Strategies for Acne. *Arch Fam Med.* 9:179-187 **2000**.

20. Stefanini, A.C. Involvement of Kallikrein-Related Peptidases in Normal and Pathologic Processes. *Dis Markers*. 2015:946572 **2015**.

21. Juliano, C. Cosmetic Functional Ingredients from Botanical Sources for Anti-Pollution Skincare Products. *Cosmetics*. 5(1):19 **2018**.

22. Apone, F. Plant tissue cultures as sources of ingredients for skin care applications. *Annual Plant Reviews*, 3, 135–150 **2020**.

23. Boncompagni, E. Sostanze vegetali in cosmetica – *Aboca* **2003**.

24. Boga, M. Chemical constituents and biological activities of Cirsium leucopsis, C. sipyleum, and C. eriophorum. *Zeitschrift für Naturforschung C*, 69(9–10), 381–390 **2015**.

25. Das, U. Ethno-herbal-medico in wound repair: An incisive review. *Phototherapy Research*, 31, 579–590 **2017**.

26. Dini, I. Nutricosmetics: A brief overview. *Phototherapy Research*, 33(12), 3054–3063 **2019**.

27. Inui, S. Improvement of acne vulgaris by topical fullerene application: Unique impact on skin care. *Nanomedicine Nanotechnology Biology and Medicine*, 7, 238–241 **2011**.

28. Jeong, D.M. Comparative antioxidant activity and HPLC profiles of some selected Korean thistles. *Archives of Pharmacol Research*, 31, 28–33 **2008**.

29. Seo, J.O. Finasteride inhibits melanogenesis through regulation of the adenylate cyclase in melanocytes and melanoma cells. *Archives of Pharmacal Research*, 41 (3), 324–332 **2018**.

30. Igawa, S. Incomplete KLK7 secretion and upregulated LEKTI expression underlie hyperkeratotic stratum corneum in atopic dermatitis. *Journal of Investigative Dermatology*, 137(2), 449–456 **2017**.

31. An, Q. High Staphylococcus epidermidis colonization and impaired permeability barrier in facial Seborrheic dermatitis. *Chinese Medical Journal*, 130(14), 1662–1669 **2017**.

32. Lijnen, P. Transforming growth factor-beta 1-induced collagen production in cultures of cardiac fibroblasts is the result of the appearance of myofibroblasts. *Methods and Findings in Experimental and Clinical Pharmacology*, 24, 333–344 **2002**.

33. Katsuta, Y. Improving the appearance of facial pores. *Cosmetics & Toiletries*, 119(10), 59–64 **2004**.

34. Li, Y. Chemical profiling of bioactive constituents in Sarcandra glabra and its preparations using ultra-high-pressure liquid chromatography coupled with LTQ Orbitrap mass spectrometry. *Rapid Communication in Mass Spectrometry*, 25(17), 2439–2447 **2011**.

35. Regueiro, J. Comprehensive identification of walnut polyphenols by liquid chromatography coupled to linear ion trap–Orbitrap mass spectrometry. *Food Chemistry*, 152, 340–348 **2014**.

36. Troise, A.D. Targeted metabolite profile of food bioactive compounds by Orbitrap high resolution mass spectrometry: The “FancyTiles” approach. *Food Research International*, 63B, 139–146 **2014**.

37. Yin J. Anti-acne vulgaris effect including skin barrier improvement and 5α-reductase inhibition by tellimagrandin I from Carpinus tschonoskii. *BMC Complementary Medicine Research*, 19, 323 **2019**.

38. Zhang, L. Defects in stratum Corneum desquamation are the predominant effect of impaired ABCA12 function in a novel mouse model of harlequin Ichthyosis. *PLoS One*, 11(8), 0161465 **2016**.

39. Zouboulis, C.C. Anti-acne drugs in phase 1 and 2 clinical trials. *Expert Opinion on Investigational Drugs*, 26, 813–823 **2017**.

40. Dong, J.B.A. Enlarged facial pores: An update on treatments. *Cutis*, 98(1), 33–36 **2016**.

41. Schütz R, Rawlings A V. Bio-derived hydroxystearic acid ameliorates skin age spots and conspicuous pores. *International Journal of Cosmetic Science*, 41(3), 240–256 **2019**.

42. Logger, J.G.M. Olydam J I. Noninvasive skin barrier assessment: Multiparametric approach and pilot study. *Cosmetics*, 6(1), 20 **2019**.

43. Yamamoto, A. Impaired water barrier function in acne vulgaris. *Archives of Dermatological Research*, 287(2), 214–218 **1995**.

44. Acker, T. The good, the bad and the ugly in oxygen-sensing: ROS, cytochromes and prolyl-hydroxylases. *Cardiovasc. Res*., 71, 195–207 **2006**.

45. Dini, I. Nutricosmetics: A brief overview. *Phytother Res*. 33, 3054–3063 **2019**.

46. Lopez-Camarillo, C. Protein kinases and transcription factors activation in response to UV-radiation of skin: Implications for carcinogenesis. *Int. J. Mol. Sci.* 13, 142–172 **2012**.

47. Laneri, S. Dosage of Bioactive Molecules in the Nutricosmeceutical Helix aspersa Muller Mucus and Formulation of New Cosmetic Cream with Moisturizing Effect. *Nat. Prod. Com*. 14, 1–7 **2019**.

48. Laneri, S. Plant cell culture extract of Cirsium eriophorum with skin pore refiner activity by modulating sebum production and inflammatory response. *Phytother Res.* 35, 530–540 **2021**.

49. Dini, I. An Extract from Ficus carica Cell Cultures Works as an Anti–Stress Ingredient for the Skin. *Antioxidants*, 10, 515 **2021**.

50. De Fabo, E.C. Mechanism of immune suppression by ultraviolet irradiation in vivo. I. Evidence for the existence of a unique photoreceptor in skin and its role in photoimmunology. *J. Exp. Med.* 158, 84–98 **1983**.

51. Dini, I. The New Challenge of Green Cosmetics: Natural Food Ingredients for Cosmetic Formulations. *Molecules*, 26, 3921 **2021**.

52. Dini, I. Spices, Condiments, Extra Virgin Olive Oil and Aromas as Not Only Flavorings, but Precious Allies for Our Wellbeing. *Antioxidants*. 10, 868 **2021**.

53. Belkaid, Y. The influence of skin microorganisms on cutaneous immunity. *Nat Rev Immunol*. 16(6), 353-66 **2016**.

54. Boxberger, M. Challenges in exploring and manipulating the human skin microbiome. *Microbiome*. 9(1), 125 **2021**.

55. De Pessemier, B. Gut-Skin Axis: Current Knowledge of the Interrelationship between Microbial Dysbiosis and Skin Conditions. *Microorganisms*. 9(2), 353 **2021**.

56. O'Sullivan, J.N. Human skin microbiota is a rich source of bacteriocin-producing staphylococci that kill human pathogens. *FEMS Microbiol Ecol*. 95 **2019**.

57. Nakatsuji, T. Antimicrobials from human skin commensal bacteria protect against Staphylococcus aureus and are deficient in atopic dermatitis. *Sci Transl Med*. 9, eaah4680 **2017.**

58. Baldwin, H.E. The role of cutaneous microbiota harmony in maintaining a functional skin barrier. *J Drugs Dermatol*. 16, 12-8 **2017**.

59. Williams, M.R. Quorum sensing between bacterial species on the skin protects against epidermal injury in atopic dermatitis. *Sci Transl Med*. 11, eaat8329 **2019**.

60. Gaitanis, G. Variation of cultured skin microbiota in mothers and their infants during the first year postpartum. *Pediatric Dermatol*. 36(4), 460-465 **2019**.

61. Sfriso, R. Revealing the secret life of skin - with the microbiome you never walk alone. *Int J Cosmet Sci*., 42(2), 116-126 **2020**.

62. Meisel, J.S. Commensal microbiota modulate gene expression in the skin. *Microbiome*. 6, 20 **2018**.

63. Schwarz, A. The Short-Chain Fatty Acid Sodium Butyrate Functions as a Regulator of the Skin Immune System. *J. Invest. Dermatol*. 137(4), 855-864 **2017**.

64. Keshari, S. Butyric Acid from Probiotic Staphylococcus epidermidis in the Skin Microbiome Down-Regulates the Ultraviolet-Induced Pro-Inflammatory IL-6 Cytokine via Short-Chain Fatty Acid Receptor. *Int. J. Mol. Sci*. 20, 4477 **2019**.

65. Russo, R. In vivo bioavailability and in vitro toxicological evaluation of the new butyric acid releaser N-(1-carbamoyl-2-phenyl-ethyl) butyramide. *Biomed Pharmacother*. 137, 111385 **2021**.

66. AOAC Appendix F: Guidelines for Standard Method Performance Requirements (SMPR). *AOAC Official methods of analysis*. **2016**

67. Ng, K.W. Skin Deep: The Basics of Human Skin Structure and Drug Penetration. Percutaneous Penetration Enhanc. *Chem. Methods Penetration Enhanc*. 3–11 **2015**.

68. Sobańska, A.W. Application of RP-18 TLC Retention Data to the Prediction of the Transdermal Absorption of Drugs. *Pharmaceuticals*. 14, 147 **2021**.

69. Todo, H. Transdermal Permeation of Drugs in Various Animal Species. *Pharmaceutics*. 9, 33 **2017**.

70. Neupane, R. Alternatives to Biological Skin in Permeation Studies: Current Trends and Possibilities. *Pharmaceutics*.12, 152 **2020**.

71. Elias, P.M. Epidermal barrier function: intercellular lamellar lipid structures, origin, composition, and metabolism. *J. Control Release*.15, 199-208 **1991**.

72. Cameron, D.R. Isolation and characterization of bacteriophages from the human skin microbiome that infect Staphylococcus epidermidis, *FEMS Microbes*. 2, xtab003 **2021**.

73. Schwarz, A. The Short-Chain Fatty Acid Sodium Butyrate Functions as a Regulator of the Skin Immune System. *J. Investig. Dermatol*. 137, 855–864 **2017**.

74. Karaki, S. Short-chain fatty acid receptor, GPR43, is expressed by enteroendocrine cells and mucosal mast cells in rat intestine. *Cell Tissue Res*. 324, 353–360 **2006**.

75. Sujka, W. Influence of porous dressings based on butyric-acetic chitin co-polymer on biological processes in vitro and in vivo. *Materials*. 12(6), 970 **2019**.

76. Traisaeng, S. A derivative of butyric acid, the fermentation metabolite of Staphylococcus epidermidis, inhibits the growth of a Staphylococcus aureus strain isolated from atopic dermatitis patients. *Toxins.* 11(6), 311 **2019**.

77. Krejner, A. Decreased expression of G-protein-coupled receptors GPR43 and GPR109a in psoriatic skin can be restored by topical application of sodium butyrate. *Arch Dermatol Res*. 310(9), 751-758 **2018**.

78. Wild, C.P. Complementing the genome with an “exposome”: The outstanding challenge of environmental exposure measurement in molecular epidemiology. *Cancer Epidemiol. Biomark. Prev*. 14, 1847–1850 **2005**.

79. Krutmann, J. The skin aging exposome. *Dermatol. Sci. J*. 85, 152–161 **2017**.

80. Vileikyte, L. Stress and wound healing. *Clin. Dermatol*. 25, 49–55 **2007**.

81. Papadimitriou, A. Regulation of the hypothalamic-pituitary-adrenal axis. *Neuroimmunomodulation*, 16, 265–271 **2009**.

82. Cohen, S. Psychological stress and disease. *JAMA* 298, 1685–1687 **2007**.

83. Chen, Y. Brain-skin connection: Stress, inflammation and skin aging. *Inflamm. Allergy Drug Targets*, 13, 177–190 **2014**.

84. Mammone, T. The induction of terminal differentiation markers by the cAMP pathway in human HaCaT keratinocytes. *Skin Pharmacol. Physiol*. 11, 152–160 **1998**.

85. Grando, S.A. Adrenergic and cholinergic control in the biology of epidermis: Physiological and clinical significance. *J. Investig. Dermatol*., 126, 1948–1965 **2006**.

86. Choi, E.H. Mechanisms by which psychologic stress alters cutaneous permeability barrier homeostasis and stratum corneum integrity. *J. Investig. Dermatol*. 124, 587–595 **2005**.

87. Romana-Souza, B. Psychological stress-induced catecholamines accelerates cutaneous aging in mice. *Mech. Ageing Dev*. 152, 63–73 **2015**.

88. Santacruz-Perez, C. Photochemistry of Lipofuscin and the Interplay of UVA and Visible Light in Skin Photosensitivity, Photochemistry and Photophysics. In Fundamentals to Applications; *IntechOpen*: London, UK, **2018**.

89. Laneri, S. Plant cell culture extract of Cirsium eriophorum with skin pore refiner activity by modulating sebum production and inflammatory response. *Phytother. Res*. 35, 530–540 **2021**

90. Apone, F. Plant tissue cultures as sources of ingredients for skin care applications. *Ann. Plant Rev*. 3, 135–150 **2020**.

91. Datwyler, S.L. On the origin of the fig: Phylogenetic relationships of Moraceae from NDHF sequences. *American Journal of Botany*, 91, 767-777 **2004**.

92. Ribeiro, J. E. L. S. Neotropikey—Interactive key and information resources for flowering plants of the Neotropics*. Royal Botanic Gardens*. **2011**.

93. Raya, F.G. The plants of the Gospels. *Biocell*, 30, 170 **2006**.

94. Salhi-Hannachi, A. Genetic diversity of different Tunisian fig (Ficus carica L.) collections revealed by RAPD fingerprints. *Hereditas*, 143 15-22 **2006**.

95. Tropicos.org. Missouri Botanical Garden. 17 Apr 2014 <http://www.tropicos.org/Name/21302044>.

96. Lansky, E.P. Ficus spp. (fig): Ethno botany and potential as anticancer and anti-inflammatory agents. *Journal of Ethnopharmacology*, 119, 195-213 **2008**.

97. Lazreg-Aref, H. Chemical composition and antibacterial activity of a hexane extract of Tunisian capri fig latex from the unripe fruit of Ficus carica. *Pharmaceutical Biology*, 50, 407-412 **2012**.

98. Mawa, S. Ficus carica L. (Moraceae): Phytochemistry, traditional uses and biological activities. *Evidence-Based Complementary and Alternative Medicine*, 8 **2013**.

99. Martínez, G.J. Farmacopea natural y tratamiento de afecciones de la piel en la medicina tradicional de los campesinos de las sierras de Córdoba (República Argentina). *Dominguezia*, 24, 27–46 **2008**.

100. Oliveira, A.P. Chemical assessment and in vitro antioxidant capacity of Ficus carica latex. *Journal of Agriculture and Food Chemistry*, 58, 3393–3398 **2010**.

101. Amorin, A. Anthelmintic activity of the latex of Ficus species. *Journal of Ethnopharmacology*, 64, 255–258 **1999**.

102. Lansky, E.P. Ficus spp. (fig): Ethno botany and potential as anticancer and anti-inflammatory agents. *Journal of Ethnopharmacology*, 119, 195–213 **2008**.

103. McCarty, R. Chronic stress and sympathetic-adrenal medullary responsiveness. *Soc. Sci. Med*. 26 (3):333–341 **1988**.

104. Sanders, V.M. Differential expression of the beta2-adrenergic receptor by Th1 and Th2 clones: implications for cytokine production and B cell help. *J. Immunol*. 158 (9):4200–4210 **1997**.

105. Marino, F. Adrenergic modulation of immune cells: an update. *Amino acids*. 45 (1):55–71 **2013**.

106. Panina-Bordignon, P. Beta2-agonists prevent Th1 development by selective inhibition of interleukin 12. *The J. Clin. Invest*. 100 (6):1513–1519 **1997**.

107. Goyarts, E. Norepinephrine modulates human dendritic cell activation by altering cytokine release. *Exp. Dermatol*. 17 (3):188–196 **2008**.

108. Grando, S.A. Adrenergic and cholinergic control in the biology of epidermis: physiological and clinical significance. *J. Invest. Dermatol*.126 (9):1948–1965 **2006**.

109. Schallreuter, K.U. Production of catecholamines in the human epidermis. *Biochem. Biophys. Res. Commun*. 189 (1):72–78 **1992**.

110. Koizumi, H. beta-Adrenergic stimulation induces activation of protein kinase C and inositol 1,4,5-trisphosphate increase in epidermis. *Exp. Dermatol*. 6 (3):128–132 **1997**.

111. Tsalokostas, G. Using Tissue Culture as an Alternative Source of Polyphenols Produced by Ficus carica L. *Ph.D. Thesis*, Faculty in Biology, City University of New York, New York, NY, USA, **2009**.

112. Gagaoua, M. Three-phase partitioning as an efficient method for the purification and recovery of ficin from Mediterranean fig (Ficus carica L.) latex. *Sep. Purif. Technol*. 132, 461–467 **2014**.

113. Nassar, A.H. Ficin production by callus cultures of Ficus carica. *Plant Phys. J.* 131, 171–179 **1987**.

114. Cuesta, A.M. The b_2-adrenergic receptor antagonist ICI-118,551 blocks the constitutively activated HIF signaling in hemangioblastomas from von Hippel-Lindau disease. *Sci. Rep*. 9, 10062 **2019**.

115. Zumwalt, J.W. Interleukin-1beta and catecholamines synergistically stimulate interleukin-6 release from rat C6 glioma cells in vitro: A potential role for lysophosphatidylcholine. *Endocrinology*, 140, 888–896 **1999**.

116. Wortsman, J. Adre-nomedullary response to maximal stress in humans. *Am. J. Med*. 77, 779–784 **1984**.

117. Garg, A. Psychological stress perturbs epidermal permeability barrier homeostasis: implications for the pathogenesis of stress-associated skin disorders. *Arch Dermatol*. Jan; 137(1):53-9 **2001**.

118. Chiu, A. The Response of Skin Disease to Stress: Changes in the Severity of Acne Vulgaris as Affected by Examination Stress. *Arch Dermatol*.139(7):897–900 **2003**.

119. Peters, E.M.J. Stressed skin?--a molecular psychosomatic update on stress-causes and effects in dermatologic diseases. *J Dtsch Dermatol Ges*. Mar;14(3):233-52; quiz 253 **2016.**

120. Dunn, J.H. Psychological Stress and skin aging: A review of possible mechanisms and potential therapies. *Dermat. Online* J. 19, 18561 **2013**.

121. Scudiero, O. Human Defensins: A Novel Approach in the Fight against Skin Colonizing Staphylococcus aureus. *Antibiotics*, 9, 198 **2020**.

122. Pero, R. Beta-defensins and analogs in Helicobacter pylori infections: mRNA expression levels, DNA methylation, and antibacterial activity. *PLoS ONE*; 14, e0222295 **2019**.

123. Damjanovic, A.K. Accelerated telomere erosion is associated with a declining immune function of caregivers of Alzheimer's disease patients. *Immun. J.* 179, 4249–4254 **2007**.

124. Hara, M.R. A stress response pathway regulates DNA damage through beta2-adrenoreceptors and beta-arrestin-1. *Nature* 477, 349–353 **2011**.

125. Romana-Souza, B. Psychological stress-induced catecholamines accelerates cutaneous aging in mice. *Mech. Ageing Dev.* 152, 63–73 **2015**.

126. Minich, D.M. A review of the clinical efficacy and safety of cruciferous vegetable phytochemicals. *Nutr. Rev.* 65, 259–267 **2007**.

127. Cormier, F. Partial purification and properties of proteases from fig (Ficus carica) callus cultures. *Biotechnol. Lett.* 11, 797–802 **1989**.

128. Chen, Y. Brain-skin connection: Stress, inflammation and skin aging. *Inflamm. Allergy Drug Targets*, 13, 177–190 **2014**.

129. Moore, A.R. The role of cAMP regulation in controlling inflammation. *Clin. Exp. Immunol*. 101, 387–389 **1995**.

130. Rinnerthaler, M. Oxidative Stress in Aging Human Skin. *Biomolecules*. 5, 545–589 **2015**.

131. Proksch, E. The skin: An indispensable barrier. *Exp. Dermatol.* 17, 1063–1972 **2008**.

132. Feingold, K.R. The role of epidermal lipids in cutaneous permeability barrier homeostasis. *J. Lipid Res.* 48, 2531–2546 **2007**.

133. Chiu, A. The response of skin disease to stress: Changes in acne severity vulgaris as affected by examination stress. *Arch Dermatol.* 139, 897–900 **2003**.

134. Peters, E.M.J. Stressed skin a molecular psychosomatic update on stress-causes and effects in dermatologic diseases. *J. Dtsch. Dermatol. Ges.* 14, 233–252 **2016**.

135. Loden, M. Role of topical emollients and moisturizers in the treatment of dry skin barrier disorders. *In Dry Skin and Moisturizers: Chemistry and Function, 2nd ed*.; CRC Press: Boca Raton, FL, USA, **2006**; pp. 771–778.

136. Fluhr, J.W. Stratum corneum pH: Formation and function of the acid mantle. *Exog. Dermatol.* 1, 163–175 **2002**.

137. Cho, U.M. Inhibitory Effect of Ficin Derived from Fig Latex on Inflammation and Melanin Production in Skin Cells. *Biotechnol. Bioproc*. 24, 288–297 **2019**.

138. Devaraj, K.B. Purification, characterization, and solvent-induced thermal stabilization of ficin from Ficus carica. *J. Agric. Food Chem.* 56, 11417–11423 **2008**.

139. Kaihui, H.U. The adverse skin reactions of health care workers using personal protective equipment for COVID-19. *Medicine*.99:24 **2020**.

140. Scarano, A. Facial skin temperature and discomfort when wearing protective face masks: thermal infrared imaging evaluation and hands moving the mask. *Int J Environ Res Public Health.*17:4624 **2020**.

141. https://www.nippon.com/en/japan-data/h00891/

142. Gerstell, E. Costumer packaged Goods Practises: How COVID-19 is changing the world of beauty. *McKinsey & Company*. **2020**.

143. Laneri, S. A New Protocol to Evaluate Waterproof Effect of Lip Gloss, *Biom. J Scien Tech Res*, 23 July **2019**.

144. Trüeb, R.M. Aging of hair. *J. Cosmetic Dermatol*. 4, 60-72 **2005**.

145. Tobin, D.J. Graying: gerontobiology of the hair follicle pigmentary unit. *Exp Gerontol* 36: 29–54 **2001**.

146. Commo, S. Human hair greying is linked to a specific depletion of hair follicle melanocytes affecting both the bulb and the outer root sheath. *Br J Dermatol* 150: 435–43 **2004**.

147. Ji, J.H. The Ethnic Differences of the Damage of Hair and Integral Hair Lipid after Ultra Violet Radiation. *Ann Dermatol*. Feb; 25(1): 54–60 **2013**.

148. Mayra, B. Hair Aging in Different Races and Ethnicities. J Clin Aesthet Dermatol. Jan; 14(1): 38–44 **2021**.

149. Anderson, R.B. Modifications of the Brunauer, Emmett and Teller equation. *J Am Chem Soc.* 70:1727-1734 **1948**.

150. Oliver, M.A. Lipid loses and barrier function modifications of the brown-to-white hair transition. *Skin Res Technol*. Jul;25(4):517-525 **2019**.

151. Martí, M. The influence of hair lipids in ethnic hair properties. *Int J Cosmet Sci*. 38:77-84 **2016**.

152. Barba, C. Moisture sorption/desorption of protein fibres. *Thermochim Acta* 552:70-76 **2013**.

153. Coderch, L. Exogenous and endogenous lipids of human hair. *Skin Res. Technol.* 23:479-485 **2017.**

154. Anderson, R.B. Modifications of the Brunauer, Emmett and Teller Equation II1. *J. Am. Chem. Soc.* 70:1727-1734 **1948**.

155. Vickerstaff T. The Physical Chemistry of Dyeing. *London: Oliver and Boyd* **1954**.

156. Natarajan, U. The thickness of 18-MEA on an ultra-high-sulfur protein surface by molecular modelling. *J Cosmet Sci*. 6:467-477 **2010**.

157. Zhang, G. Measuring changes in chemistry, composition, and molecular structure within hair fibers by infrared and Raman spectroscopic imaging. *J Biomed Optics*. 16:056009 **2011**.

158. Martí M. The influence of hair lipids in ethnic hair properties. *Int J Cosmet Sci*. 38:77-84 **2016**.

159. Meredith, P. The physical and chemical properties of eumelanin. *Pigment Cell Res*. 19(6):572-594 **2006**.

160. Franbourg, A. Current research on ethnic hair. *J Am Acad Dermatol*. Jun; 48 (6 Suppl) : S115-9 **2003**.

161. Dekio, S. Hair low-sulfur protein composition does not differ electrophoretically among different races. *J Dermatol*. Oct;15(5):393-6 **1988**.

162. Oliver, MA, Ethnic hair: Thermoanalytical and spectroscopic differences. *Skin Research and Technology*. March; 617-626 **2020**.

163. Coderch L, External lipid function in ethnic hairs. *J Cosmet Dermatol*. December;1912-1920 **2019**.

ACKNOWLEDGMENTS

I would like to thank the people who have helped me in this challenging course, even in a few words.

A special acknowledgment is dedicated to Prof. Sonia Laneri, who gave me this great opportunity. If it were not for her, I would not be here now. She engaged with force to support my research activity and helped me to achieve my goals. She is more than a professor for me. She is the woman that I hope to be someday.
I want to thank Prof. Antonia Sacchi, a mentor with her great life experience.
Thank you, Prof. Luisa Coderch, for showing me how to be more analytical and organized. You are a great scientist, and I spent a beautiful time at your laboratory.
Thank you to Vitalab Srl for the technical support.

CURRICULUM VITAE

Ritamaria Di Lorenzo obtained a Master's Degree in Pharmaceutical Chemistry in October 2017 at the University of Naples Federico II, Department of Pharmacy, and she discussed an experimental thesis entitled: "A New Protocol to Evaluate Waterproof Effect of Lip Gloss" that was also published on a peer-reviewed journal of the cosmetic sector.

In 2019 she entered the XXXIV cycle of the Ph.D. program in Pharmaceutical Sciences, Dept. of Pharmacy in Naples at the RD Cosmetics Laboratory. Her research focuses on the development and execution of tests to evaluate efficacy and activity research to identify new APIs to be conveyed in skincare and haircare products. Until October 2021, she was engaged in Spain at the DermoCosmetic Assessment service of the Institute of Advanced Chemistry of Catalonia (IQAC), carrying out research projects in hair aging and interracial differences that regulate the different permeation of cosmetic treatments in hairs.

.

UNIVERSITY CAREER

2019 – present: Ph.D. student in Pharmaceutical Sciences, University of Naples Federico II

August 2021 – present: fellowship in collaboration with Vitalab S.r.l. "Ricerca e sviluppo di nuovi attivi funzionali in prodotti cosmetici" – Ref. FARM/BS/16/2021

September 2020 – June 2020: fellowship in collaboration with Public Health Department. "Tecniche di analisi di fluidi biologici" – Ref. FARM/BS/13/2020

June 2020 – August 2020: fellowship in collaboration with Cosmetica Italia Servizi S.r.l. "Valutazione di efficacia di nuovi estratti dermocosmetici" - Ref. FARM/BS/09/2020

May 2019 – May 2020: fellowship in collaboration with Cosmetica Italia Servizi S.r.l. "Studi per la valutazione di efficacia di cosmetici in base al Regolamento EU 1223/2009" - Ref. FARM/BS/11/2019

April 2018 – September 2018: fellowship in collaboration with Cosmetica Italia Servizi S.r.l. "Valutazione di efficacia di prodotti cosmetici anti-aging mediante tecniche strumentali non invasive" - Ref. FARM/BS/04/2018

PUBLICATIONS

- Laneri S, Di Lorenzo R, Sacchi A, Dini I. “A New Protocol to Evaluate Waterproof Effect of Lip Gloss.”, *Biomedical Journal of Scientific & Technical Research*. LLC, vol. 19(5), 14676-14678, **2019.**

- Laneri S, Di Lorenzo R, Sacchi A, Dini I. “Dosage of Bioactive Molecules in the Nutricosmeceutical Helix aspersa Muller Mucus and Formulation of New Cosmetic Cream with Moisturizing Effect.”, *Natural product communications*, August: 1–7 **2019**.

- De Caro C, Raucci F, Saviano A, Cristiano C, Casillo GM, Di Lorenzo R, Sacchi A, Laneri S, Dini I, De Vita S, Chini MG, Bifulco G, Calignano A, Maione F, Mascolo N. “Pharmacological and molecular docking assessment of cryptotanshinone as natural-derived analgesic compound.”, *Biomed Pharmacother*. June; 126:110042 **2020**.

- Dini I, Di Lorenzo R, Senatore A, Coppola D, Laneri S. “Validation of rapid automated analysis of acetic acid in vinegar.” *Foods*, June; 9(6), 761 **2020**.

- Laneri S, Di Lorenzo R, Bernardi A, Sacchi A, Dini I “Aloe barbadensis: A Plant of Nutricosmetic Interest.”, *Natural product communications*, July; 15(7): 1–6 **2020**.

- Laneri S, Dini I, Tito A, Di Lorenzo R, Bimonte M, Tortora A, Zappelli C, Angelillo M, Bernardi A, Sacchi A, Colucci M G, Apone F. “Plant cell culture extract of Cirsium eriophorum with skin pore refiner activity by modulating sebum production and inflammatory response.”, *Phytotherapy Research*;1–11 **2020**.

- Dini I, Falanga D, Di Lorenzo R, Tito A, Carotenuto G, Zappelli C, Grumetto L, Sacchi A, Laneri S, Apone F. “An Extract from Ficus carica Cell Cultures Works as an Anti-Stress Ingredient for the Skin.”, *Antioxidants*, 10(4), 515 **2021**;

- Dini I, Di Lorenzo R, Senatore A, Coppola D, Laneri S. “Comparison between Mid-Infrared (ATR-FTIR) Spectroscopy and Official Analysis Methods for Determination of the Concentrations of Alcohol, SO2, and Total Acids in Wine.”, *Separations*, 8(10), 191 **2021**.

- Russo G, Laneri S, Di Lorenzo R, Ferrara L, Grumetto L. The occurrence of selected endocrine-disrupting chemicals in water and sediments from an urban lagoon in Southern Italy. *Water Environ Res*. Oct;93(10):1944-1958 **2021**.

- Di Lorenzo, R.; Bernardi, A.; Grumetto, L.; Sacchi, A.; Avagliano, C.; Coppola, S.; de Giovanni di Santa Severina, A.F.; Bruno, C.; Paparo, L.; Laneri, S.; Dini, I. Phenylalanine Butyramide Is a New Cosmetic Ingredient with Soothing and Anti-Reddening Potential. *Molecules.* 26, 6611 **2021**.

POSTER AND ORAL COMMUNICATIONS

Poster communication:

Validation of rapid automated analysis of acetic acid in vinegar - “Incontri di Scienza delle Separazioni”, 28 - 29 November 2019 - Naples, Italy

Analysis and in vivo evaluation of physio-balancing and soothing effect of emulsions containing ALOE ARBORESCENS GEL – “28° Italo-latinamerican congress of ethnomedicine”, 16 – 20 September 2019, La Habana, Cuba

Dermocosmetic efficacy of a nutricosmetic concentrated oil-soluble fraction from Vitis vinifera grape marc on the skin hydrolipidic barrier and wrinkles - “Cosmetic Dermatology and Aesthetic Medicine”, 22 - 23 June 2020 - Paris, France

Herbal extracts rich in phytochemicals as potential ingredients in anti-aging nutricosmetics – “International Conference and exhibition on Cosmetology&Plastic Surgery”, 13 – 14 August 2020 – Venice, Italy

Oral communication:

Keratin Reconstruction: Evaluation of Green Peptides Technology on Hair Performance – “15. International Conference Cosmetic and Plastic Surgery”, 18 -19 November 2021 – Paris, France